Role of PIP binding motifs on the nucleolar localization and function of ErbB3 binding protein 1

SHAOOR AHMAD KHAN

UNIVERSITY OF BERGEN
Faculty of Mathematics and Natural Sciences

Department of Biological Sciences

Norway

June 2020

This thesis is submitted in partial fulfillment of the requirements for the degree of

Master of Science

Acknowledgments

The work in this manuscript was carried out from August 2019 to April 2020 at University of Bergen. I am grateful to God for giving me strength and courage to follow on with my aspirations.

First and foremost, I would like to thank my supervisor Associate Professor, **Aurelia Lewis** for all the discussions, back to back meetings, both online and in person. Thank you for creating a friendly working environment and cheery vibe which really helped during stress periods. Thank you for giving the tips on SDS and immunoblotting and introducing me to fluorescence microscopy. After that my co-supervisor **Andrea Morovicz** for her assistance in PyMOL and also during experiments. Your experimental tips made life easier. A special thanks to **Felicity Ashcroft** from NTNU for her utmost help in Cell Profiler analysis and helping in designing the pipeline.

Thank you to all the NucReg members for each and every small help. All the nice people especially **Diana, Sandra** and **Linda.** I am sorry if I missed anyone. Thank you for the discussions, help with the fluorescence microscope and experimentation. Also I had a good time with other master fellows; **Malene**, **Marie, Mette**. The lunch breaks with fun discussions helped a lot!

I would also thank my family, particularly my father who allowed me to take my own path and invested his time and life savings to help me come to a country like Norway and follow my passion and dreams. I am certainly indebted to you for life. My mother who has always been my support and showered her love and countless prayers. My siblings who I look forward to as inspiration for moving forward in life and achieving my goals.

I want to particularly also mention my Aunt and her children who became the second family in Norway. My aunt who became the second mother to me and specially **Iyaz bhai** who became a brother to me and helped me a lot for completing the long journey. Thank you so much for your love and support. A special thanks to you guys.

Some particular friends I want to mention because without them the two years would have been difficult. **Rustum** and **Malin**, thank you so much for the teas, making food and doing the house chores on my part during the writing time! Your love and moral support helped me pass through the difficult time. I also thank all my other friends from Norway and home country for their support and motivation. You know who you are!

Contents

Key Abbreviations

PIP	Polyphoshphoinositide phosphates
PtdIn	Phosphatidylinositol
PPIn	Polyphosphoinositide
PA2G4	Proliferation associated 2 G4
EBP1	ErbB3 binding protein 1
FL	Full length
DAPI	4′,6-diamidino-2-phenylindole
EU	Ethyl- Uridine
rRNA	ribosomal RNA
rDNA	ribosomal DNA
FC	Fibrillar center
DFC	Dense fibrillar component
GC	Granular component
PI3K	PhosphoInositide-3 Kinase
mTOR	mammalian target of rapamycin
PIP4K	Phosphatidyl- 5 phosphate 4 kinase
PIP5K	Phosphatidyl- 4 phosphate 5 kinase
PLC	Phospho Lipase C
DAG	Diacylglycerol
PBR	Polybasic regions
UBF	Upstream binding factor
PTEN	Phosphatase and Tensin homolog
RNP	Ribonucleoprotein

dsRBD	double stranded RNA binding domain
FMDV IRES	Foot and mouth Disease Virus , Internal ribosome entry site
EMCV	encephalomyocarditis virus
INPP5D	Inositol- Polyphosphate-5 phosphatase D
INPPL1	Inositol- Polyphosphate phosphatase Like 1
HDM2	Human double minute 2 homolog
CDK	Cyclin dependent kinase
HSP70	Heat shock protein 70

Abstract

Sub-cellular localization is key to the specific function of proteins. Proteins can be recruited to different cell compartments via their interaction with the signaling lipids, polyphosphoinositides (PPIn). While their actions have been comprehensively documented in cytoplasmic membranes, these lipids are also present in membrane-less compartments within the nucleus. To understand the function of PPIn in the nucleus, we thought to identify nuclear PPIn binding proteins using quantitative mass spectrometry combined with PPIn affinity pull down. Using this approach, we identified ErbB3-binding protein 1 (EBP1), known to contribute to many cellular functions through interactions with RNA, DNA as well as other proteins. Using biochemical and biophysical approaches, we have demonstrated a direct interaction between EBP1 and PPIns via two lysine rich motifs located in the N- and C-termini. The C-terminal motif was shown to be required for the localization of EBP1 in nucleoli. A frameshift tumor mutant which introduced additional basic residues in the C-terminal motif led to an increase in PPIn binding and nucleolar localization of EBP1. Here we showed that the nucleolar presence of EBP1 correlated with the presence of rRNA for the WT and the frameshift tumor mutant but not the C-term PPIn-binding mutant. This suggests a molecular link between EBP1's localization and its subsequent effect on nucleolar processes thereby playing a role in cells transformation. We also performed CRISPR/CAS genome editing of exon 2 on *PA2G4* gene in HEK293T cells however it didn't yield any fruitful outcomes. The clones analyzed by sequencing were wild type with no expected change, though few clones showed reduction at protein level with one clone suggesting an in-frame deletion

Introduction

Polyphosphoinositides

Polyphosphoinositides (PPIn) are low in abundance but essential phospholipids in eukaryotes. They are present as minority acidic phospholipids in the eukaryotic cell membranes (Falkenburger et al, 2010). Polyphosphoinositides are derivatives of phosphatidylinositol (PtdIns) (Michell et al, 2006) which is a glycerol-based phospholipid composed of two hydrophobic fatty acids (mostly stearic and arachidonic acids) and a phosphodiester linked to a *myo*-inositol ring (Figure 1A). When the inositol head group is reversibly mono or multi phosphorylated on 3, 4, or 5 positions, it results in seven different combinations of PtdIns-phosphates with distinct biological functions, termed as PPIn (Figure 1B). The metabolism of different PPIn regulated by different kinases and phosphatases as shown in Figure 1B. Since their discovery by Hokin and Hokin (Hokin & Hokin, 1953) in the 1950s, these lipids have established to become important signaling mediators driving several cellular functions. They exert their function either indirectly as precursors of second messengers such as inositol- 1,4, 5-triphosphate (Ins(1,4,5)P_3) and diacylglycerol (DAG) or directly by association with the effector proteins stimulating different signaling cascades (Payrastre, 2001; Toker, 2002; Blind et al, 2014).

Cellular localization and function

Although PPIn constitute only 1% of total phospholipids, they are one of the most universal signaling entities in eukaryotic cells and involved in almost all cellular aspects. PtdIns is primarily synthesized in the endoplasmic reticulum (ER) and delivered to the plasma membrane (PM) and other membrane compartments (*e.g.* Golgi, lysosomes and the nucleus) by vesicular transport or via cytosolic PtdIns transfer proteins (Di Paolo & De Camilli, 2006).

PPIn controlled signaling pathway is mediated in two distinct ways, directly via PPIn or indirectly via other second messengers such as DAG and Ins(1,4,5)P_3. PtdIns(4,5)-bisphosphate is the precursor of these second messengers which is hydrolyzed at PM by PLC in response to receptor activation, thus contributing to the regulation of intracellular Ca^{2+} homeostasis via its production (William et al, 2013). Ins(1,4,5)P_3 can be further phosphorylated to generate higher phosphorylated inositol phosphates (Tsui & York, 2010) and play role in several aspects, but they will not be detailed more here.

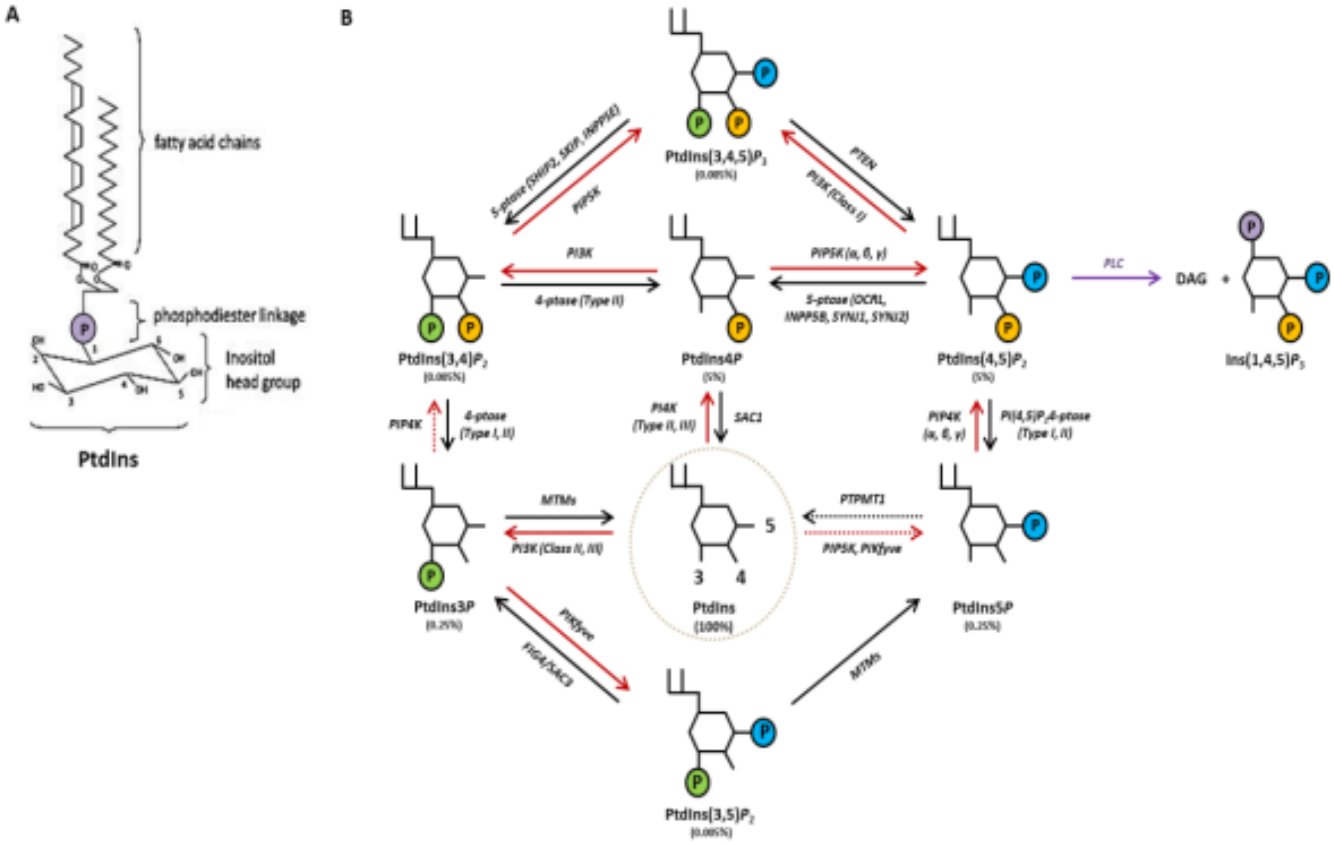

Figure 1. PtdIns and its phosphorylated derivatives polyphoshoinositides (PPIn). **A)** Structural representation of phosphatidylinositol (PtdIns) with two fatty acid tails and an inositol head group linked to the glycerol backbone. **B**) Pathway of polyphosphoinositide (PPIn)-generation in mammalian cells. PtdIns in the gray dashed circle shows the labeled positions of the phosphorylation sites. All seven PPIn-products (see text above) are presented with their PPIn-metabolizing enzymes (in italic). Red arrows designate phosphorylation by given kinases, and black arrows are for dephosphorylation by phosphatases. Dashed arrows indicate PPIn-synthesis *in vitro*. DAG and Ins(1,4,5)P_3 are products of PtdIns (4,5)P_2 hydrolysis by Phospholipase C (in purple). Percentages under PPIns indicate the relative abundances of these lipids relative to PtdIns in resting cells. Figure taken from (Fiume et al., 2015) and modified using (Maffucci, 2012) and (Leslie & Downes, 200

Membrane anchored PPIn, on the other hand, play a fundamental part on the membrane–cytosol interface by recruiting proteins that recognize the head groups via their PPIn-binding domain or motifs to PM and often transduce downstream signals. These lipids mediate acute responses, but also act as constitutive signals that define the identity of organelles. Besides acting as a signal transducer at the cell surface, PPIn play important roles in the regulation of membrane traffic, cytoskeleton remodeling, endocytic and exocytic processes, cell survival and proliferation and nuclear events (Balla, 2013; Shah et al., 2013).

Nuclear polyphosphoinositide signaling

Phospholipids have not only been shown to play structural roles in membranes but also initiate signaling pathways. However, they have also been found to be vital constituents of nuclei, not only just in nuclear envelope but also within nuclei, the nuclear matrix and also associated with the chromatin (Albi et al, 2003 & Hunt, 2006). This pool of endonuclear PPIn make up 6-10% of the total PtdIn composition (Postle et al, 2007) and ~~a~~re found in nucleus with their enzymes responsible for the interconversions (Barlow et al, 2010; Flume et al, 2012; Schramp et al, 2012; Shah et al, 2013; Jacobsen et al, 2019). Until now, several studies have provided evidence about the presence of PPIn and metabolizing enzymes: lipases, kinases and phosphatases in several sub nuclear compartments. This generates a PPIn pool involved in distinct functions such as chromatin remodeling, DNA repair, transcriptional processing and regulating gene expression (Castano et al, 2019; Fiume et al, 2019; Jacobsen et al, 2019). Smith and Wells in 1983 showed not only the presence of PtdIn in the nucleus but also the lipid kinases which generate phosphatidylinositol 4,5-bisphosphate PtdIns(4,5)P_2 to be also present there. While the studies by Smith and Wells confirmed the presence of PPIn and their metabolizing enzymes in purified nuclear envelopes, Van and colleagues further showed their presence within the nucleus as well (Van et al, 1997). Washing highly purified rat liver nuclei with Triton X 100 0.04% removed the membrane but the mass level of PPIn only decreased by 40%. Moreover under similar conditions nuclei labelling with ^{32}P-ATP showed significant presence of PtdOH, PtdIns4*P* and PtdIn(4,5)P_2. Figure 2A shows the PPIn species found in different compartments of the nucleus and 2B highlights the enzymes which are involved in their metabolism. Further studies showed that PtdIns 4-kinase (PI4K) is localized to the outer matrix of the nucleus and PtdIn4*P*-5-Kinase PIP5K to the inner matrix (Payrastre et al, 1992). As stated earlier these PPIn are reported to be involved in different nuclear functions, and PtdIn (4,5)P_2 has been shown to directly be related to chromatin remodeling (Zhao et al, 1998) and PtdIn(3,4,5)-trisphosphate PtdIn(3,4,5)P_3 is also involved in mRNA export by interacting with Aly, a RNA-binding adaptor protein required for transcription export complex in nuclear speckles (Masuda et al., 2005).

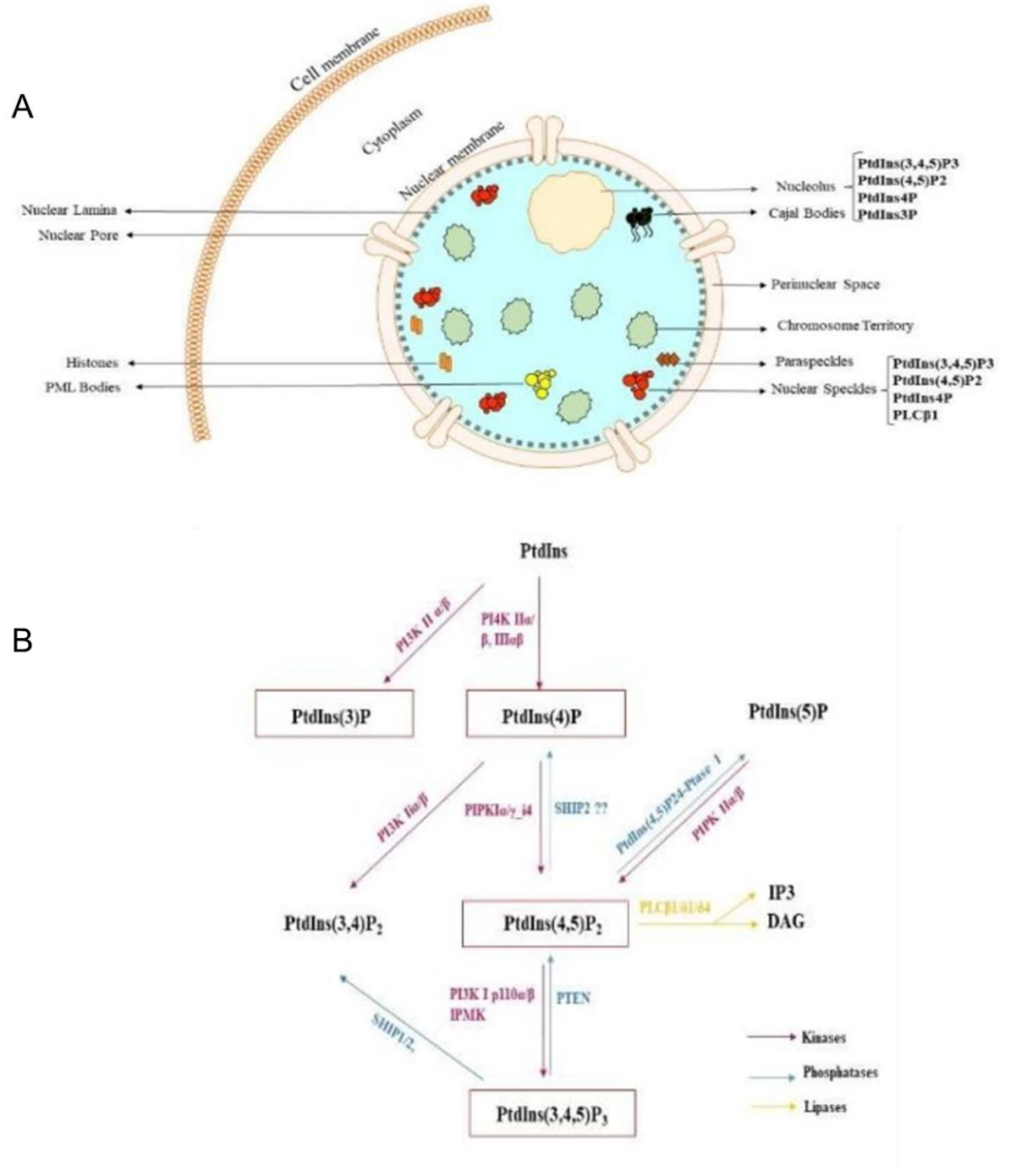

Figure 2. **Nuclear sub compartments and nuclear polyphosphoinositide signaling**. **(A)** Membrane less sub compartments where different PPIn: PtdIn(3,4,5)P_3, PtdIns(4,5)P_2, PtdIns4*P* are found. **(B)** Nuclear PPIn metabolism along with respective enzymes involved: PI4K, PIP5K, PLCβ1 and other lipid kinases shown. Boxed PPIn represent nuclear/nucleolar PPIn while un-boxed are non-nuclear. Figure adapted from Xian et al, 2020. PtdIn(3,4,5)P_3: Phosphatidylinositol 3,4,5 triphosphate. PI4K: PtdIns 4-kinase, PIP5K: PtdIns 4P-5-Kinase, PLCβ1: Phospholipase C beta 1.

Nucleolus

Structure

When the nucleus is stained with fluorescent DNA dyes such as 4′,6-diamidino-2-phenylindole (DAPI), the nucleolus is seen as a dark dense structure, DAPI negative, amongst the more brightly stained chromatin which is an indication of the presence of active rDNA throughout the structure (Figure 3A). As evident by electron microscopy, the nucleolus in many animal cells have been identified as a structure with tripartite architecture. This consists of lightly stained regions fibrillar centers (FCs) surrounded by a dense fibrillar component (DFC): the remaining which appears to be granular in nature is called Granular component (Shaw & Jordan, 1995), Figure 3B.

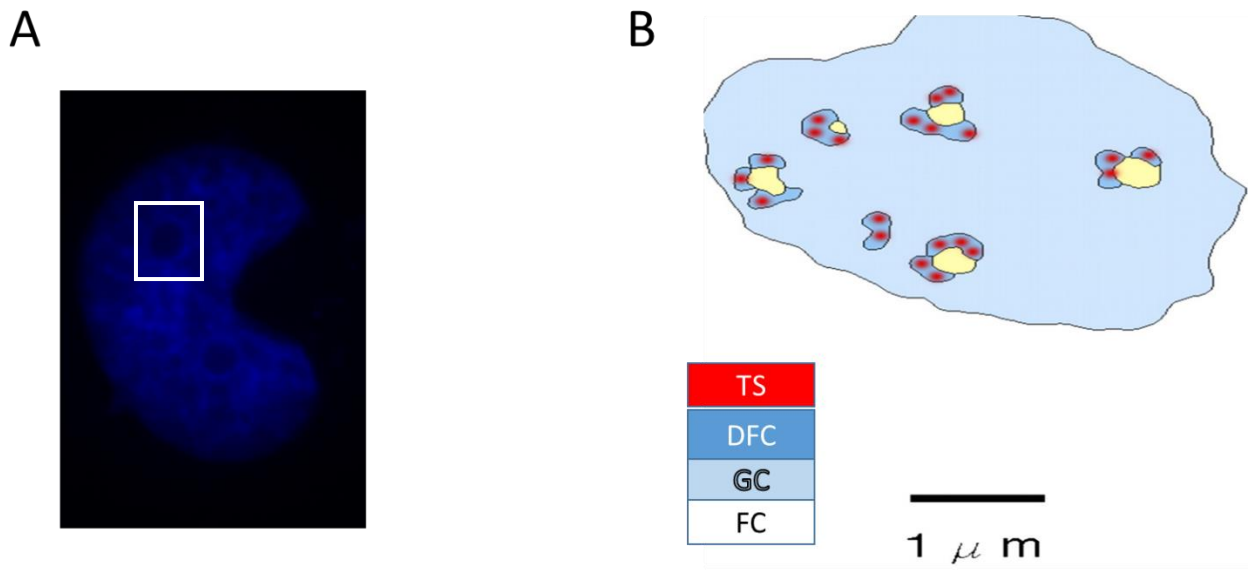

Figure 3. Nucleolar structure and different regions. A) Darkly stained nucleoli (white box) against light staining of chromatin (DAPI, blue). **B)** Shows the cartoon diagram of the nucleolus highlighting DFC, GC and FC regions. TS represents the transcription site. **A** is from this work and **B** adapted from Peter and John, 2012. DFC: Dense fibrillar component, GC: Granular component and FC: Fibrillar center.

Functions

Ribosome biogenesis (Figure 4) is the key function of nucleolus. It is an orchestrated process occurring in the nucleolus consisting of the transcription of rRNAs, and processing of polycistronic 47S pre-rRNA into smaller transcripts (18S, 5.8S and 28S rRNAs). The rRNA synthesis is catalyzed by RNA Polymerase 1. Moreover the assembly of ribosome unit (association of ribonucleoprotein (RP) and rRNAs as well as export of assembled ribosomes to cytoplasm also happen (Bosivert et al, 2007; Henras et al, 2008, Lindstrom et al, 2009; Moss et al, 2007; Rodnina & Wintermeyer, 2009; Thomson et al, 2013; Woolfbord & Baserga, 2013). Ribosome biogenesis is a well-regulated process important for cell cycle and growth however under stress conditions, the cells respond by downregulating it because of its energy expense aspect (Grummt et al, 2013). Although ribosome biogenesis is the key function of nucleolus, it is now established that the nucleolus also serves many additional roles which have no apparent link with ribosome synthesis. Signal recognition particle (SRP) assembly (Politz et al, 2000), U2 and U6 spliceosome small RNA modification (Ganot et al, 1999; Yu et al, 2001) are for instance non-ribosomal roles that have been clearly reported. Other visiting molecules present in the nucleolus which are involved in cellular functions like cell growth control, telomere maintenance, protein degradation and some microRNAs (Politz et al, 2009; Reyes- Gutierrez et al, 2014) have been studied as well. More than 700 nucleolar proteins have been evidently shown to be un-related to ribosome biogenesis after a proteomic analysis on purified nucleoli from HeLa cells by two groups (Anderson et al, 2002 & 2005; Scherl et al, 2002). Pederson and Tsai, 2009 later showed that a few of them were closely connected to cell cycle progression and cell division.

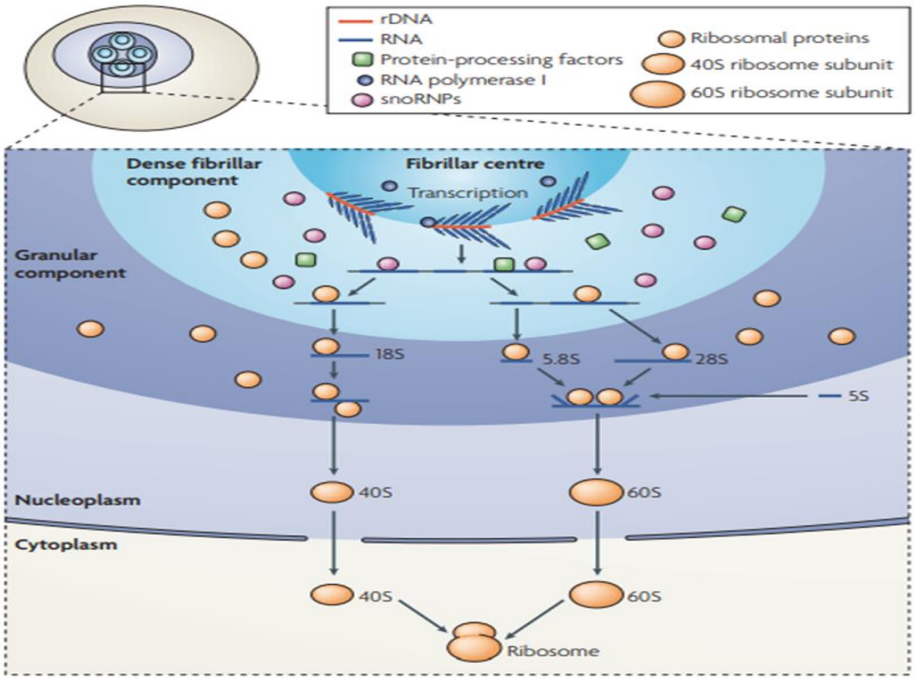

Figure 4. Model of ribosome biogenesis. Transcription of the ribosomal DNA (rDNA) occurs in the dense fibrillar component (DFC) region or at the boundary of fibrillar center (FC) and DFC. These transcripts are spliced into small rRNAs by small nucleolar ribonucleoprotiens (snoRNPs) and the final maturation and assembly occurs in Granular component (GC) where 5.8S rRNA, 28S rRNA combine with 5S transcript to make the 60S subunit and 18S assembles alone into 40S. Figure adapted from Boisvert et al, 2007

PPIn signaling

Until now, PPIn have been reported to be a part of cytoplasm and nuclear compartments, however recent studies have also now elucidated the presence of these unique molecules in the nucleolus, regulating rRNA synthesis in normal and transformed cells. Table 1 shows the summary of some PPIn and involved enzymes. Previously our group also identified p110β and PtdIns (3, 4, 5)P_3 in nucleoli of AU565 breast cancer cell line (Karlsson et al, 2016).

Table 1. Summary of nucleolar PPIn and enzymes reported. Table updated from Jacobsen et al, 2019 and Victoria Arnesen's master thesis.

PPIn/PPIn enzymes	Identified function in the nucleolus	Reference
PtdIn(4,5)P_2	Promotes RNA Pol 1 transcription but not as a source for DAG and IP3 Structural role	(Yildirim et al, 2013) (Sobol et al, 2013
PtdIns(3,4,5)P_3	Binds to nucleolar protein nucleophosmin (alias B23) Binds EBP1	(Ahn et al, 2005) (Karlsson et al, 2016)
PI4K230/IIIα	Possibly in complex with DNA and RNA	(Kakuk et al, 2006, 2008)
PIP5KIα	Member of rDNA silencing complex	(Chakrabati et al, 2015)
p110β	Unknown	(Karlsson et al, 2016)
PTEN	Contributes to phenotypic changes of nucleolus	(Li et al, 2014)
SHIP1	Localizes in the nucleolar cavity upon proteasome inhibition, unknown function	(Ehm et al, 2015)
PtdIn4*P*	Unknown	(Kalasova et al, 2016)
PtdIn3*P*	Unknown	(Gillooly et al, 2000)

Cancer predisposition linked with ribosome biogenesis

Nucleolar proteins have been linked with predisposition to cancer which is further associated with disrupted ribosome biogenesis and rRNA synthesis. Dyskeratosis congenita syndrome (Heiss et al, 1999) in which the nucleolar protein, Dyskerin's low expression has been linked to abnormally low levels of rRNA's pseudouridylation in some specific tumors (Montanaro et al, 2006). Similarly nucleophosmin/B23, has been identified to have both oncogenic and suppressor effects. Mutation in *B23* is implicated in hematological cancers (Grisendi et al, 2005; Naoe et al, 2006). There are also other proto-oncogenes and tumor suppressor proteins which affect production of the ribosomes, highlighted in the sections below.

Oncogenes up-regulate ribosome biogenesis

Mitogens and growth factors stimulate the PI3K pathway which activates MYC (Zhu et al, 2008), which is the main modulator of ribosome biogenesis. It enhances the process by increasing RNA Pol 1 transcription by recruiting Selective factor 1 (SL1) to the promoter, stimulates ribosomal protein synthesis by Pol 1 transcriptional activity and promotes RNA Pol III activity by transcription factor IIIB, TFIIIB mediated pathway (White et al, 2005; Gomez et al, 2006; Van et al, 2010). Oncogenic transformations due to highly increased production of ribosome biosynthesis, therefore, result in changes in nucleolar function and morphology, like increased size and number which has been observed in cancer tissues (Donizy et al, 2017). This has been highlighted in this thesis.

Tumor Suppressor genes down-regulate ribosome biogenesis

Once the cell enters mitosis, the ribosome biogenesis is regulated by the factors controlling the cell cycle progression, including the transcription factor retinoblastoma (RB). Active un-phosphorylated pRB inhibits rRNA transcription by binding to UBF (Cavanaugh et al, 1995; Voit et al, 1997; Hannan et al, 2000; Ciarmatori et al, 2001) and Pol III transcription by binding to TFIIIB (White et al, 1996; Felton et al, 2003). Hence the progressive phosphorylation of pRB during a cell cycle progression also increases rRNA synthesis from G1 to G2 phase. Another negative regulator of ribosome biogenesis is p53, which works by inhibiting the factor SL1 which helps recruit RNA Pol1 to rRNA promoter (Zhai et al, 2000) and Pol III transcription by inhibiting TFIIIB (Felton et al, 2003). This negative regulation is also supported by p14ARF which disrupts the recruitment of UBF factor on the transcription process and further increases p53 activity. It also inhibits nucleophosmin, a nucleolar protein involved in rRNA processing (Ayrault et al, 2006).

Ribosome biogenesis is up-regulated in cancers

Together, the oncogenic and suppressor genes controlling cell proliferation also regulate ribosome biogenesis and neoplastic transformation is characterized by either uncontrolled activity of oncogenes or inactivation of tumor suppressor genes. Both cases result in the hyper activation of MAPK/ERK pathway, increasing rRNA synthesis (Hanhan & Weinberg, 2000) *TP53* mutations leading to p53 inactivation have been characterized in 50% of tumors in humans (Vogelstein et al, 2000; Vousden et al, 2007) and mutated p53 no longer exerts its negative control over rRNA transcription. Similarly ARF14 inhibition results in enhancement of ribosome biogenesis both through p53 stabilization and directly (Sher, 2001; Low & Sher, 2003). Also tumor suppressor *PTEN* is very frequently mutated in cancers (Yin & Shen, 2008) losing its repression on Pol 1 transcriptional activity.

Nucleolar PPIn signaling landscape in Cancer

The PI3K pathway is hyperactivated in cancers mostly due to alteration in several gene members of the pathway (Engelmann, 2009; Fruman & Rommel, 2014; Thorp et al, 2015). Interestingly, the pathway has also been linked with nucleolar activity. Although, the localization has not been defined, the class I PI3K catalytic p110β and regulatory p85 subunits were found to interact with insulin receptor substrate (IRS-1) and UBF, upon stimulation of insulin like growth factor (IGF), enhancing rRNA transcription (Drakas et al, 2004). Nuclear upregulation of PI3K pathway involving p110β has also been linked with increase rDNA transcription in endometrial cancer cells (Fatemeh et al, 2019*****). Moreover PI3K-Akt/mTOR pathway also interacts with c-MYC, which is dysregulated in 15-20% of human malignancies either by enhanced translocation or expression. (Wendel et al, 2004; Udin et al, 2006). In addition part of the role in malignancy development is also attributed to its ability to promote ribosome biogenesis (Rugerro & Pandolfi, 2003; Poortinga et al, 2004; Grandori et al, 2005; Barna et al, 2008; Dai et al, 2008). The level of PtdIn(3,4,5)P_3 is also modulated by PTEN, another nucleolar protein and somatic mutations targeting *PTEN* (Ali et al, 1999) causing increased signaling in the pathway have been identified (Catalogue of Somatic mutations in Cancer, see for more information). Loss of function of this tumor suppressor is implicated in several sporadic cancers; endometrial, breast, ovarian, gliomas, melanomas, lung, renal and prostrate (Maehama, 2007). Other target proteins which might be involved in this pathway are 5-Phospahatases 1 such as SH-domain- including 5-Phosphatase 1 (SHIP1) encoded by *INPP5D* and SHIP2 by *INPPL1*. There are several lines of studies which have shown the oncogenic implications of SHIP1. *Inpp5d*$^{-/-}$ mouse developed a myeloproliferative disease, similar to Chronic myelogenous leukemia (CML) (Helgason et al, 1998). Similarly activation of SHIP1 by some inhibitory molecules has shown to reduce the levels of PtdIn(3,4,5)P_3 in

haematapoetic and myeloma cells (Ong et al, 2007; Kennah et al, 2009). Moreover PI4KIIIα among the four types of PI4K which is the kinase enzyme generating PtdIn4*P* and also linked with Akt/PI3K pathways have been identified in various cancers (Waugh, 2012). Although PtdIn4*P* nucleolar function has not yet been identified (see table 1), its metabolizing enzyme PI4KIIIα is associated with more invasive phenotypes in pancreatic cancers (Ishikawa et al, 2003) as well as linked with poor prognosis in hepatocellular carcinoma (Ilboudo et al, 2014). Recently, a studied reported that the upregulation of PI4KIIIα enhanced the invasion and metastasis by prostate cancer cells (Sbrissa et al, 2015). A recent study has shown the relationship between upregulation of PIP5K1α (Table 1) circular RNA in non-small cell lung cancer (Zhang et al, 2018) and another report has shown the relationship between upregulation of circular PIP5K1α RNA and colon cancer development (Zhang et al, 2019). PtdIn(4,5)P_2, the product of PIP5KI pathway has also been associated with invadopodia development in human breast cancer cells and was found to regulate several components localized at invadopodia such as N- WASP(Neural Wiskott Aldrich syndrome protein), coflin and dynamin (Takenava & Itoh 2001; Ling et al, 2006). Nucleolar functions of most of the PPIn and their metabolizing enzymes still need to be identified (refer to table 1), however their roles in tumorigenesis have been reported extensively, evident by the studies mentioned above.

ErbB3 binding protein 1

Background and Structural insights.

ErbB3 binding protein 1 (EBP1), also known as Proliferation-associated 2G4 protein *(PA2G4*) was originally identified as an ErbB3 binding protein (Yoo et al., 2000a). *PA2G4* gene is located on chromosome 10D3 (chromosome12q13.2), and composed of ten exons. ErbB3 belongs to the epidermal growth factor receptor (EGFR) family of receptor tyrosine kinases, and is activated by the ligand heregulin (HRG). Due to its lack of tyrosine kinase activity, ErbB3 heterodimerizes with other ErbB receptors, preferentially ErbB2 to transduce its downstream signaling. ErbB3 is frequently overexpressed in breast cancer and co-expression of ErbB2/3 is a poor prognostic indicator (Hamburger, 2008). By using the yeast two-hybrid system, Yoo et al, 2000 have identified EBP1 interacting with the first 15 amino acids of juxtamembrane domain of unphosphorylated ErbB3 receptor. The association of EBP1 with ErbB3 appears to be regulated by PKC activity, although the details are not clear (Lessor and Hamburger, 2001). Treatment of the breast cancer AU565 cells with HRG but not EGF, however, resulted in dissociation of EBP1 from ErbB3, and subsequently, translocation from the cytoplasm into the nucleus (Yoo et al., 2000a). EBP1 is mostly involved in cell growth and differentiation by acting as a transcriptional and translational regulator in addition to participating in ribosome assembly (Squatrito et al., 2004).

EBP1 is highly conserved in eukaryotes and is ubiquitously expressed in a wide variety of tissues and organisms (Yamada et al., 1994, Xia et al., 2001b, Horvath et al., 2006), including hematopoietic cells, which do not express the ErbB receptors (Pinkas-Kramarski et al 1997; Xia et al., 2001b). Previously, EBP1 was discovered as a murine cDNA encoding a 38 kDa protein named p38-2G4 (Radomski & Jost, 1995), and later, the human homologue was identified as *PA2G4* gene product (Lamartine et al., 1997).

Its crystal structure was first reported in 2007 by two separate groups which provided the same structures for the murine and human proteins (Kowalinski et al., 2007; Monie et al., 2007). The structure revealed a pita-bread fold forming a hydrophobic cavity in the center, and an insert domain of unknown function (Figure 5). This pita-bread fold is conserved in methionine aminopeptidase (MAP), and human MAP2 was identified as the closest homologue of EBP1. Although EBP1 shares the structural similarity of the binding pocket with MAP2, it showed that EBP1 lacks the enzymatic activity. Compared to MAP2, EBP1 has a C-terminal elongation of 57 residues, part of which is ordered (aa 340-362), including a short α-helix (α10) (Kowalinski et al., 2007). The last part (aa 364-373) is unstructured, and was not unresolved in these 3D-structure. But it is now included in the cryo_EM structure.

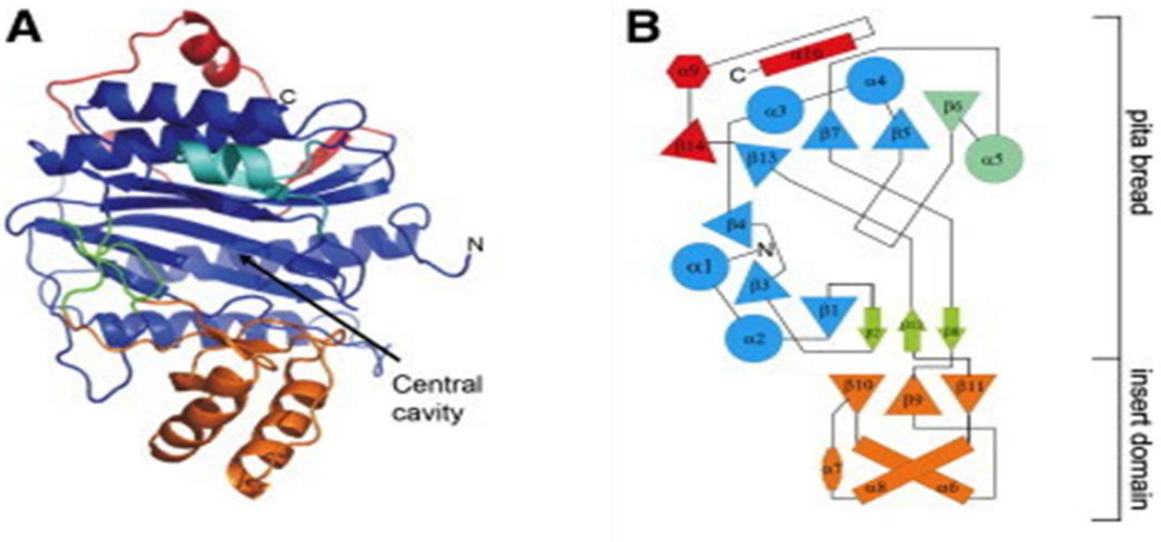

Figure 5. Structure of EBP1. A) EBP1 is shown in a ribbon representation with the beta barrel forming the hydrophobic cavity in the center (indicated by an arrow). The pita-bread domain is colored in blue, the insert domain in orange, the β-sheet connecting these domains in green, the EBP1 specific helix at the entrance of the cavity in turquoise and the C-terminal elongation in red. **B)** Topology diagram of EBP1. For clarity, the orientation is chosen 90° rotated compared to (A). β-Strands are represented by arrows and triangles, α-helices by cylinders and circles, and 3_{10} helices by hexagons. Figure from Kowalinski et al, 2007.

Nucleolar localization, RNA-binding properties of EBP1 and its growth regulation.

After EBP1 was identified in the nucleolus, its RNA-binding property was first discovered in 2004 by Squatrito *et al.,* using mass spectrometry. Analysis of the data showed that EBP1 was part of the pre-ribosomal ribonucleoprotein (RNP) complexes. Moreover, EBP1 associated with some rRNA precursors and the mature rRNAs, such as 28S, 18S and 5.8S through its σ^{70}-like motif, a eukaryotic RNA-binding domain. In addition, EBP1 interacted also with 5S and other RNA species, thus suggesting its role in ribosome biosynthesis, particularly in maturation of the 60S subunit. This study showed also that EBP1 mutant lacking this motif did not have any growth-suppressing activity, in contrast to WT (Squatrito et al., 2004). By the same group, a dsRNA-binding domain (dsRBD) was also identified in EBP1 (aa 91-156), and it showed that this domain can drive EBP1 to the nucleolus as well as σ^{70}-like motif. Both motifs were shown to be required for its nucleolar localization and the formation with the RNP complexes. Thus, deletion of either of them led to accumulation in the cytoplasm and failure of RNP complexes constitution (Squatrito et al., 2006).

Squatrito et al, 2004 also demonstrated that sequences in both the C and N termini were responsible for the nucleolar localization. Mutants with K20 and K22 and R364 and K365 substituted to Alanines failed to localize properly in the nucleolar compartment. The K20A-K22A mutant, but not the R364A-K365A lost the ability to suppress cell growth compared to Wild type protein (Squatrito et al, 2004). Later on our group also identified that amino acids K369-K372 were also involved in the nucleoar signal at the C-terminus (Karlsson et al, 2016) which has also been validated in this thesis. These experiments provided the evidence of the co-relation between EBP1's localization to nucleolus and the binding capacity to different RNA forming RNP complexes leading to their maturation.

EBP1 as a translational regulator.

In the cytoplasm, EBP1 was shown to regulate translation, primarily by binding to mature RNA 40S. Previously, Pilipenko et al, 2000 demonstrated EBP1's role in initiating the 48S complex formation on the Foot and mouth disease Virus Internal ribosomal entry site (FMDV IRES) by biophysical toe-printing analysis. This was later on confirmed in a study conducted by Monie et al, 2007 in which by RNAi mediated reduction of EBP1, 55% of the IRES activity was shown to reduce whereas Encephalomyocarditis virus (EMCV) IRES and cap dependent translation was unaffected. Both studies reveal the potential role of EBP1 at translational level. In Castration resistant prostate cancer cells (CRPC), EBP1 was found to inhibit Androgen receptor (AR) translation (Zhou et al, 2010), consistent with the previous findings that it associates with 40S, 60S and 80S ribosomes and is a part of ribonucleoprotein complex in HeLa cells (Squatrito

et al, 2004; Squatrito et al, 2006. Most recently, a cryo-EM structural study revealed the interaction of EBP1 with mature 80S non-translating ribosome tunnel exit site by recruiting rRNA expansion segment ES27L (Figure 6) to it via specific interactions with rRNA consensus sequences (Wild et al, 2020).

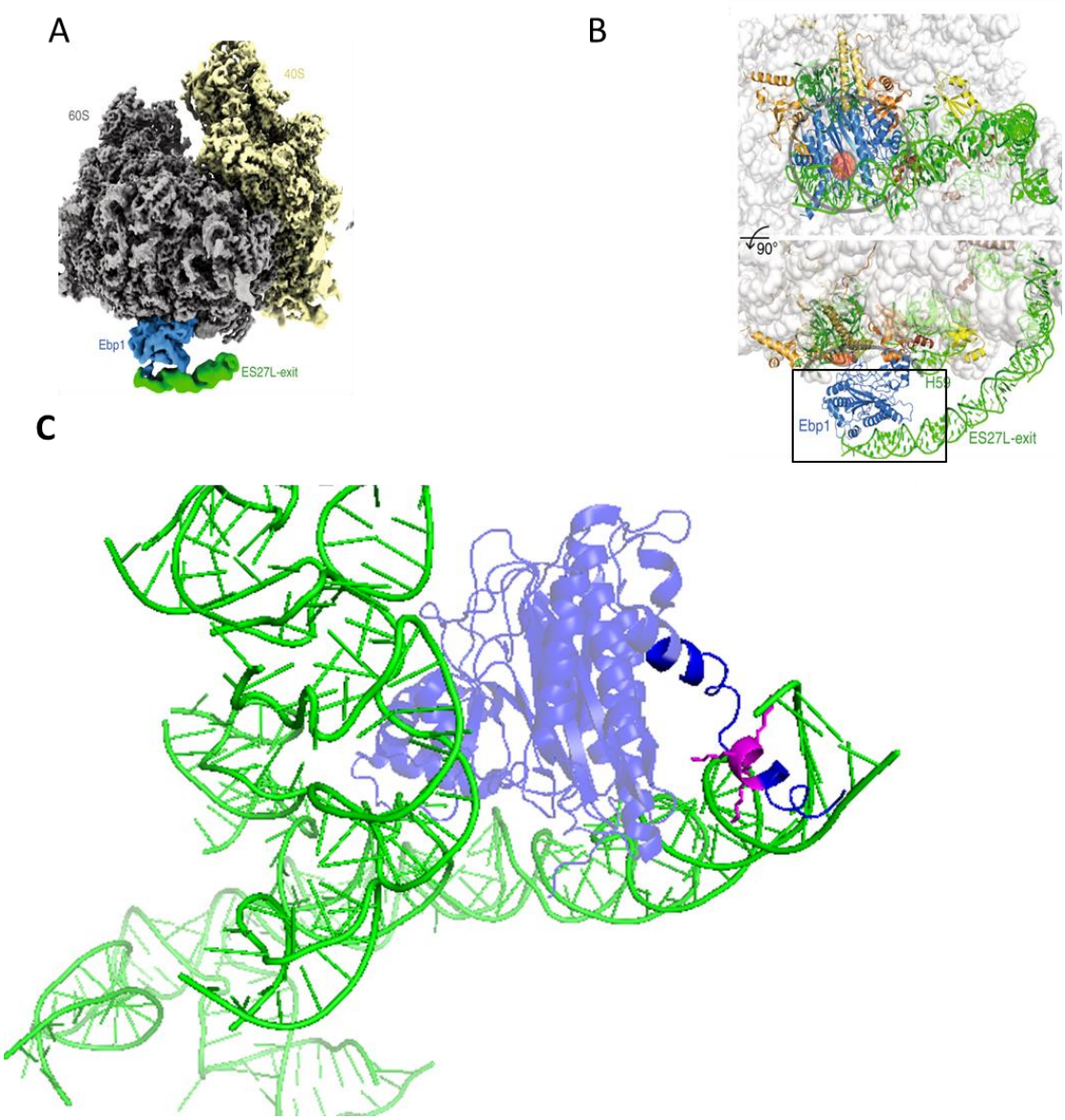

Figure 6. Cryo EM EBP1-ribosome complex composite. **A.** larger subunit (gray), smaller subunit (yellow), EBP1 (blue) and ES27L (green) are depicted. **B** shows ribosome-EBP1 complex, rRNA (green), ribosomal proteins (yellow orange and brown) and EBP1 (blue). **C** cryo-EM structure of EBP1-ribosome complex, EBP1 (blue) modified showing rRNA expansion segments (green) and the C-terminus binding motif ^{369}**KKKK**^{372} (purple). Figure adapted from Wild et al, 2020 and modified in PyMol. PDB ID: 6SXO. Modified part shown in black box

Role of EBP1 in tumorigenesis.

EBP1 has been reported to be closely related in the development of several cancers. Altered expression of EBP1 has been observed, and associated with higher histological grade as well as poor prognosis in some cancers. However, EBP1 can function as an oncogene or tumor suppressor, depending on the tissue and cancer type.

EBP1 as a tumor suppressor

Upon HRG stimulation, EBP1 was shown to be dissociated from ErbB3, followed by its translocation into the nucleus, which resulted in increased cell arrest in G2/M (Lessor et al., 2000). Transfection of the *PA2G4* cDNA into AU565 cells localized in the nucleus, and appeared to mimic some of the growth suppressing and differentiating effects of HRG, in absence of HRG. In addition to reduced cell growth and increased cell cycle arrest in G2/M, cellular differentiation was also induced, with appearance of increased lipid droplets, and production of milk protein casein. Overexpression of the *PA2G4* gene in androgen-dependent LNCaP prostate cancer cells also resulted in inhibition of cell growth (Zhang et al., 2002). This *in cellulo* effect of EBP1 was also observed in severe combined immunodeficiency (SCID) mice injected with LNCaP cells overexpressing EBP1 (Zhang et al., 2005b). The tumor growth in those prostate cancer xenografts developed slower in EBP1 transfected cells. The inhibitory properties of ectopic EBP1 was shown to be beneficial in salivary adenoid carcinoma as well (Yu et al., 2007). In clinical studies of human bladder cancer and hepatocellular carcinoma, EBP1 expression was low, and the reduction of EBP1 was associated with enhanced cell growth and tumor progression (He et al., 2013, Hu et al., 2014).

Further studies have shown that EBP1 decreases cell proliferation in prostate and breast cancer cells by directly binding to the androgen receptor (AR) and tumor suppressor retinoblastoma (Rb) and inhibiting transcription of AR and E2F1 regulated genes, such as prostate specific antigen (PSA) and genes involved in cell cycle progression such as Cyclin E, cyclin D1 and c-myc (Xia et al., 2001a; Zhang et al., 2002,). Although interaction with Rb was required to bind E2F1 promotor, EBP1 can repress the E2F1 regulated genes in Rb negative cells, and the mechanism is thus unclear (Zhang et al., 2003). In both cases, addition of HRG enhanced EBP1 binding to E2F1 and AR, and the repression of their transcriptional activity (Zhang & Hamburger, 2004; Zhang & Hamburger, 2005). The same group has also shown that EBP1 recruits histone deacetylase 2 (HDAC2) and Sin3A (a corepressor of Sin3) to the AR and E2F promoters to repress the transcription of AR and E2F-mediated genes (Zhang et al., 2003, Zhang

et al., 2005a). Phosphorylation at S363 in EBP1 was required for its protein-protein interaction with HDAC and Sin3A, whereas the S363A mutant could still bind to E2F1 but without repressing transcription (Akinmade et al., 2007a). EBP1 acts also as a suppressor by negatively regulating Annexin A2, which is often upregulated in breast cancer cells and known to enhance the proliferation and invasion of breast cancer cells (Zhang et al., 2015).

EBP1 with oncogenic functions

On the other hand, there are emerging evidences where EBP1 promotes cell proliferation and cancer progression. Several studies on the expression of EBP1 in tumor tissues and its clinical pathological relevance show often an association of overexpressed EBP1 with tumorigenesis. Patients with breast cancer expressing high levels of EBP1 have poor clinical outcomes, suggesting it may promote aggressive behavior (Ou et al., 2006). EBP1 was overexpressed in colorectal cancers compared to normal areas adjacent to the cancer (Santegoets et al., 2007). Characterization of EBP1 expression in prostate cancer patients showed also high levels of EBP1 to correlate with the occurrence of prostate cancer (Gannon et al., 2008). EBP1 also promotes cell growth and invasion in human glioblastoma (GBM), and high levels of EBP1 was correlated with poor prognosis in GBM patients (Kim et al., 2010; Kim et al., 2012, Thus overexpression of EBP1 in these cancers associates with tumorigenesis.

It is reported that in NGF-treated PC12 cells, EBP1 acted in an anti-apoptotic manner, thus increasing cell survival (Ahn et al., 2006). EBP1 also promotes cell proliferation and invasion in human glioma cells through downregulation of the tumor suppressor, p53 (Kim et al., 2010). In unstressed cells, p53 is maintained at low levels by HDM2, also known as MDM2, an ubiquitin ligase that mediates its degradation (Li et al., 2003). EBP1 binds to HDM2, enhancing HDM2-p53 association and thereby, promoting p53 polyubiquitination and degradation (Kim et al., 2010). Another mechanism suggested by the same group is that EBP1 stabilizes Akt-mediated HDM2 phosphorylation, thus preventing HDM2 self-ubiquitination, and confining HDM2 in the nucleus to antagonize p53 (Kim et al., 2012). However, a recent study has shown that phosphorylation of serine 34 by CDK2 led to an accelerated tumor cell growth, thus suggesting that this phosphorylation is critical for tumorigenic function of EBP1 (Ko et al., 2014).

In addition to its role in promoting cell growth and inhibition of apoptosis, EBP1 regulates other proteins that are responsible for malignant transformation in cancer cells. Recently, a study showed that EBP1 upregulates podoplanin expression and promotes oral cancer progression. Podoplanin is normally expressed in lymphatic endothelial and fibroblastic reticular cells, but is highly expressed in various human cancers (Wicki & Christofori, 2007) and promotes tumorigenesis in oral squamous cell carcinoma (OSCC) (Yuan et al., 2006). An investigation

by Mei *et al.*, on the regulation of podoplanin expression has shown that EBP1 indirectly binds to the *podoplanin* promoter, thus resulting in a dramatic increase of podoplanin (Mei et al., 2014). OSCC cells express *podoplanin* mRNA despite the fact that no protein can be detected until the cells reach confluency, and when EBP1 is translocated into the nucleus and acts as transcriptional activator, hence contributing to oral tumorigenesis.

Isoforms and their antagonizing roles in cancer development.

PA2G4 encodes two alternatively spliced EBP1 isoforms p42 and p48 (p48 used in this study) which are transcribed into two mRNA transcripts, however interestingly speaking the gene *PA2G4* has three in frame ATG codons (Liu et al, 2006). Translation for p48 begins at the first ATG codon and the protein tends to migrate at an apparent molecular weight of 48 kDa on SDS polyacrylamide gels. p48 is 54 amino acids longer at the N terminus than the p42 isoform which is translated at the third ATG codon removing a 29 nucleotide exon and hence the elimination of second ATG codon. p42 migrates at the molecular weight of 42 kDa (Liu et al, 2006). In rat PC12 cells, they localize differently and regulate cell proliferation, survival and differentiation in opposite way. p42 localizes predominantly in the cytoplasm and suppresses cell growth and induces differentiation, while p48 localizes in both the cytoplasm and the nucleolus, and enhances cell growth in addition to inhibiting apoptosis (Liu et al., 2006). Figures 7 depicts the schematic models of p42 mediated oncogenic suppressor activity and p48 driven tumorigenesis respectively. The fact that p42 is missing the 54 amino acids may account for the unstable nature of the protein and the different roles of the isoforms (Monie et al, 2007).

A

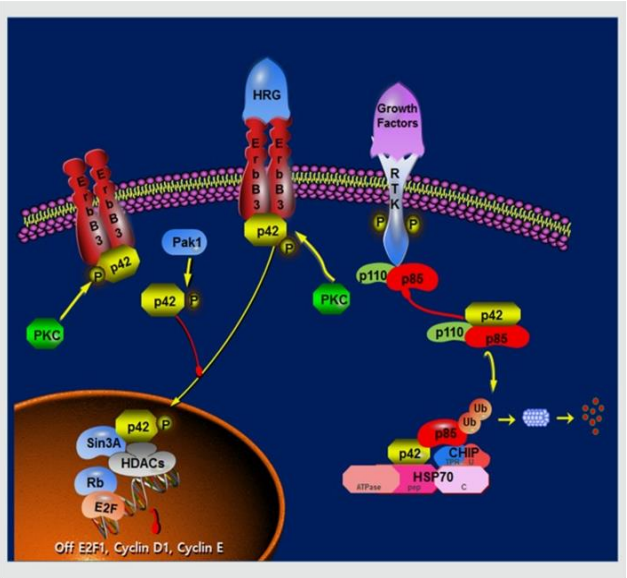

B

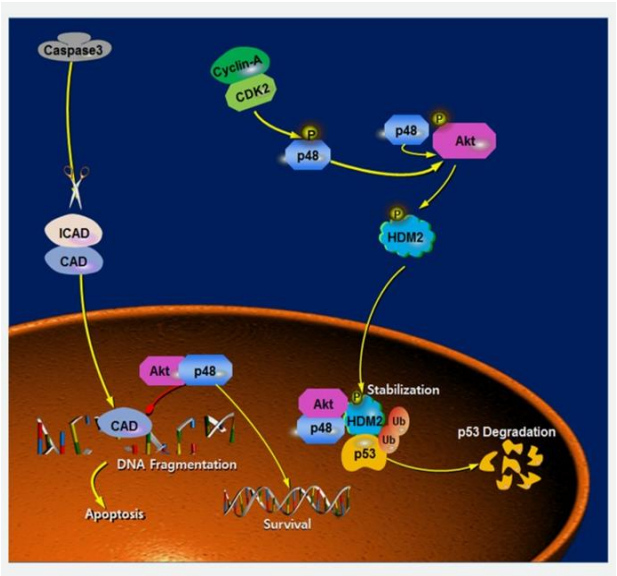

Figure 7. Opposing roles of two isoforms in human cancer cells. **A** shows p42 mediated tumor suppressing activity. When p42 levels are low, p85 cannot interact with heat shock protein 70 (HSP70/CHIP) mediated ubiquitation and degradation which results in higher PI3K activity. However when p42 is up-regulated, it associates p85 with HSP70/CHIP complex inhibiting the PI3K pathway and suppressing tumor. **B** shows the opposing role of p48 which is localized in cytoplasm and nucleus. In the nucleus p48 linked with Akt inhibits Carbamoyl-phosphate synthetase 2, aspartate transcarbamylase, and dihydroorotase (CAD) suppressing DNA degradation and increasing cell survival. P48 also enhances tumorigenesis by an alternative mechanism i.e by activating Akt which increases the level of Human double minute 2 homolog (HDM2) and this in turn causes degradation of p53 which is a tumor suppressor. In addition p48 is also phosphorylated at Ser 34 by Cyclin dependent kinase 2 (CDK2/Cyclin A) which enhances the oncogenic properties of p48 Ebp1. Figures adapted from Ko et al, 2016.

Aims of the study

Previously, Lewis et al identified EBP1 as one of the potential nuclear PPIn binding proteins through PtdIn(4,5)P_2 interactomics coupled with MS, (Lewis et al, 2011). Moreover two lysine rich motifs, one at the C terminus (^{364}RKTQKKKKKK^{373}) and another at the N-terminus (^{65}KKEKEMKK^{72}) were shown to be involved in the interaction of EBP1 with PPIn (Karlsson et al, 2016). In addition, the C-terminal motif was shown to be necessary for the nucleolar localization of the protein. In Figure 8, it is shown that the N terminal KR motif is located right after the RBD α^{70} like region and the C-term motif consists of R364-K365 which was previously shown to contribute to nucleolar localization.

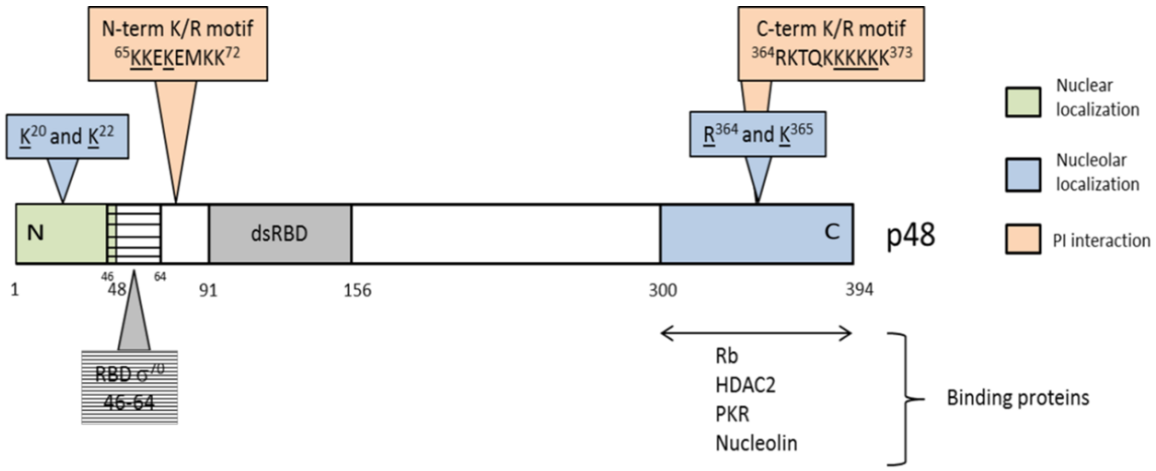

Figure 8. Characterized motifs and their roles in EBP1. K/R motifs at N- and C-terminal ends (orange) are responsible for binding to PPIns (Karlsson et al, 2016). EBP1 interacts with RNA via its RNA binding domain (RBD) (46-64) and the first 48 amino acids (green) are critical for nuclear localization whereas K20-K22 (blue) and R364 and K365 (blue) are responsible for nucleolar localization (Squatrito et al, 2004 and 2006). EBP1 binds to other proteins Rb, HDAC2, PKR and Nucleolin by C-term region. Figure by Lewis AE.

The aim of this project was to determine how PPIn interaction regulate the function of EBP1 by influencing its subcellular localization and to elucidate its effect on ribosomal RNA synthesis, which has effect on cell proliferation and subsequent transformation. Moreover we also investigated into an EBP1 tumor mutant's effect on the nucleolar localization and rRNA synthesis. Lastly, the CRISPR\CAS mediated editing of *PA2G4* aimed at generating a Knocked out cell line in order to better understand the physiological role of the protein.

Materials and Methods

Materials and instruments

Table 2. Chemicals

Name	Abbreviation	Supplier
2-amino-2hydroxymethyl-propane-2,3-diol	Tris	Merck
2,2',2'',2'''-(Ethane-1,2-diyldinitrilo)tetraacetic acid	EDTA	Merck
4-(1,1,3,3-Tetramethylbutyl)phenyl-polyethylene glycol	Triton-X100	Sigma
Acrylamide/Bisacrylamide	-	Sigma
Ammonium persulfate	APS	Bio-Rad
Ampicillin	amp	Sigma
Agarose	-	Bio-Rad
B-glycerophosphate	-	Sigma
Bovine serum albumin	BSA	Sigma
Bromophenol blue	BPB	Lonza
Calcium chloride	$CaCl_2$	Sigma
Deoxycholic acid	-	Sigma
Dimethyl sulfoxide	DMSO	Sigma
DL-Dithiothreitol	DTT	Merck
Essentially fatty acid free bovine serum albumin	-	Sigma
Ethanol	EtOH	Merck
Fetal bovine serum	FBS	Sigma
Hydrogen chloride	HCl	Sigma
Isopropanol	-	Sigma
LB Agar	-	Sigma
Magnesium chloride	$MgCl_2$	Kemetyl
Methanol	MeOH	Sigma
N,*N*,*N*′,*N*′-tetramethyl-ethane-1,2-diamine	Temed	Sigma
Sodium chloride	NaCl	Merck
Sodium hydroxide	NaOH	Merck
Non-fat milk powder	-	Sainsbury
PFA	PFA	
Polyoxyethylenesorbitan monolaurat	Tween 20	Sigma
Potassium chloride	KCl	Merck
Sodium Chloride	NaCl	Merck
Tryptone	-	Bacto™
Yeast extract	-	Bacto™

Table 3. Commercial kits

Plasmid Mini Kit I	Small scale plasmid purification	Omega
Plasmid Maxi Kit (25)	Big scale plasmid purification	QIAGEN
Big Dye Terminator version 3.1	Sequencing	Biosystems
SuperSignal®West-Pico Chemiluminescent	Immunoblotting	Thermofisher scientific
SuperSignal®West-femto Maximum	Immunoblotting	Thermofisher Scientific
Pierce® BCA Reagent A	Protein assay	Thermofisher Scientific
Pierce® BCA Reagent B	Protein assay	Thermofisher Scientific
Click It™ RNA Alexa flour 594 imaging kit	RNA labelling	Thermofisher Scientific.
TOPO® TA cloning kit	Sequencing	Invitrogen

Table 4. Commercial reagents, buffers and solutions

Name	Purpose	Supplier
0,5 M Tris-HCl pH 6,8	SDS PAGE	Biorad
1,5 M Tris-HCl pH 8,8	SDS PAGE	Biorad
ProLong® Gold antifade reagent with DAPI	Mounting solution	Molecular Probes
SDS Solution 20 % (w/v)	SDS PAGE	Biorad
Sequencing buffer	Sequencing	UiB Sequencing lab
Restore™ Western Blot Stripping buffer	Strip WB	Thermofisher
Lipofectamine 3000	Transfection	Thermofisher
Goat serum	Blocking	Invitrogen
Cas/Grna proteins	CRIPSR/CAS	Sigma Aldrich

Table 5. Buffer recipes.

Name	**Recipe**
SDS Loading dye	11mM Tris-HCl pH 6.8, 1% v/v SDS, 4% v/v glycerol, 0.05% M DTT, 0.04% w/v BPB
Transfer buffer	192mM Glycine, 25mM Tris-HCl pH 8.3, 10% v/v Methanol
1x TBST	50mM Tris pH 7.5, 150mM NaCl, 0.1% v/v Tween 20
RIPA	50 mM Tris HCl pH 8, 1.5 mM KCl, 2.5 mM $MgCl_2$, 5 mM NaF, 2 mM Na_3VO_4, 1:100 v/v mPIC*

**mammalian protease inhibitor cocktail*

Table 6. List of in house plasmids used. F= Full length, fs= frame-shift. M=mutant, W= wild type

Plasmid name	Description	Abbreviated name
pEGFP-C2-EBP1	WT Full length EBP1 a1-394	pEGFP-C2-FW
pEGFP-C2-EBP1-K369A-K370A-K371A-K372A	C-terminal motif mutant	pEGFP-C2-FM3
pEGFP-C2-EBP1-K65A-K66A-K68A	N-terminal motif mutant	pEGFP-C2-M57
pEGFP-C2-EBP1-K65A-K66A-K68A-K369A-K370A-K371A-K372A	N and C terminal mutant	pEGFP-C2-FM357
pEGFP-C2-EBP1-K372Rfs c1108delA	K372Rfs tumour mutant	pEGFP-C2-F-K372Rfs c1108delA

Table 7. Primers used PCR amplification of CRIPSR clones

Primer	Sequence
Forward	5' TTGGAAACCTTTTGGGATACTG 3'
Reverse	5' CCTGAAAACATGGAGTAGAGGG 3'

Table 8. Cell lines

Name	Type	Source
AU565	**Breast cancer cells**	Dr. Elisabet Ognedal Berge, Klinisk institutt 2, UiB
HEK293T	**Human embryonic kidney cells**	Research group

Table 9. Culture reagents

Name	Abbreviation	Source
Dulbecco's modified eagles medium	DMEM	Sigma Aldrich
Roswell Park Memorial Institute medium,	RPMI	Sigma Aldrich
Fetal bovine serum	FBS	Sigma Aldrich
0.25% Trypsin-EDTA solution	Trypsin	Sigma Aldrich
100 x Penicillin-Streptomycin	PS	Sigma Aldrich
Dimethyl sulfoxide	DMSO	Sigma Aldrich
Phosphate buffer saline	PBS	-

Table 10. Primary and secondary antibodies

Antibody/1^0 And 2^0	Type	Dilution LB/WB	Supplier	Catalog #
EBP1	Mouse monoclonal	1:1000	Santacruz	Sc-393114
β-actin	Mouse	1:2000	Santacruz	Sc-69879
Lamin A/C	Mouse	1:10.000	Santacruz	Sc-376248
2^0	Anti-mouse Goat IgG HRP	1:10.000	Invitrogen	G21040

1^0: Primary 2^0: Secondary

Table 11. Instruments

Name	Purpose	Manufacturer
Allegra® X-15R Centrifuge	Centrifugation	Beckman Coulter
Alpha™ unit block for DNA Engine Systems	PCR	Biorad
Avanti® J-26 XP	Centrifugation	Beckman Coulter
ChemiDoc™ XRS+	Western and lipid blot imaging	Bio-Rad
Fluorescence microscope DMI 6000 B	Immunostaining	Leica
GelDoc™ EZ imager	Gel imaging	Bio-Rad
NanoDrop ND-1000™	DNA quantification	Saveen-Werner
Spectrophotometer w/Take 3 plate	Protein assay	BioTek
BD Facs Aria SORP	Single cell sorting	Beckton Dickinson

Table 12. Softwares and programs

Name	Purpose	Manufacturer/developer
Imagelab	Western blot and gel imaging	Biorad
Leica X	Cell imaging	Leica Microsystems
Fiji Image J	Cell imaging and processing	National institute of Health
Cell Profiler	Quantification	McQuin et al, 2018

Methods

Cell culturing.

All cell culturing procedures were carried out under sterile conditions in a Laminar flow cell culture bench with a High efficiency particulate air filter (HEPA). AU565 which is a breast cancer cell line were grown following the general cell culturing guidelines using RPMI-250 supplemented with 10% Fetal Bovine Serum (FBS) and 1% Penicillin-Streptomycin (PS) and the growth was monitored on a frequent basis by light microscope. HEK293T cells were similarly cultured using complete Dulbecco's Modified Eagles Medium (DMEM) with low glucose plus 10% FBS and 1% PS and grown under standard cell culturing conditions.

Cell passaging

When the cells reached 70-80% confluency, they were split. For this, the medium was aspirated, cells were washed with 1x Phosphate Buffer Saline (PBS), pre-warmed to 37℃, and 0.25% Trypsin-EDTA was added. The cells were incubated at 37 ℃ with trypsin until they were detached. Cell detachment was observed under the microscope. As AU565 were hard to detach, the plate was shaken a bit or the dish sides were hit with a mild force. When the cells were observed to be flowing freely, trypsin was inactivated by adding fresh RPMI (supplemented with 10% FBS and 1% PS). The medium was pipetted up and down multiple times and transferred to a new plate. AU565 were split in 1:2 or 1:3 and HEK293T 1:3 or 1:4. Similarly HEK293T cells were trypsinised and split but they detached comparatively easily.

Plasmid transfection

When AU565 cells reached 70-80% confluency, they were split in a 6-well plate containing a coverslip. Before carrying out transfection, the medium was replaced with fresh RPMI (supplemented with 10% FBS). 2 µg of each plasmid construct was added to 250 µL of pre-warmed OPTI-MEM. The transfection reagent Lipofectamine^{R} 3000 (6 µL) was mixed separately with the same volume of OPTI-MEM. Then the diluted plasmids were slowly added to the diluted Lipofectamine, mixed slowly and incubated for complex formation at RT for 20 min. After the prescribed period, the mixture was added drop by drop to the cells and incubated at 37℃ for 24 h. After 24 h, the medium was changed to RPMI (supplemented with FBS and PS) and incubated at 37℃ for another 24 h.

RNA EU labelling

Click^{IT} RNA imaging assay is used to detect global RNA synthesis temporally and spatially in cells and tissues[1]. Utilizing an alkyne-modified nucleoside, 5-ethyluridine (EU) and click chemistry, newly synthesized RNA can be detected. Detection uses the 'click' reaction between the fluorescent dye (azide modified dye or hapten) and alkyne base modified RNA (Figure 9).

At 48 h post-transfection, 2 ml from the initial 3 ml medium was aspirated leaving 1 ml on cells. 1 mM EU in pre-warmed medium was added to the cells and incubated at 37^{0}C for 15 min. After washing in PBS, the cover slips were transferred to a separate 6 well plate and placed in PBS. The remaining cells, attached to the plate were collected and lysed (see whole cell extraction) for use in Western immunoblotting. Cells on cover-slips were fixed using pre-warmed 3.7% Paraformaldehyde in PBS for 10 min and washed with PBS thrice. The wash buffer was removed and cells were permeabilised with 0.5% Triton X -100/PBS at RT for 15 min. After washing once in PBS, 500 µL of the Click^{it} cocktail: 1x Click^{it} reaction RNA buffer, 100 mM Copper (II) Sulfate, 1x Click^{it} reaction buffer additive using the Alexa Fluor 594 azide was added per slip and incubated in the dark for 30 min. Afterwards, the cocktail was removed and cells washed briefly with 1x reaction rinse buffer. The cells were mounted with ProLong® Glass antifade mountant with NucBlue on glass slides and stored at 4°C and imaging was done the next day or the day after.

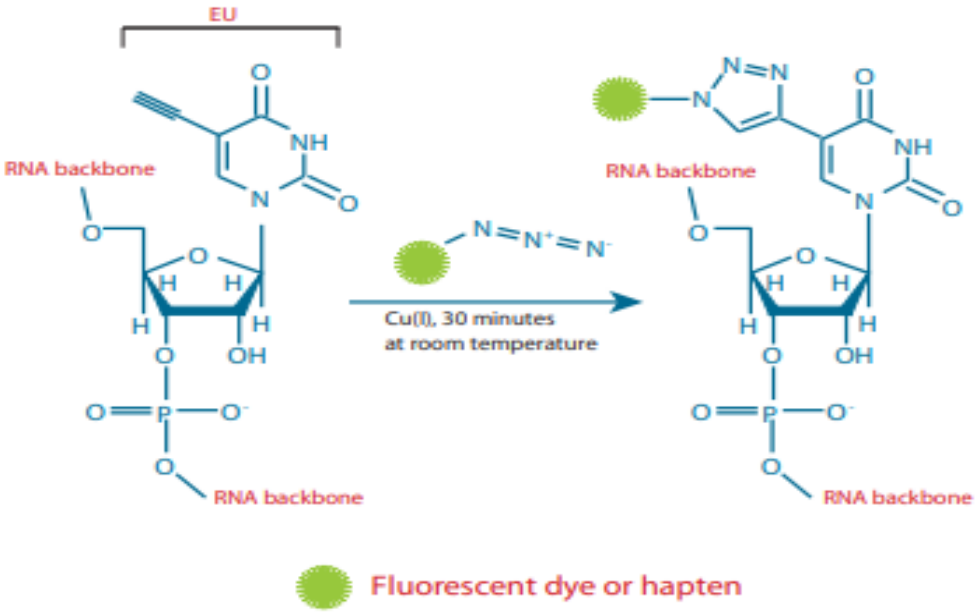

Figure 9. Click chemistry between RNA and fluorescent azide dye. 5-Ethyl-Uridine Incorporates into RNA first followed by reaction with the fluorescent dye. The fluorescence was later detected with a Leica microscope. Figure adapted from Thermofisher Scientific product protocol.

Imaging, Acquisition, Quantification

The glass slides were imaged using a Leica microsystems fluorescence microscope DMI 6000 equipped with three filters: blue band pass for the excitation of DAPI (4′,6-Diamidino-2-phenylindole dihydrochloride) (DNA), red band pass for Alexa594 and green band pass for GFP. The acquisition settings for EU fluorescence intensity was kept constant for all the constructs. The images were processed using Cell Profiler (for quantifying the EU fluorescence intensity in the nucleoli, and Leica X imaging tool (for quantifying the transfection and EU labelling.

Inhibition of RNA expression

The RNA expression was inhibited by using 1 µM RNA Pol 1 inhibitor BMH21 for 2 h 45 min followed by 15 min of EU labelling.

Whole cell extract preparation

To detect the overall expression of different proteins in different cell lines, the cells were lysed and the whole cells extracts were subjected to western blotting. Cells at 70-90 % confluency were washed twice with cold PBS, and lysed with 150 µl of cold RIPA buffer: 50 mM Tris HCl pH 8, 1.5 mM KCl, 2.5 mM $MgCl_2$, 5 mM NaF, 2 mM Na_3VO_4 and 1:100 v/v mPIC (mammalian protease inhibitor cocktail from Sigma). Cell debris and the DNA were pelleted by centrifuging the lysate at 13,000 x g, 4 °C for 5 min and the supernatant was collected as whole cell extract (WCE) and stored at – 80 °C for further analysis. For CRISPR/CAS9 experiment (following later), the extracts were also sonicated before centrifugation step: 3 x sonication for 5 sec with 1 min rest between each.

Bicinchoninic acid protein assay

The protein concentration in the cell lysates obtained was determined using Thermo Scientific™ Pierce™ BCA™ (Bicinchoninic acid) Protein Assay kit. It uses the peptide bond's ability to reduce Cu^{2+} to Cu^{+}, and the reduced Cu^{+} will be proportional to the amount of protein present in the solution. BCA in the reagent chelates with Cu^{+} and forms a purple-colored product which is measureable by a standard spectrometer at 562 nm. For this purpose, the cell lysates were run in duplicates on a 96 well plate along with the blank buffer (RIPA) and serial dilutions: 0 µg/µl, 0.625 µg/µl, 0.725 µg/µl, 1.25 µg/µl, 2.5 µg/µl, 5.0 µg/µl and 7.5 µg/µl made from the stock of 10 mg/ml Bovine Serum Albumin (BSA) in RIPA buffer. 200 µl of Pierce™ BCA™ Protein Assay reagent mix was added to each well containing 2 µl of the lysates in duplicate as well as BSA standard dilutions and the blank and incubated at 37℃ for 10 min. Absorbance measurements were performed at 562 nm on the Epoch microplate spectrophotometer and concentrations calculated using Excel. A linear graph was constructed

with x-axis representing the standard BSA concentrations vs absorbance values on y-axis. The equation of the graph was used to determine the concentrations of protein.

Sodium dodecyl Sulfate Polyacrylamide Gel Electrophoresis.

Sodium Dodecyl Sulfate Polyacrylamide Gel Electrophoresis (SDS-PAGE) is a routine method for separating proteins based on the molecular weights. 30 µg of cell extracts were resolved on the SDS gel. The samples were mixed with 5x loading dye: 13 mM Tris-HCl pH 6.8, 1% w/v SDS, 4% v/v glycerol, 50 mM Dithiothreitol (DTT), 0.04% w/v Bromophenol Blue (BPB)and boiled for 5 min. The gel was run at 120 V for about 1 h 30 min until the dye reached the bottom end of the gel.

Western Immunoblotting

Western blotting is a routine molecular biology method that allows the detection of specific proteins from extracts made from cells or tissues, and can be used to semi-quantitatively compare protein levels between extracts. Proteins are separated by size using SDS-PAGE and transferred to a membrane where they are probed with antibodies specific to the target proteins.

Proteins from the gel were transferred onto nitrocellulose membrane with 0.45 µm pores via blotting method. First, a 3 mm thick Whatman Filter paper and matching the size of the gel was pre-soaked in the transfer buffer: 192 mM Glycine, 25 mM Tris-HCl pH 8.3, 10% v/v Methanol. Following the wet western blotting protocol, the transfer was conducted overnight at 4°C. Once the transfer was completed, the membrane was blocked with 10 ml of 5 % (w/v) powdered skim milk in TBST (5 mM Tris pH 7.5, 15 mM NaCl, 0.01% v/v Tween 20) for 1h at RT. After blocking, the membrane was rinsed with TBST and probed with primary antibody (Table 10) diluted in TBST for 1 h at RT or o/n at 4 °C followed by 3 x 10 min washes in TBST. To detect the protein bound to the primary antibody, the membrane was incubated with Horseradish peroxidase (HRP)-conjugated secondary antibody diluted 1:10, 000 in TBST for 1 h at RT followed by 3 x 10 min washes in TBST. All incubations and washes were done on the shaker. The protein-antibody complexes were detected using SuperSignal® West Pico Chemiluminescent Substrate (ECL-PLEX) from Thermo Scientific per membrane. The membrane was incubated for 5 min with ECL-PLEX and detected with Bio-Rad's Molecular Imager® ChemiDoc™ XRS+ using ImageLab™ Software Version 3.0.

Clustered regularly interspaced short palindromic sequences/Cas9 (CRISPR/CAS9) mediated genome editing

CRISPR/CAS9 is increasingly becoming popular in the fields of genomic editing and gene regulation. Based on a type II prokaryotic immune system, this mechanism provides acquired immunity gained through resistance against foreign elements (Wiedenheft et al, 2012). The mechanism was first identified as a bacterial defense against viruses.

Genomic editing via the use of CRISPR, by creating a single stranded gRNA (guide RNA) directed to the gene of interest and recruiting Cas9, several genes have been studied and their function determined using this system (Feng et al, 2015).

Identifying the desired sequence and designing gRNA. *In-silico*

In this project we aimed to disrupt the *PA2G4* gene in order to understand the function of its encoded protein Ebp1. For this purpose, we targeted the exon 2 in *PA2G4* located on chromosome 12. Firstly, by using CHOP-CHOP **https://chopchop.cbu.uib.no/** several guide RNA (gRNA) sequences were identified and the most suitable gRNA sequence was selected based on the best Score and maximum efficiency with minimum off-targets.

Preparation of Cas9/gRNA ribonucleoprotein complex.

Trans-activating (tracrRNA) and Crispr RNA (crRNA) conjugated to ATT0590 from Sigma Aldrich were re-suspended to a final concentration of 100 µM each in 10 mM nuclease-free Tris-HCl pH 7.8. Lyophilized EGFP-Cas9 was re-suspended to a total concentration of 2.5 µg/µl in the reconstitution buffer (50% glycerol in water). 3 µl of 100 µM crRNA and ATT0590-tracrRNA were mixed together forming the gRNA (1:1) and then mixed with 4 µl of 2.5 µg/µl Cas9 to finally form the ribonucleoprotein complex (5:1). They were mixed thoroughly and incubated on ice for 20 min.

Transfection of HEK293T cells with CRISPR/CAS9 complex product.

HEK293T cells were seeded in a 6-well plate and left to recover for 18-24 h before being transfected. The required confluency was 80%. Next day the medium was changed to DMEM and 10% FBS. The cells were transfected with CAS9/gRNA complex using 18.75 µl TransIT-CRISPR® Transfection Reagent (Sigma-Aldrich, Catalog Number T1706) as transfection agent and were allowed to grow at 37 °C in a CO_2 incubator for 48 h post transfection.

Fluorescence assisted Cell Sorting.

Cells were washed with 1x PBS, trypsinized and centrifuged in 2 ml PBS at 900g for 5 min. This was repeated once and cells were suspended in 0.6 ml PBS containing 10% FBS and were sorted by Fluorescence assisted Cell sorting (FACS), to select the EGFP (Cas-9 green fluorescent) and m-cherry (Atto-590 fluorescent gRNA) positive cells and re-plated in 1-2 wells of a 6 well plate and left for recovery for two days. After recovery they were washed again as before and were FACS single-cell sorted for EGFP and Atto590 into 96 well plates and grown in a mix of conditioned medium previously collected from HEK-293 cells and fresh growth medium (1:1). Each clone was further cultured in 48, 24, 12, 6 well plates to finally reach 10 cm dishes. The procedure is shown in Figure 10

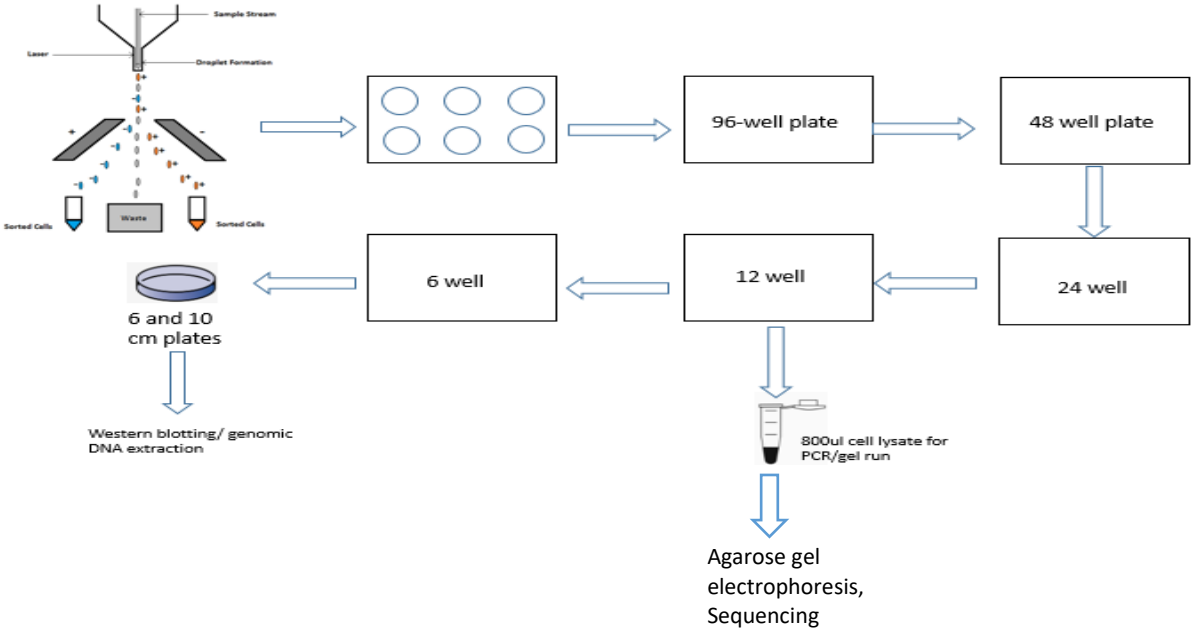

Figure 10. Fluorescence assisted cell sorting. EGFP-Cas9 and Atto-gRNA red fluorescent cells were sorted by FACS and sequentially grown in 96, 48, 24, 12 and 6 well plates. 800 µl was separated for PCR/restriction digestion and sequencing. Remaining was transferred to 6 well plates and then cultured in 6 cm and 10 cm plates for whole cell extraction.

Preparation of lysates

When cells grown in the 12 well plate reached 80% confluency, they were washed with 1x PBS, trypsinized following the usual protocol and 800 µl was collected and the remaining 1.2 ml was transferred to 6 well plate for further growth. Cells were centrifuged at 17000xg for 2 min at 4°C. Supernatant was removed and the pellet was re-suspended in 1 ml 10 mM Tris-HCl pH 8.5 and centrifuged again at 17000xg for 2 min. The cell pellets were re-suspended in 25-100 µl 10 mM Tris, vortexed thoroughly and heated at 95°C for 15 min followed by a quick cool down on ice. Cells were incubated with 4 µl Proteinase K at 50°C for 30-45 min and the enzyme was inactivated at 95°C for 10 min. After cooling on ice for a short time, the cell lysates were ready for PCR.

Polymerase Chain Reaction

15 µl of cell lysate was mixed with 1x HotFire Pol^{R} master mix, 0.5 M $MgCl_2$, 10 µM of forward and reverse primers in 10 mM Tris HCl pH 8.5 in a total volume of 20 µl (refer to Table 5 for primer sequences). PCR was performed with the following running conditions. A total of 40 cycles were run.

Table 13. Running conditions for PCR.

Stage	Time	Temperature/°C	
Initial Denaturation	12 min	95	
Denaturation	30 sec	95	40 cycles
Annealing	20 sec	50	
Initial Extension	45 sec	72	
Final Extension	7 min	72	
Hold	∞	4	

Agarose gel electrophoresis

Samples were mixed with DNA loading buffer and run on a 2-3.5 % agarose gel made in 1x Tris Acetate- EDTA (TAE) buffer: 40 mM Tris base, 1 mM EDTA pH 8.0 and 20 mM Acetic acid containing 1.2 µg/µl EtBr along with 2log DNA marker. To visualize the PCR amplification products, the gel was run for 30 min at 100V and for restriction digestion analysis, it was run for 15 min, imaged and then run for further 15 min at 100V.

Purification of PCR product

The remaining PCR product for M3 and S3 clones was purified using Macherey^{TM} Nagel Nucleospin^{TM} Gel and PCR clean up kit from Thermofisher Scientific.

Restriction digestion

The purified PCR product (212 ng M3 and 243 ng S3) was digested with N1aIV restriction endonuclease, 1x SmartCut buffer in a total volume of 20µl followed by incubation at 37℃ for 1 hour.

DNA sequencing

M3 and S3 were sequenced following the BigDye v.3.1 Protocol. 1 µl of each product was added to 10 µM forward primer (**5′TTGGAAACCTTTTGGGATACTG'3**) and 1x Sequencing buffer. PCR was ran for 27 cycles with the following conditions. After PCR the final volume was made to 10 µl and samples delivered for sequencing at the UIB sequencing facility.

Table 14. Running conditions for Big Dye PCR.

Stage	Time	Temperature/℃	
Initial Denaturation	5 min	96	
Denaturation	10 sec	96	27 cycles
Annealing	5 sec	50	
Extension	4 min	60	
Hold	∞	10	

Results

EBP1 localizes to the nucleolus via its C-terminus PBR.

EBP1 has been shown previously to localize into the nucleolus of HeLa and NIH-3T3 cells (Squatrito et al, 2004) and in the breast cancer cell line AU565. The group identified the lysine rich binding motifs at N and C terminus which are involved for interacting with PPIns with the C-terminal motif contributing the most to the nucleolar localization (Karlsson et al, 2016). In the present study, we first revalidated the previous findings. AU565 were transfected with EGFP-tagged EBP1 FL WT and the following mutants; EGFP-FL-C term: ^{369}**KKKK**^{372} to **AAAA**, EGFP-FL-N term: ^{65}**KK**E**K**^{68} to **AA**E**A** and EGFP-FL C-term and N-term double mutant (Figure 1 A). The expression of the EGFP-tagged protein was also checked against endogenous EBP1 in AU565 cells using Western immunoblotting (Figure 1 B). The endogenous EBP1 protein was found approximately near 50 kDa which matches with the known molecular weight of p48-EBP1 i.e 48 kDa (Liu et al, 2006). EGFP-EBP1 was observed at approximately 75 kDa. It is clear from the figure that EGFP-FL WT EBP1 and EGFP-FL C term had almost the same signal strength of bands than the endogenous EBP1 while EGFP-FL N term and EGFP-double mutant had stronger bands.

The transfected AU565 were examined by fluorescence microscopy and representative pictures are shown in (Figure 2). The cells were further quantified for nucleolar and non-nucleolar EBP1 for wild type and mutants. Results were gathered as percentage of EGFP positive cells being nucleolar or non-nucleolar (Figure 1 C). The Graph shows that 80% of the cells expressing EGFP-FL WT showed a nucleolar localization which was greatly decreased in all the mutants. FL-EGFP N terminal mutant had a higher percentage of cells with nucleolar EBP1 than the C-terminus mutant and the double mutant showed the lowest nucleolar EBP1 localization. Hence it was established that the C-terminus binding motif does contribute the most to nucleolar localization.

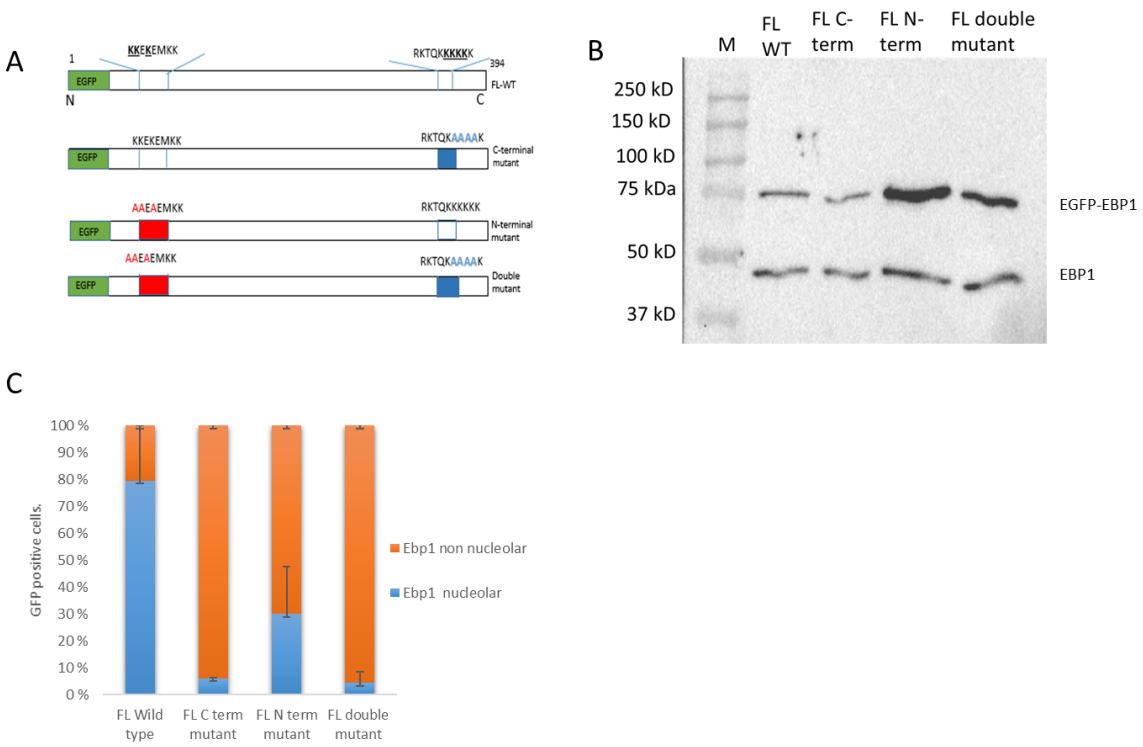

Figure 1. Schematic illustrations for EGFP-wild type EBP1 and respective mutants, expression relative to endogenous EBP1 and nucleolar quantification. A: Diagram of the constructs used in this study. Top most shows wild type Ebp1 with the N and C terminal KR motifs. <=. N-terminal mutant ^{65}**KK**E**K**^{68} to **AA**E**A**, *mutation highlighted in red*) and C terminal-mutant (^{369}**KKKK**^{372} to **AAAA**, *mutation highlighted in blue*) and double mutant (*Red and blue)* are shown. **B:** AU565 were transfected with the constructs: EGFP-Full length Wild type EBP1, EGFP-FL C terminal, EGFP FL-N terminal mutants and EGFP- FL C and N term and then whole cell extracts were obtained and protein expression of our constructs checked on western blot. FL WT: Full length wild type, C term: FL C terminal mutant, N term: FL N terminal mutant, **C**: EGFP positive cells were quantified for nucleolar and non-nucleolar Ebp1. C is the average quantification of a biological triplicate.

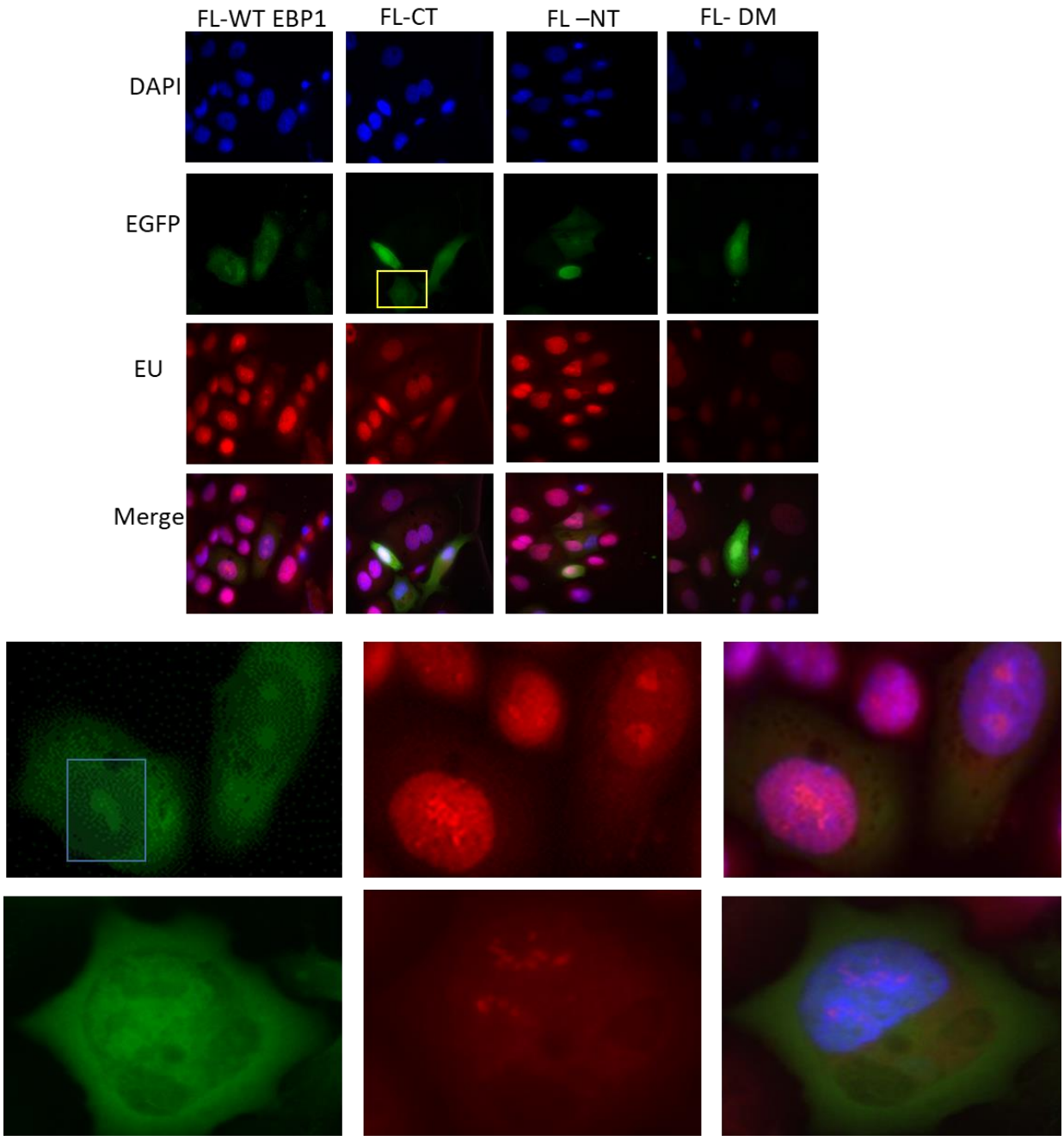

Figure 2. EBP1 subcellular localization and EU pattern for wild type protein and mutants. AU565cells were transfected with EGFP-EBP1 Full length wild type and mutant constructs: EGFP-FL C term, EGFP-FL N term and EGFP-FL C and N term. RNA was labelled by EU labelling followed by fluorescence microscopy. Separate lane of magnified images of FL-WT nucleolar EBP1 (Blue square) and EU while FL CT (cell in the yellow square) showing empty nucleoli in GFP positive cell as well as for EU (mainly nuclear). The images are representative of three biological experiments. FL-WT: Full length wild type, CT: C-terminal mutant, NT: N-terminal mutant, FL-DM: Full length double mutant.

Localization of EBP1 in the nucleolus correlates with the presence of nascent rRNA in the nucleolus.

As it has already been established that the C- terminal binding motif contributes the most to EBP1's nucleolar localization, the next objective was to investigate into the effect of the PPIn interaction on rRNA synthesis. We tried to find out if there is any co-relation between the nucleolar sub-cellular localization of EBP1 and the presence of nascent ribosomal RNA, as labelled by EU. Figure 3 A represents the quantification as percentage of cells for wild type and mutants. 50% of EGFP positive cells expressing FL-WT EBP1 had nucleolar EU and all the mutants showed a decrease in the percentage for nucleolar EU with double mutant being the least nucleolar. The C terminal mutant was about 20% nucleolar and 80% non-nucleolar and N- terminal mutant compared to C- terminus was more nucleolar(25%) and 75% non-nucleolar. Overall the mutants showed empty nucleoli that is no or very weak signal of EU in the nucleolus. (Figure 2).

4 different patterns were studied to analyze the correlation between localization of EBP1 and nascent ribosomal RNA as labelled by EU. Figure 3 B shows the quantified results and Table 1 summarizes the patterns observed and their corresponding percentages. FL WT EBP1 demonstrated a strong correlation between the presence of EBP1 in the nucleolus together with rRNA. More than 50% of the cells were positive for both nucleolar EBP1 and EU and about 17.9% of the cells had non-nucleolar EBP1 and EU. As for the C-terminal mutant 0% of cells had both nucleolar EU and EBP1 while the N-terminal was 18.7%. Interestingly double mutant had a slight percentage (2.78) of cells with nucleolar EBP1 and EU nevertheless more than 90% were non-nucleolar for both EBP1 and EU.

Table 1.0. Summary highlighting the correlation between localization of EBP1 and presence of EU in the nucleolus.

EGFP-EBP1 plasmids	EU and EBP1 non-nucleolar (%)	EU and EBP1 nucleolar (%)	EU non- nucleolar EBP1 nucleolar (%)	EU nucleolar EBP1 non-nucleolar (%)
FL WT	17.9	56.04	29.6	0.86
FL C term mutant	69.5	0.00	2.80	24.5
FL N term mutant	61.8	18.7	9.31	10.3
FL double mutant	90.6	2.78	0	5.32

A

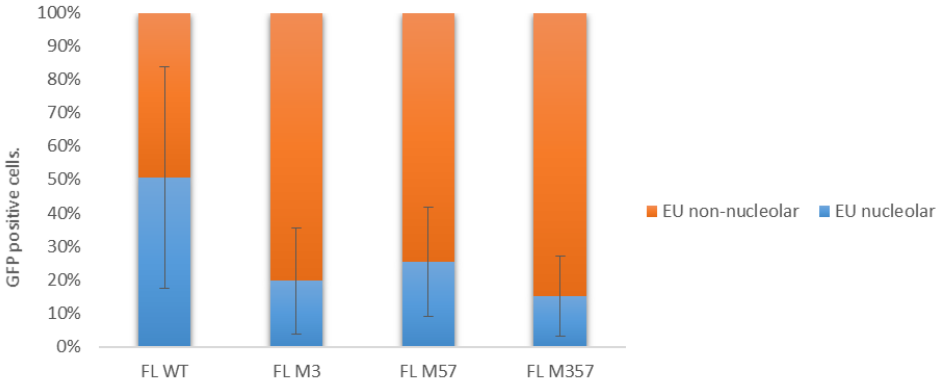

B

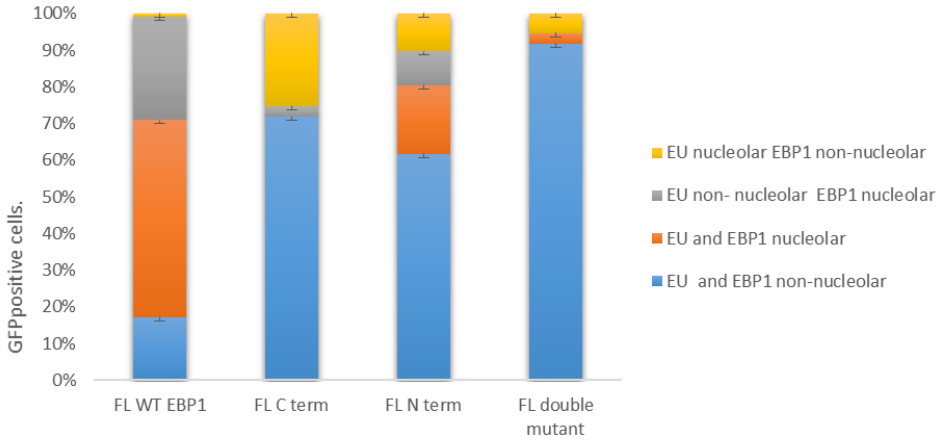

Figure 3. Study of the RNA level in relation to localization of EBP1. AU565 cells were transfected with the constructs: EGFP-FL WT EBP1, EGFP-FL C term, EGFP-FL N term and EGFP-FL C and N term mutants and RNA labeled by EU. 20-25 EGFP positive cells were quantified for each construct and 3 biological experiments were analyzed. The figures show the average ± SDs of the triplicate. **A**: Bar graph showing the percentage of EGFP-positive cells with nucleolar and non-nucleolar EU for EGFP-EBP1 wild type and mutants. **B**: Bar graph highlighting the correlation between the localization of EBP1 and presence of EU in the nucleolus corresponding to wild type and mutants. FL M3: C term FL M57: N term FL M357: C and N term mutant.

RNA Pol 1 inhibitor BMH21 treated cells were EU negative.

AU565 cells were transfected with EGFP-FL WT EBP1, treated with or without the RNA Pol 1 BMH21 inhibitor and EU-labelled (Figure 4). The inhibitor blocks the transcription of nascent rRNA without interfering with GFP signal hence empty nucleoli were observed in the cells for EGFP-FL WT treated with BMH21 while the positive control i.e EGFP-FL WT EBP1 minus BMH21 expressed rRNA showing presence of EU in the nucleolus.

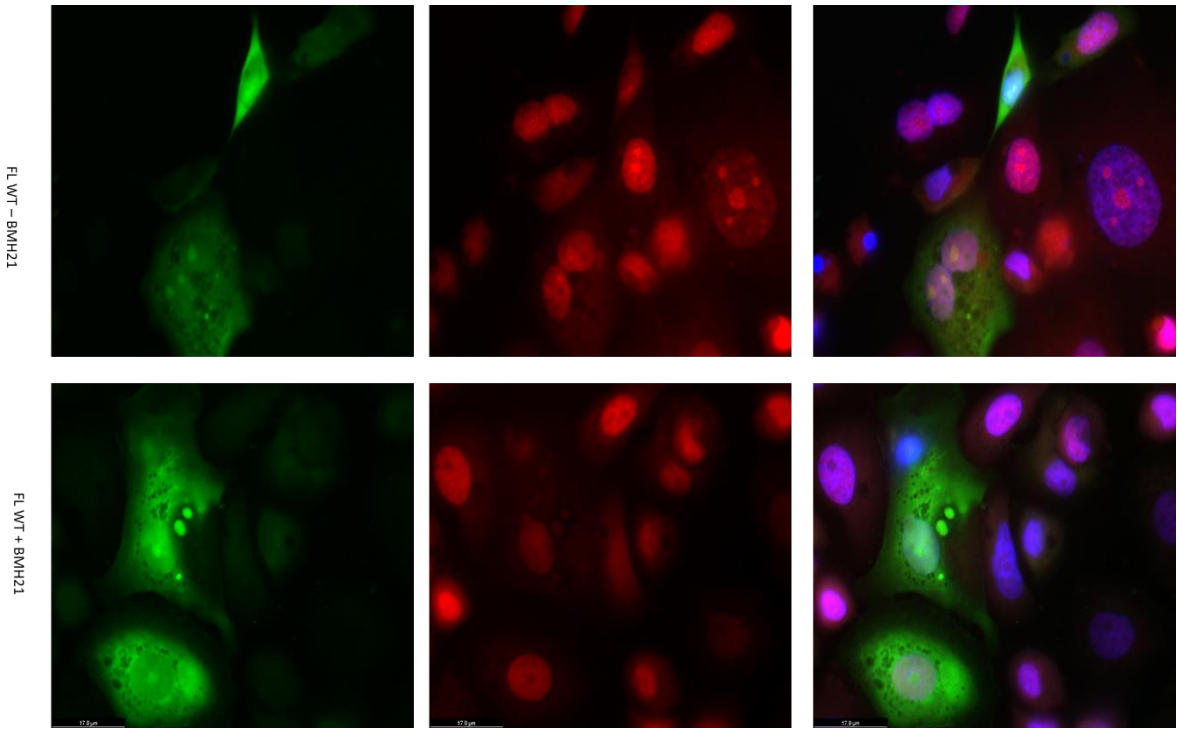

Figure 4. AU565 cells treatment with RNA Pol 1 inhibitor BMH21. AU565 cells were transfected with EGFP- FL WT EBP1 and treated with (+) or without (-) the RNA Pol 1 inhibitor BMH21 followed by EU labelling and examination by epifluorescence microscopy. Treated cells showed empty nucleoli for EU (FL WT + BMH21) and untreated cells expressed rRNA hence presence of EU did not change in the nucleolus (FL WT – BMH21).

An EBP1 tumor mutant showed a stronger nucleolar localization and rRNA levels than Wild type EBP1

EBP1 as a growth regulatory protein has been documented to be involved in cancer development. K372Rdel-fs is one of characteristic mutations identified in a pancreatic, large intestine, stomach and ovary cancer according to the public data from the Catalogue of Somatic Mutations in Cancer (COSMIC, v91). A former master student worked partially on it and we decided to take forward the findings because the mutant has been linked to the nucleolar localization of EBP1. The mutation lies in the C term motif and that the frameshift deletion altered the part of the motif and changed the protein sequence, Figure 5 A highlights the location of the mutation within the motif along with wild type protein. AU565 cells were transfected with the constructs; Full length wild type EGFP-tagged EBP1 and K372Rdel-fs mutant. In addition, cells were treated with the RNA polymerase I inhibitor, BMH21 to demonstrate as a control for EU labeling as shown earlier. The negative control showed a decrease in the level of rRNA. The cells were again monitored by fluorescence microscopy (5B). Percentage of transfected cells with nucleolar and non-nucleolar EBP1 and EU was also determined. K372Rdel- frame shift tumor mutant had a higher % of cells with nucleolar EBP1 (100% nucleolar) and EU (92.5%) compared to wild type (87.7% nucleolar EBP1, 12.24% non-nucleolar EBP1; 85.81% nucleolar EU, 14.17% non-nucleolar EU). Figure 6 A and B show the results.

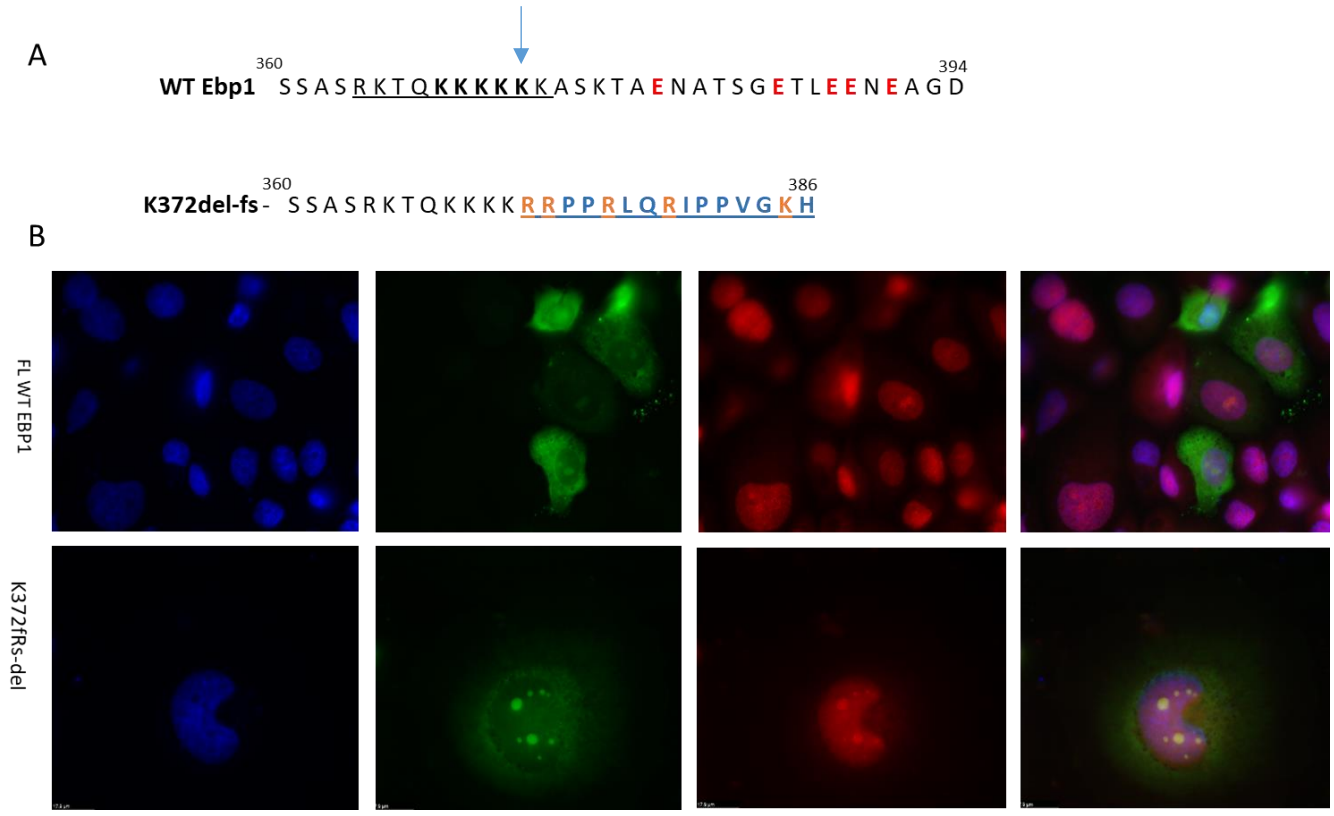

Figure 5. Schematic constructs and Subcellular localization of EBP1 and EU signaling for wild type and Tumor mutant. A: WT shown as the 394 amino-acids long protein with KR motif intact (underlined in the sequence). Tumor mutant protein (K37Rdel-fs) was shorter than the wild type and due to the mutation at -Lysine 372 (arrow), there was a frameshift caused by the deletion of 1 base (c.1115) (underlined in the mutant) in the reading frame encoding a shorter and more positive protein. **B:** Fluorescence microscopy of AU565 cells transfected with WT EBP1 and K372Rdel-fs and EU labelled. K372Rdel-fs showing a strong GFP-EBP1 signal as well as EU in the nucleolus. K372Rfs-del: deletion frame shift mutant. Image is representative of two biological repeats.

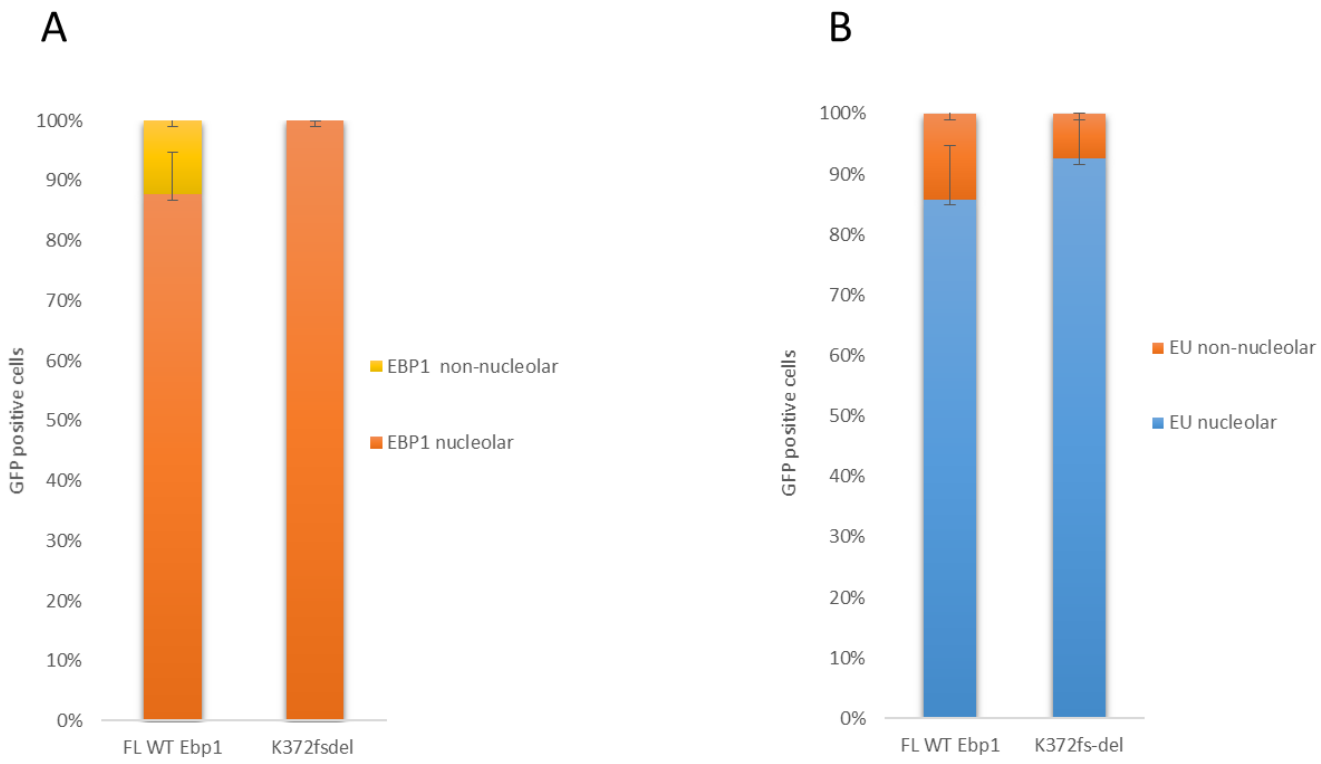

Figure 6. Percentage of transfected cells with nucleolar/non-nucleolar EBP1and EU for wild type, and tumor mutant. 20-25 GFP positive cells were counted for K372del-fs and FL-WT EBP1. Tumor mutant was 100% nucleolar for EBP1 **(A)** and more than 90% of the cells also had nucleolar EU compared to FL wild type (more than 80% nucleolar and 10-20% non-nucleolar EBP1 and EU **(A and B).** Results represent the duplicate.

K372Rdel-fs increased the number of nucleoli

K372Rdel-fs tumor mutant and the wild type Ebp1 were also analyzed for the number of nucleoli in the EGFP-positive cells. The nucleoli were counted per cell. K372Rdel-fs tumor mutant showed an increase in the number of nucleoli compared to wild type as shown in Figure 7; Figure 7 A and B show the results for two separate experiments. For experiment 1, approximately 18-20 EGFP positive cells were analyzed. A shows that the tumor mutant had 1-2 cells with enhanced number of nucleoli (9/cell) and most of the cells still had 2, 3, or 4 nucleoli. Most cells transfected with FL-WT EBP1 had one or two nucleoli (Figure 7 A), 12 cells had only one nucleolus. Experiment 2 (B) also showed a similar trend although the number of GFP positive cells taken into account were less compared to experiment 1, nevertheless it was established that K372Rdel-fs mutant tend to increase the number of nucleoli.

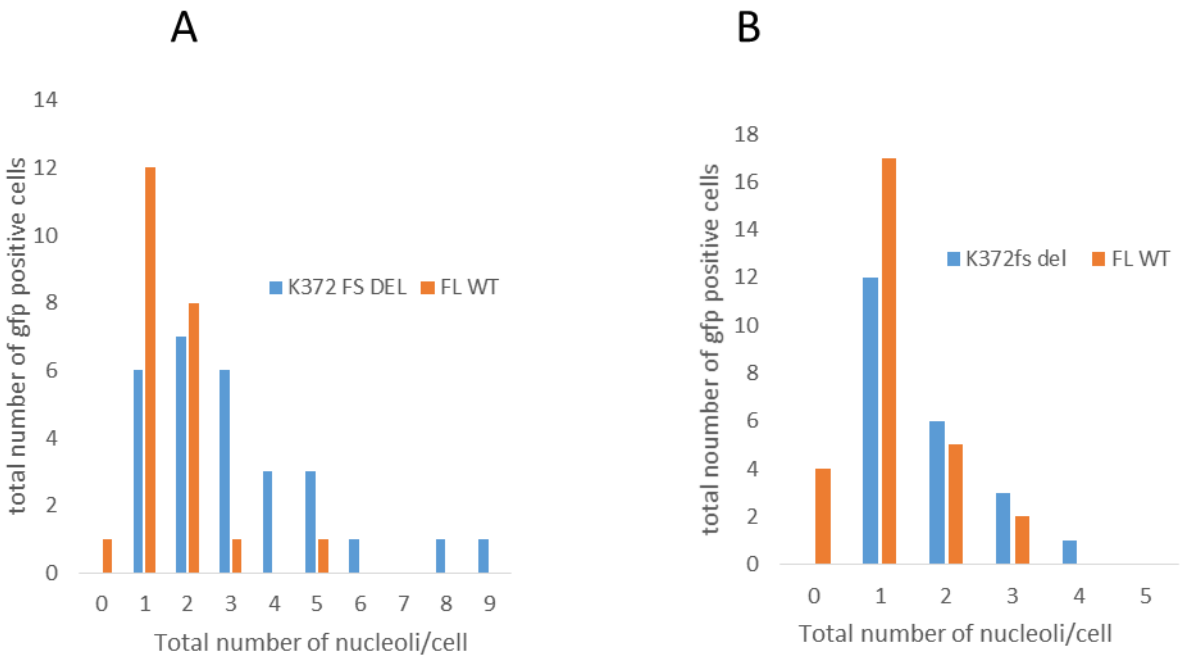

Figure 7. Number of nucleoli in GFP positive cells for tumor mutant and FL Wild type EBP1. Experiment 1 **(A)**: 12 EGFP positive cells had one nucleolus for wild type whereas 6 cells had one nucleolus for K372del-fs. The highest number recorded was 9 nucleoli for K372del-fs. Experiment 2 **(B)** showed a similar trend and K37del-fs had the highest number of 4 while FL-WT highest number was 3 and most cells still had 1 or 2 nucleoli.

Integrated EU intensity in the nucleolus was lower for the K372Rdel-fs tumor mutant.

A procedure was developed to quantify the intensity of EU in the nucleoli of EGFP-positive cells transfected with the tumor mutant and FL-WT EBP1. Approximately 30 GFP-positive cells were analyzed for each construct from comprising of 8 sets of images and 2 biological replicates for each construct was taken into account. For this purpose we used the software Cell profiler (Figure 8). The images were run through a designed pipeline relevant to the objective and analyzed (Figure 8 A-B). The program first detects the nucleus via the DAPI channel and this allows for the detection of GFP signal within the nucleus and excluding the cytoplasm (Figure 8 C). Then it is set to detect the nucleoli based on a suitable threshold factor which was selected according to the GFP signal in the image (see Supplementary Figure S3). Cell profiler then creates a filtered image of the nucleoli further refining the threshold parameter and gives the output as a csv file for Integrated EU intensity and other parameters but they were not considered. The results were plotted as Average Integrated Nucleolar EU intensity against the total number of GFP positive cells of the constructs**.** Interestingly, the calculated average for the tumor mutant was lower than the Wild type EBP1 (Figure 9).

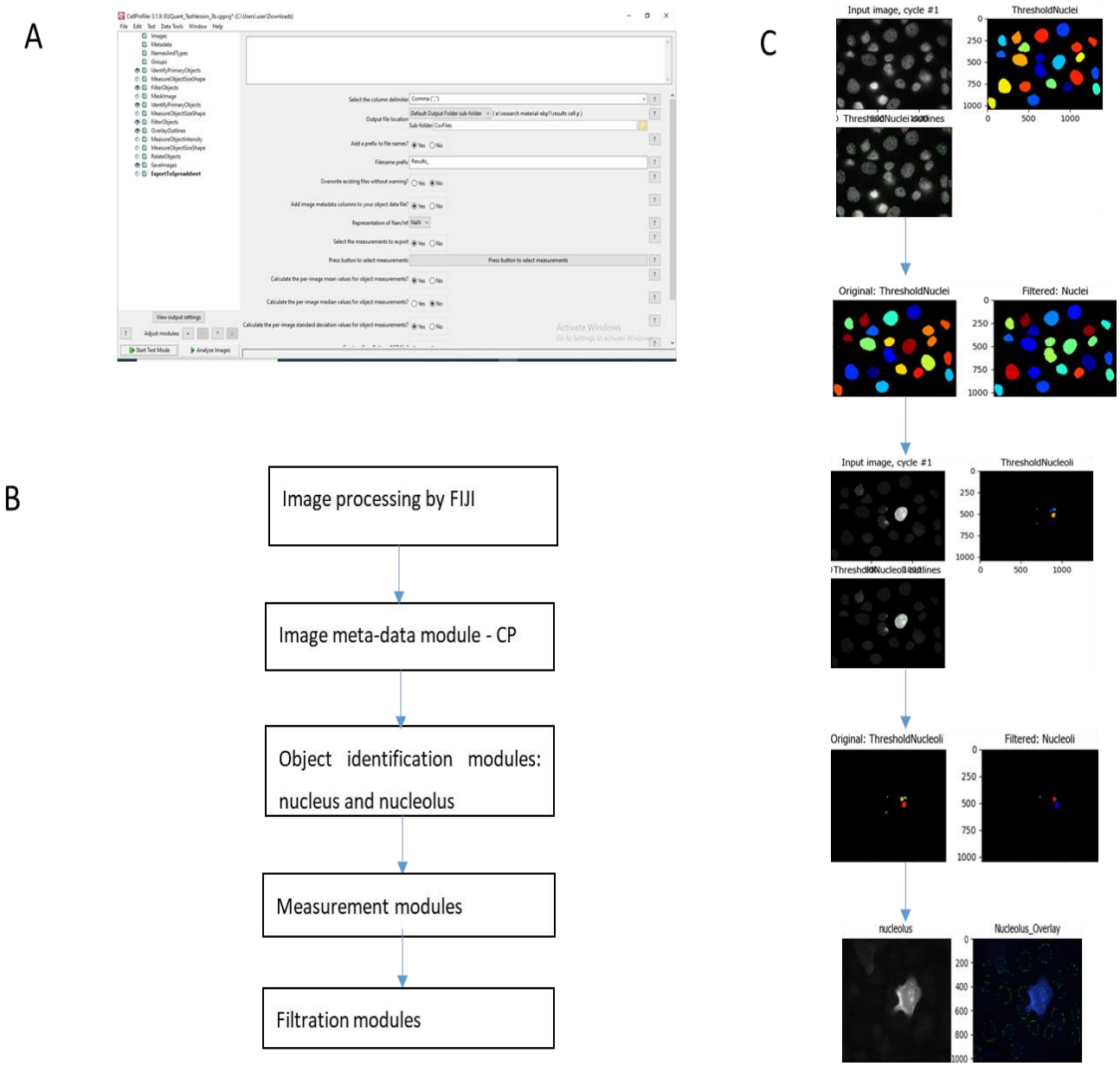

Figure 8. Cell profiler overview and features. (A) Main interface of cell profiler and pipeline used shown. **(B)** Overview of modules in the pipeline and identification of the region of interest in the cell (nucleolus in this case) and output generated as an excel file. **(C)** Images obtained from a run highlighting thresholding, filtration modules and final nucleolus overlay in AU565 cells. CP: Cell profiler

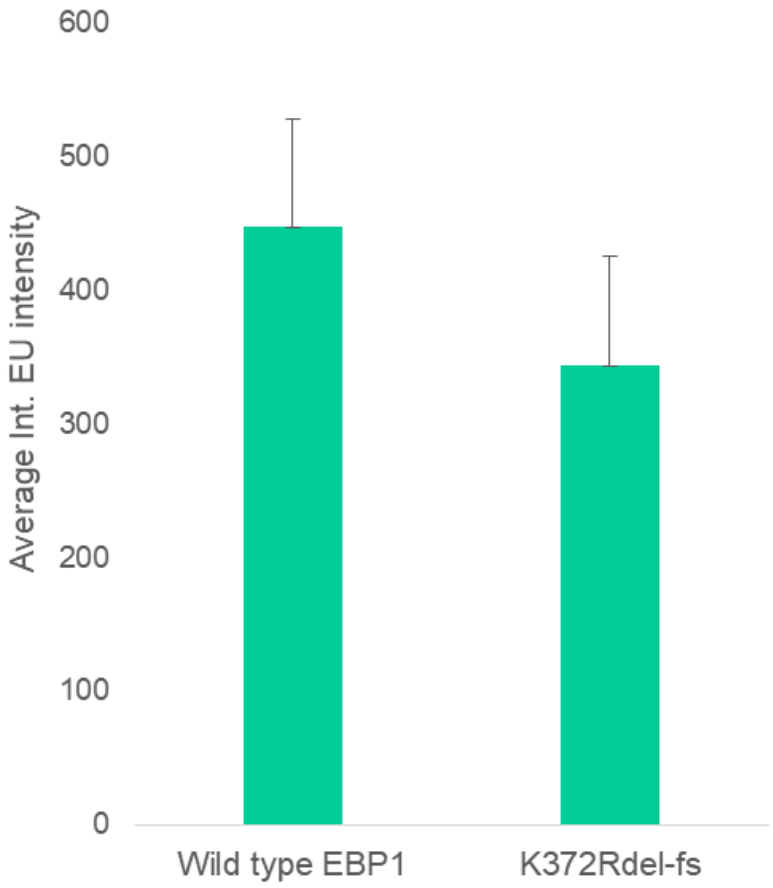

Figure 9. Average Integrated Nucleolar EU intensity. 30 GFP positive cells for each construct were analyzed through cell profiler. Bar graph showing Average Integrated Nucleolar EU intensity for EGFP-FL WT EBP1 and K372Rdel-fs mutant. EGFP-FL WT EBP1 had a higher intensity (447.86 $\pm$ SD) than K372Rdel-fs tumor mutant (344.18 $\pm$ SD) as seen above. Graph represents two biological repeats.

CRISPR/CAS editing of *PA2G4*

In parallel, we tried to generate a *PA2G4* gene knocked out cell line by CRISPR/CAS. By using ENSMBL genome browser an early exon on the gene was identified and we used CHOPCHOP to design a gRNA that would target that exon of the gene, with the lowest off target possibilities and the highest efficiency. Figure 10 A and B shows CHOP-CHOP output. Top 10 scoring gRNA target sites are shown in table attached with Figure 10 A. As depicted by the table, the only coding region in the gene which is targeted by our gRNA was on *exon* 2 (rank 2). For our CRISPR/CAS experiments, we applied the gRNA targeting approximately the middle of exon 2 (5'GGGTTGGCACCTACTTCTGCTGG 3') which also harbored the restriction site for N1aIV (Figure 11). Successful transfection of the CRISPR/CAS9 ribonucleoprotein complex in HEK293T cells should result in the double strand break in *PA2G4* gene.

A

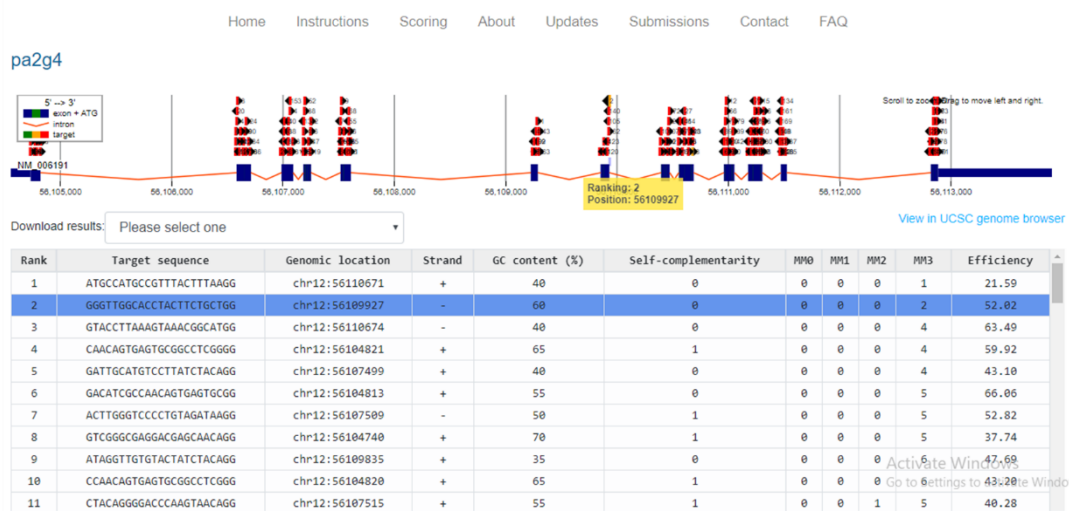

Rank	Target sequence	Genomic location	Strand	GC content (%)	Self-complementarity	MM0	MM1	MM2	MM3	Efficiency
1	ATGCCATGCCGTTTACTTTAAGG	chr12:56110671	+	40	0	0	0	0	1	21.59
2	GGGTTGGCACCTACTTCTGCTGG	chr12:56109927	-	60	0	0	0	0	2	52.02
3	GTACCTTAAAGTAAACGGCATGG	chr12:56110674	-	40	0	0	0	0	4	63.49
4	CAACAGTGAGTGCGGCCTCGGGG	chr12:56104821	+	65	1	0	0	0	4	59.92
5	GATTGCATGTCCTTATCTACAGG	chr12:56107499	+	40	0	0	0	0	4	43.10
6	GACATCGCCAACAGTGAGTGCGG	chr12:56104813	+	55	0	0	0	0	5	66.06
7	ACTTGGGTCCCCTGTAGATAAGG	chr12:56107509	-	50	1	0	0	0	5	52.82
8	GTCGGGCGAGGACGAGCAACAGG	chr12:56104740	+	70	1	0	0	0	5	37.74
9	ATAGGTTGTGTACTATCTACAGG	chr12:56109835	+	35	0	0	0	0	5	47.69
10	CCAACAGTGAGTGCGGCCTCGGG	chr12:56104820	+	65	1	0	0	0	5	43.20
11	CTACAGGGGACCCAAGTAACAGG	chr12:56107515	+	55	1	0	0	1	5	40.28

B

Figure 10. Exon 2 Identification on *PA2G4* gene using CHOP-CHOP tool and selection of potential off targets. A: CHOP-CHOP utilized to identify target sites on *PA2G4* gene with exon 2 (Ranking 2, highlighted by yellow box) being the most efficient target site (shown in the table, highlighted blue). **B**: Further information on exon 2, target site shown in red circle.

A

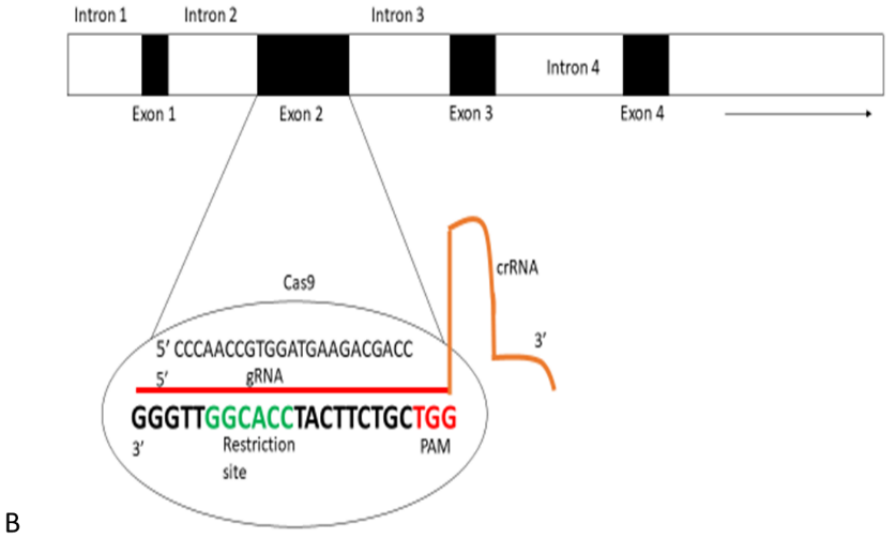

B

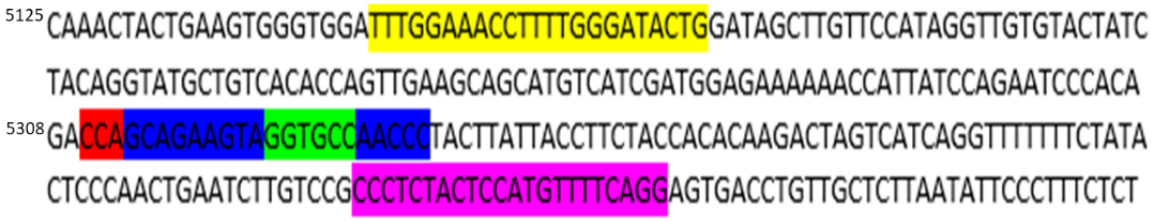

Figure 11. Schematic representation of *PA2G4* gene and Cripsr/Cas mediated genome editing. A: Cartoon diagram of *PA2G4* showing the first 4 of the 13 exons and adjacent introns. Exon 2 has been further magnified highlighting the sequence targeted by the crRNA for CRISPR/Cas9 editing. **B**: Part of the DNA sequence of *PA2G4* (5125-5491 bp) and exon 2 (at 5308 bp) with the crRNA shown in blue, restriction site highlighted in green, PAM in red and forward (yellow) and reverse (purple) primers. PAM: Protospacer adjacent motif. CrRNA: CRISPR RNA

Selection of positive clones by FACS.

Following transfection of HEK293T cells with the gRNA/CAS9 ribonucleoprotein complex, the positive cells were sorted using Fluorescence assisted cell sorting (FACS). First they were sorted as Cas9-GFP fluorescent and Atto-red-g RNA m-cherry fluorescent cells and re-plated in 1-2 wells of a 6 well plate and then FACS single cell sorting was done on 5 96 well plates. Figure 12 A, B,C and D show the screening results by FACS and D highlights the EGFP-Cas9/Atto-red gRNA positive cells A total of 37 clones were able to grow from the 5 96 well plates and further expanded on 48, 24, 12, 6 well plates until we reached 10 cm dish. Each clone was allocated an ID to keep track.

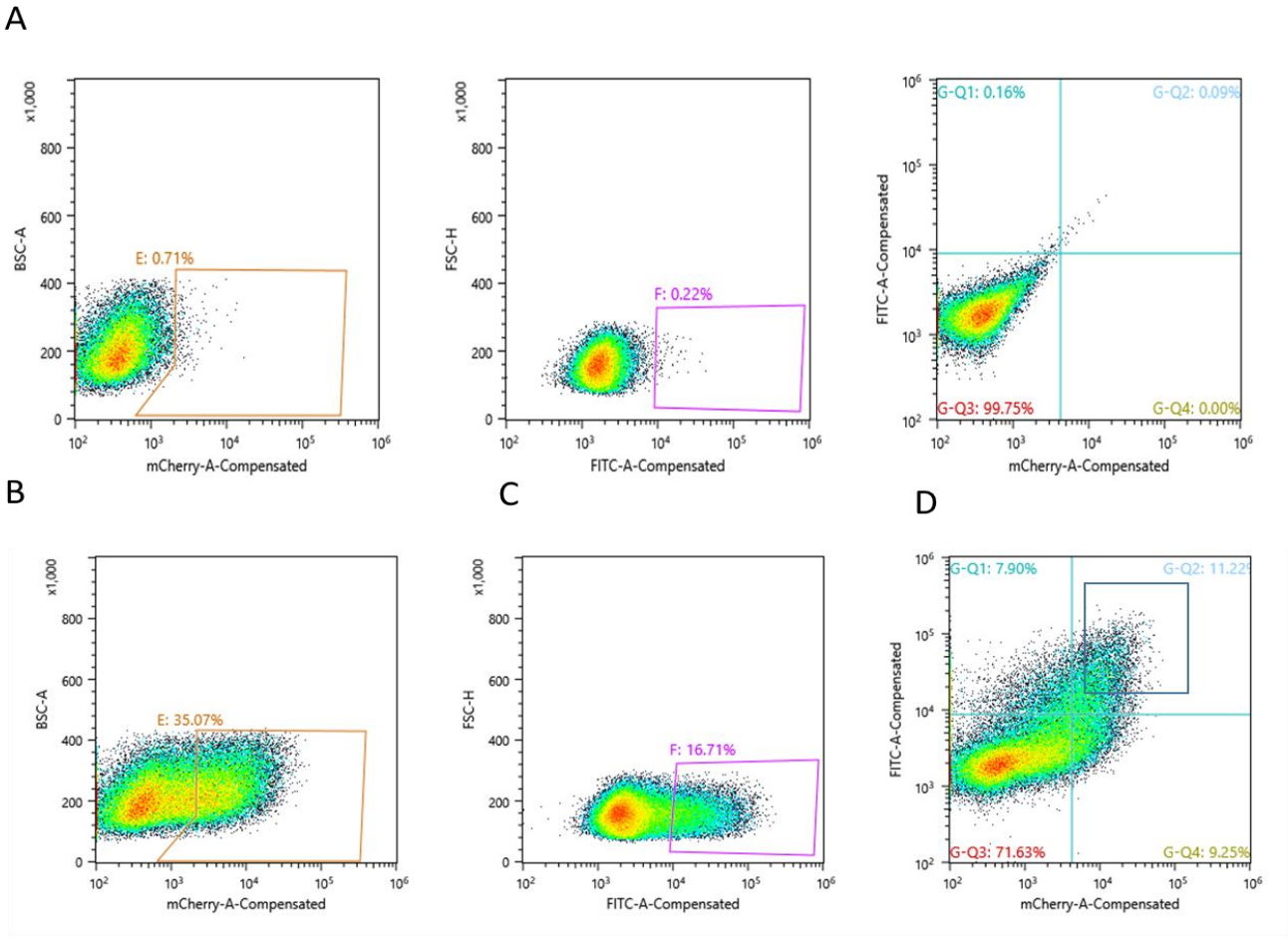

Figure 12. Cell sorting by FACS of Cas9/gRNA positive HEK293T cells. HEK293T cells were transfected with ribonucleoprotein complex and first sorted in 1-2 wells of a 6 well plate and then FACS single sorted. A: Wild type HEK-293 cells. **B**: EGFP-Cas9 positive HEK-293 cells **C**: Atto-red gRNA positive cells marked by m-cherry fluorescence and **D**: Cas9/ gRNA positive cells both green (FITC compensated) and red (m-cherry-A compensated): Area shown by blue box.

PCR amplification, restriction digestion, DNA sequencing and immunoblotting.

Cell lysates from a few clones were used to generate the templates for PCR amplification followed by agarose gel electrophoresis and PCR product purification. The clones S3 and M3 showed a light PCR between 200 and 300 marker matching the size of 244 bp expected product. (Figure 13 A). Figure 13 B shows amplification of a few other clones. M3 and S3 were purified and digested with the NIaIV restriction endonuclease (Figure 13 C) and sequenced. Restriction gel revealed two products at expected 101 bp and 143 bp for each clone if the restriction site was kept intact, this would likely suggest that M3 and S3 are wild type. Figure 14 A shows the S3 and M3 sequences with target site and cut off sequence and B1 and B2 shows the sequencing results of the parts of S3 and M3 DNA respectively The chromatograms revealed both clones to be wild type with no expected change.

We first followed the approach of analyzing DNA followed by western blotting to check expression of the clones which was not feasible hence decided to re-direct to first immunoblot and then if there is any positive result, follow on with the PCR purification and digestion. Therefore we performed the immune blot of clones C2 and C3 as they showed a strong band for PCR amplification (Figure 13 B). Cell extracts were collected using RIPA buffer and sonicated followed by centrifugation and resolving on SDS PAGE. 30 µg of protein for each clone was resolved and transferred overnight for western blotting (Figure 15).There was reduction at protein for C2 but C3 seemed to have increased. Other clones which were not amplified by PCR but only checked for protein reduction were G1, 1v and 2v and all had a lower expression (checked against Lamin A/c). Band for 2v was also found to be slightly lower than WT and its lower expression suggests an in-frame deletion. C31 did not have any band when amplified and resolved on agarose gel (result not shown) but was reduced at protein level (Figure 15). The clones were not subjected to restriction digestion.

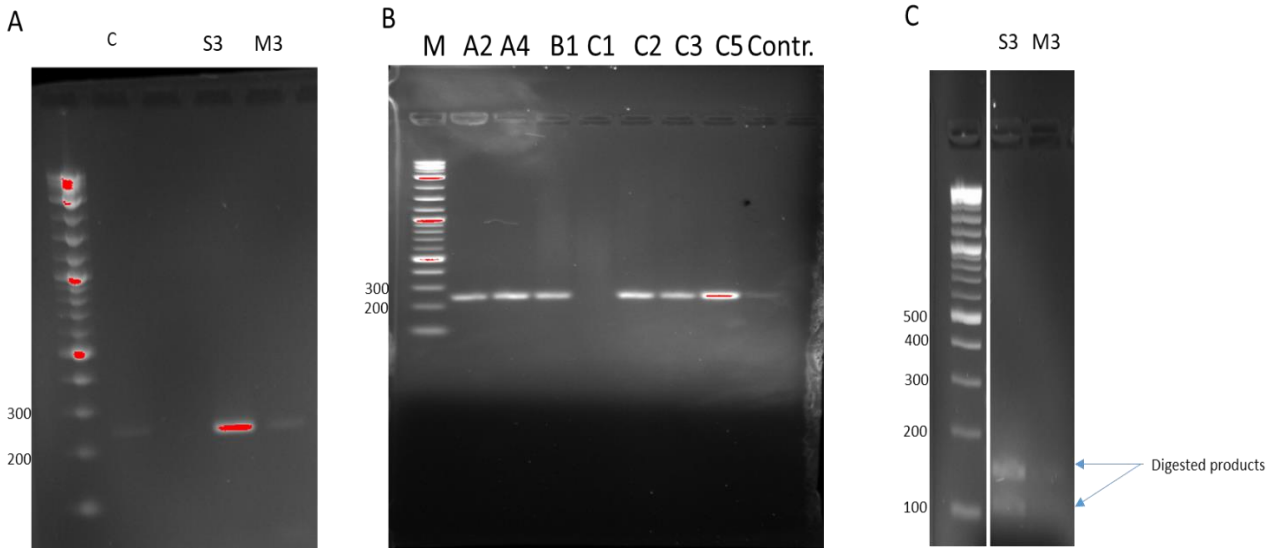

Figure 13. PCR amplification and restriction digestion of CRISPR clones. **A:** PCR amplification of S3 and M3 clones on 2% agarose gel. M3 and S3 observed between 200 and 300 bp which matches the expected product size i.e 244 bp. **B:** PCR amplification of A2, A4, B1, C1, C3 and C5 clones with HEK293 control cell lystate resolved on a 2% agarose gel. **C:** Restriction digestion of S3 and M3 with N1aIV and PCR products resolved on 3.5% agarose gel with two products seen at 102 and 143 bp for each clone

A

S3

NNNNNNNNNNNNNNTTGTGTACTATCTACAGGTATGCTGTCACACCAGTTGAAGCAGCATGTCATCGATGGAGAA
AAAACCATTATCCAGAATCCCACAGACCAGCACAAGTAGGTGCCAACCCTACTTATTACCTTCTACCACACAAGA
CTAGTCATCAGGTTTTTTTCTATACTCCCAACTGAATCTTGTCCGCCCTCTACTCCATGTTTTCAGGNAAGTTTT
ACAGTAGAGGTANGACTTTCTTGGNNTTNGCTGCNTTTCCTCCGAGGGACCNATGAATACATTATCATNTTTCAT
CTAGCCTGATTATGTCTCNAAACACAAGNAGGTGGCTGTTTANGNGCCTTNTTN

M3

NCTACAGGTATGCTGTCACACCAGTTGAAGCAGCATGTCATCGATGGAGAAAAAACCATTATCCAGAATCCCACA
GACCAGCACAAGTAGGTGCCAACCCTACTTATTACCTTCTACCACACAAGACTAGTCATCAGGTTTTTTTCTATA
CTCCCAACTGAATCTTGTCCGCCCTCTACTCCATGTTTTCAGGA

Figure 14. Schematic diagram of S3 and M3 sequences and DNA sequencing chromatograms. A: S3 and M3 sequences shown with gRNA site highlighted in green and PAM in red. Cas9 cleavage downstream PAM sequence and 3 nucleotides after GCA (light blue)**. B:** DNA chromatograms of parts of S3 (B1) and M3 (B2) DNA sequencing respectively. PAM cut off at CCA (shown by black lines, S3 at 102 bp and M3 at 78 bp).

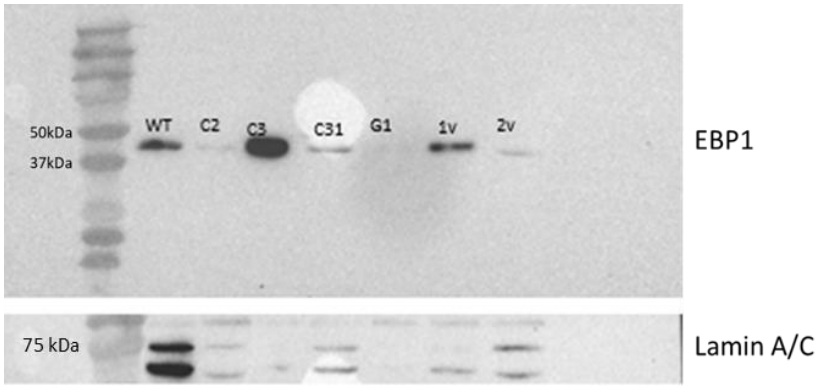

Figure 15. Protein expression of Crispr/Clones by western blot. Cell lysates from the indicated clones were checked for protein reduction by immunoblotting against wild type using an anti-EBP1 antibody and anti-Lamin A/C used as the loading control.

Discussion

Previously, EBP1 has been identified as a potential PtdIn(4,5)P_2 binding protein by combining PtdIns(4,5)P_2 pull down from neomycin displaced nuclear proteins and quantitative MS (Lewis et al, 2011). In this present study, we first reconfirmed the contributing role of C terminal motif to the nucleolar localization of EBP1 in AU565 cells (Karlsson et al, 2016). EBP1 doesn't harbor PPIn binding motifs such as PH, PX or FYE domains (Lemmon, 2008) but stretches of basic amino acids at C and N terminus producing a polybasic binding motif region (PBR) following the sequence K/R-($X_{n\ =3-7}$)-KXKK, have been reported for electrostatic interactions between EBP1 and PPIns(Martin, 1998). Specifically the C terminus harbors the nucleolar retention signal (NoRs) and the nuclear export signal NES (Squatrito et al, 2004). Another protein SAP30L has also been found to harbor the nucleolar signal located C-terminus of its nuclear localization signal (NLS) and also involved in PPIn interaction (Viiri et al, 2009). When the polybasic sequence $_{120}$RRYKRHYK$_{127}$ was mutated to Alanines (all the residues), SAP30L was found to exclude from nucleolus and retain in nucleus (Viiri et al, 2006), consistent with the behavior of C- terminal PBR of EBP1. Our results were coherent with these previous findings as Wild type EBP1 with intact C-terminal motif had the highest percentage of cells with nucleolar EBP1 compared to corresponding mutants in which the PBR positive stretch of Lysine was mutated to Alanine hence the C terminal motif may provide a stronger binding probabilities to several PPIns with differently spaced phosphates on inositol ring, at least *in vitro* and also help the protein's nucleolar localization.

It had already been established that the C-terminal binding motif contributes more to nucleolar localization of EBP1 (Squatrito et al, 2004; Karlsson et al, 2016). We aimed to find out the effect of this interaction on the function of EBP1 with respect to rDNA transcription and ribosome biogenesis. The results showed that Full length Wild type EBP1 not only localized more strongly into the nucleolus but its localization also correlated with the presence of nascent RNA including the rRNA as labelled by EU compared to mutant constructs. C-terminal mutant also showed lower nucleolar EU signal than N-terminal mutant hence aligning with the stronger binding of EBP1 with PPIns when it is intact as stated earlier. It had also been speculated that EBP1 interferes with the rRNA synthesis. Nyugen et al, 2015 for the first time demonstrated the inhibitory action of mycophenolic acid (MPA) on GTP which affected the interaction of TIF-IA factor with Ebp1 which played a key role in regulating PCNA (proliferating cell nuclear antigen) and rRNA synthesis. Similarly Squatrito et al, 2004 demonstrated EBP1 as a part of ribonucleoprotein (RNP), suggesting that its localization, interaction with RNP and proliferation inhibition are tightly connected.

EBP1 has been documented to be involved in cancer development extensively. While p42 isoform has shown to be a tumor suppressor, the pro-oncogenic characteristics of p48 has been documented in various cancers (Santegoets et al., 2007; Kim et al., 2010; Ko et al, 2015; Nguyen et al., 2016; Nguyen et al 2018). The synthesis of pre-ribosomal RNA which reflects the overall transcription of RNA is increased in various human cancers and is indeed one of the hall marks of tumor (Pelletier et al, 2018). K372Rdel-frameshift tumor mutant when analyzed against Full length Wild type Ebp1, not only showed an enhanced nucleolar signal but also more than 90% of the transfected cells had a stronger nucleolar EU suggesting higher rRNA levels. The encoded shorter, yet more positive protein harboring additional Arginine and Lysine due to the K372R mutation may offer stronger PPIn binding chance, hence stronger nucleolar localization. Moreover addition of prolines might also have a stabilization effect leading to a greater retention in the nucleolus (Yutani et al, 1991). This stronger retention and localization could have had enhanced the rRNA synthesis through several ways which still need to be uncovered, however few identified mechanisms including TIF-90 mediated pathway as evident in colon tumor cells (Nyugen et al, 2019), or regulation of rRNA through Pol 1 activity and stabilization of PCNA as reported in Acute myelogenous leukemia cells (Nyugen et al, 2016) might be involved. The actual tumorigenic property of this mutant also needs to be verified.

K372Rdel-fs mutant also enhanced the number of nucleoli. Hypertrophy of nucleoli, manifested by their increased size and number has been correlated with increased cell proliferation rate and growth in cancer tissues (Donizy et al, 2017). Consistently, increased size and number is related with higher rRNA transcriptional activity by multiple regulating factors such as upstream binding factor (UBF), DNA topoisomerase, fibrillarin and agryophylic proteins (AgNOR), snoRNPs, and small as well as large subunit proteins (Derenzini et al, 1998; Chang et al, 2016). What effect the K372R mutation might have on EBP1 and its binding capacity needs to be further investigated, however the effect is coherent with the documented studies describing increased nucleoli number and size as hallmarks of cancer.

We hypothesized that increased nucleolar localization of K372Rdel-fs tumor mutant will enhance the intensity of EU in the nucleolus. Though as described earlier that more than 90% of the cells had nucleolar EU, the nucleoli number and size were increased, the integrated nucleolar EU intensity determined by the program contradicted our hypothesis. Full length Wild type EBP1 had a higher Int. EU intensity than the tumor mutant. Despite the contradicting results, we concluded it might be possible that EBP1 regulate rRNA synthesis by different mechanism which still needs to be uncovered and doesn't interfere directly with rRNA synthesis

The CRISPR/CAS experiment did not yield fruitful outcomes. Almost all the clones analyzed after FACS were wild type as shown by PCR amplification. The clones digested and sequenced also showed wild type nature. Some of the clones did show a reduction at protein level and one particular clone even suggests in-frame deletion, however the results are not conclusive yet. In addition, the protein extracts of the potential KO clones were collected when we had trouble with the incubators showing low CO2 levels. This was in contrast to the WT protein extract collected under normal cell growth and that may account for the different levels of protein in the clones compared to the WT sample. Due to time constraint, I was not able to further validate these or other clones. No previous study is linked with the CRISPR/CAS mediated editing of the gene, hence it will be beneficial to generate a knocked out cell line as it will help refine the study and give a more clear answer to the physiological role of EBP1.

In summary, EBP1's multifactorial role in the nucleolus have been investigated previously. It interacts with many RNAs; mRNA, rRNA, ribosomal subunits (Squatrito et al, 2004 and 2006) as well as other proteins such as Nucleolar protein nucleophosmin 1(NPM 1) promoting ribosome biogenesis (Okada et al, 2007). Its varying role in tumor development has also been reported with respect to two antagonizing isoforms however whether a friend or a foe, this still needs to be further investigated.

Concluding remarks and future perspectives

In a nutshell, we validated the more contributing role of C-terminal motif in the nucleolar localization of EBP1 in AU565 breast cancer cells which aligned with the previous findings by our group and other reports. Moreover we also proved that the nucleolar localization of EBP1 correlates with the presence of nascent rRNA in the nucleolus. We also investigated into the tumor mutant which suggests possible effect of mutated EBP1's role in cancer development through enhanced nucleolar localization and retention and increased nucleolar number as well as size. A correlation was shown between the nucleolar presence of EBP1 and rRNA synthesis, due to the C-term motif which could also be further validated by more precise methods such a as luciferase assay, though due to unfortunate circumstances of covid-19 situation, I could not continue that. In addition to, we also need to test and compare the transforming properties of the N-term and C-term PPIn binding mutants to WT EBP1. This would tie an oncogenic role of EBP1 to PPIn interaction. The question regarding the exact mechanism of EBP1 mediated rRNA synthesis still needs to be answered. Whether EBP1 retention in the nucleolus is solely due to PtdIn interaction or there is more to it? It also would be interesting to find out the exact localization of EBP1 in the nucleolus (FC/DC or GC region?). These are some of the intriguing questions that are linked with this study and need further research and investigation. We also

tried to generate a *PA2G4* knocked out cell line in order to find out the lethality if there is any due to low or no expression of its protein EBP1 on the cells. The clones collected will be further analyzed. The purpose of the KO cell lines was to stably reintroduce the different EGFP-EBP1 constructs (WT and mutants) and to test them for cell proliferation, transforming properties, rRNA synthesis.

References

AHN, J. Y., LIU, X., CHENG, D., PENG, J., CHAN, P. K., WADE, P. A., & YE, K. 2005. Nucleophosmin/B23, a nuclear PI(3,4,5)P(3) receptor, mediates the antiapoptotic actions of NGF by inhibiting CAD. *Molecular cell, 18*(4), 435–445.

AHN, J. Y., LIU, X., LIU, Z., PEREIRA, L., CHENG, D., PENG, J., WADE, P. A., HAMBURGER, A. W. & YE, K. 2006. Nuclear Akt associates with PKC-phosphorylated Ebp1, preventing DNA fragmentation by inhibition of caspase-activated DNase. *The EMBO journal,* 25**,** 2083-2095**.**

AKINMADE, D., LEE, M., ZHANG, Y. & HAMBURGER, A. W. 2007b. Ebp1-mediated inhibition of cell growth requires serine 363 phosphorylation. *International journal of oncology,* 31**,** 851-8.

ALBI E, Cataldi S, ROSSI G, MAGNI MV, J HEPTOL. 2003. A possible role of cholesterol-sphingomyelin/phosphatidylcholine in nuclear matrix during rat liver regeneration. May; 38(5): 623-8.

ALI I. U., SCHRIML, L. M., & DEAN, M. 1999. Mutational spectra of PTEN/MMAC1 gene: a tumor suppressor with lipid phosphatase activity. *Journal of the National Cancer Institute*, *91*(22), 1922–1932.

ANDERSEN, J. S., LYON, C. E., FOX, A. H., LEUNG, A. K., LAM, Y. W., STEEN, H., MANN,M. & LAMOND, A. I. 2002. Directed proteomic analysis of the human nucleolus. *Current biology,* 12**,** 1-11.

ANDERSEN, J. S., LAM, Y. W., LEUNG, A. K., ONG, S.-E., LYON, C. E., LAMOND, A. I. & MANN, M. 2005. Nucleolar proteome dynamics. *Nature,* 433**,** 77-83.

AYRAULT, O., ANDRIQUE, L., FAUVIN, D., EYMIN, B., GAZZERI, S., SEITE, P. 2006. Human tumor suppressor p14ARF negatively regulates rRNA transcription and inhibits UBF1 transcription factor phosphorylation. *Oncogene*, *25*(58), 7577–7586.

BALLA, T. 2013. Phosphoinositides: tiny lipids with giant impact on cell regulation. *Physiological reviews,* 93**,** 1019-1137.

BARLOW, C. A., LAISHRAM, R. S. & ANDERSON, R. A. 2010. Nuclear phosphoinositides: a signaling enigma wrapped in a compartmental conundrum. *Trends in cell biology,* 20**,** 25-35.

BARNA, M., PUSIC, A., ZOLLO, O., COSTA, M., KONDRASHOV, N., REGO, E., RAO,P. H., & RUGGERO, D. 2008. Suppression of Myc oncogenic activity by ribosomal protein Haplo-insufficiency. *Nature, 456*(7224), 971–975.

BLIND RD, SABLIN EP, KUCHENBECKER KM, CHIU HJ, DEACON AM, DAS D, FLETTERICK RJ, INGRAHAM HA. 2014. The signaling phospholipid PIP3 creates a new interaction surface on the nuclear receptor SF-1. Proc Natl Acad Sci U S A; 111:15054–15059.

BROSH, R. M., Jr, KARMAKAR, P., SOMMERS, J. A., YANG, Q., WANG, X. W., SPILLARE, E. A., HARRIS, C. C., & BOHR, V. A. 2001. p53 modulates the exonuclease activity of Werner syndrome protein. *The Journal of biological chemistry*, *276*(37), 35093–35102.

BOISVERT, F. M., VAN KONINGSBRUGEN, S., NAVASCEUS, J., & LAMOND, A. I. 2007. The multifunctional nucleolus. *Nature reviews. Molecular cell biology*, *8*(7), 574–585.

CARPENTER, C. L., DUCKWORTH, B. C., AUGER, K. R., COHEN, B., SCHAFFHAUSEN, B. S., & CANTLEY L. C. 1990. Purification and characterization of phosphoinositide 3-kinase from rat liver. *The Journal of biological chemistry*, *265*(32), 19704–19711.

CASTANO, E.; YILDIRIM S.; FABEROVA, V.; KRAUSOVA, A.; ULICNA, L. PAPRCKOVA, D, SZTACHO, M, HOZAK, P. 2019. Nuclear Phosphoinositides: Versatile Regulators of Genome Functions. *Cells*, *8*, 649

CAVANAUGH, A. H., HEMPLE, W. M., TAYLO, L. J., ROGALSKY V., TODOROV, G., & ROTHBLUM, L. I. (1995). Activity of RNA polymerase I transcription factor UBF blocked by Rb gene product. *Nature*, *374*(6518), 177–180.

CHANG, C. Y., LAI, M. T., CHEN Y., YANG, C. W., CHANG, H. W., LU, C. C., CHEN, C. M., CHAN, C., CHUNG, C., TSENG, C. C., HWANG, T., SHEU, J. J., & TSAI, F. J. 2016. Up-regulation of ribosome biogenesis by MIR196A2 genetic variation promotes endometriosis development and progression. *Oncotarget*, *7*(47), 76713–76725.

CHAKRABARTI, R., SANYAL S., GHOSH, A., BHAR, K., DAS C., & SIDDHANTA, A. (2015). Phosphatidylinositol-4-phosphate 5-Kinase 1α Modulates Ribosomal RNA Gene Silencing through Its Interaction with Histone H3 Lysine 9 Trimethylation and Heterochromatin Protein HP1-α. *The Journal of biological chemistry*, *290*(34), 20893–20903.

Ciarmatori, S., Scott, P. H., Sutcliffe, J. E., McLees, A., Alzuherri, H. M., Dannenberg, J. H., te Riele, H., Grummt, I., Voit, R., & White, R. J. (2001). Overlapping functions of the pRb family in the regulation of rRNA synthesis. *Molecular and cellular biology*, *21*(17), 5806–5814.

DAI, M. S., & LU, H. 2008. Crosstalk between c-Myc and ribosome in ribosomal biogenesis and cancer. *Journal of cellular biochemistry*, *105*(3), 670–677

DERENZIINI, M., TRERE, D., PESSION, A., MONTANARO, L., SIRRI, V., & OCHS, R. L. 1998. Nucleolar function and size in cancer cells. *The American journal of pathology*, *152*(5), 1291–1297.

DI PAOLO, G. & DE CAMILLI, P. 2006. Phosphoinositides in cell regulation and membrane dynamics. *Nature*, 443**,** 651-657.

DONIZY, P., BIECEK, P., HALON, A., MACIEJCZYK, A., & MATKOWSKI, R. 2017. Nucleoli cytomorphology in cutaneous melanoma cells - a new prognostic approach to an old concept. *Diagnostic pathology*, *12*(1), 88.

DRAKAS R, TU X, BASERGA R. 2004 Control of cell size through phosphorylation of upstream binding factor 1 by nuclear phosphatidylinositol 3-kinase. Proceedings of the National Academy of Sciences of the United States of America. 101(25):9272-9276

EHM, P., NALASKOWSKI, M. M., WUNDENBERG, T., & JUCKER, M. 2015. The tumor suppressor SHIP1 co-localizes in nucleolar cavities with p53 and components of PML nuclear bodies. *Nucleus (Austin, Tex.), 6*(2), 154–164.

ENGLEMAN JA. 2009 Targeting PI3K signaling in cancer: opportunities, challenges and limitations. *Nat Rev Cancer*.; 9(8):550-562.

FALKENBURGER BH, JENSEN JB, DICKSON EJ, SUH BC, HILLE B 2010. Phosphoinositides: lipid regulators of membrane proteins. *J Physiol*; 588(Pt 17): 3179-3185.

Fatemeh Mazloumi Gavgani, Thomas Karlsson, Ingvild L Tangen, Andrea Papdiné Morovicz, Victoria Smith Arnesen, Diana C. Turcu, Camilla Krakstad, Julie Guillermet-Guibert, Aurélia E Lewis. 2019. Nuclear upregulation of PI3K p110β correlates with increased rRNA transcription in endometrial cancer cells. *Pre-print.

FENG Y, SASSI S, SHEN JK, YANG XQ, GAO Y, OSAKA E 2015. Targeting Cdk11 in Osteosarcoma Cells Using the CRISPR-cas9 System. *Journal of Orthopaedic Research*. ; 33

FELTON-EDKINS, Z. A., KENNETH, N. S., BROWN, T. R., DALY, N. L., GOMEZ ROMAN, N., GRANDORI, C., EISENMAN, R. N., & WHITE, R. J. 2003. Direct regulation of RNA polymerase III transcription by RB, p53 and c-Myc. *Cell cycle (Georgetown, Tex.), 2*(3), 181–184

FIUME R., KEUNE W.J., FAENZA I., BULTSUMA Y., RAMAZZOTI G., JONES D.R., MARTELLI A.M., SOMMER L., FOLLO M.Y., DIVECHA N., COCCO 2012. L. Nuclear phosphoinositides: location, regulation and function. Subcell. Biochem. 59:335–361.

FIUME, R., STIJF-BULTSMA, Y., SHAH, Z. H., KEUNE, W. J., JONES, D. R., JUDE,J. G. & DIVECHA, N. 2015. PIP4K and the role of nuclear phosphoinositides in tumour suppression. *Biochim Biophys Acta,* 1851**,** 898-910.

FIUME, R., FAENZA, I., SHETH, B.; POLI, A.; VIDALLE M.C.; MAZZETTI, C.; ABDUL, S.H.; CAMPAGNOLI, F.;FABBRINI ,M.; KIMBER S.T. 2019, Nuclear Phosphoinositides: Their Regulation and Roles in Nuclear functions. *Int. J. Mol. Sci., 20*.

FOLLO MY, MANZOLI L, POLI A, McBUREY JA, COCCO L. 2015. PLC and PI3K/Akt/mTOR signaling in disease and cancer. *Adv Biol Regul*. ; 57:10-16.

FRUMAN, D. A., & ROMMEL, C. (2014). PI3K and cancer: lessons, challenges and opportunities. *Nature reviews. Drug discovery*, *13*(2), 140–156.

GANOT, P., JÁDY, B. E., BORTOLIN, M.-L., DARZACQ, X. & KISS, T. 1999. Nucleolar factors direct the 2′-O- ribose methylation and pseudouridylation of U6 spliceosomal RNA. *Molecular and cellular biology,* 19**,** 6906-6917.

GANNON, P. O., KOUMAKPAYI, I. H., LE PAGE, C., KARAKIEWICZ, P. I., MES-MASSON, A.-M. & SAAD, F. 2008. Ebp1 expression in benign and malignant prostate. *Cancer Cell Int,* 8**,** 18.

GILLOOLY, D. J., MORROW, I. C., LINDSAY, M., GOULD, R., BRYANT, N. J., GAULLIER, J. M., PARTON, R. G., & STENMARK, H. 2000. Localization of phosphatidylinositol 3-phosphate in yeast and mammalian cells. *The EMBO journal*, *19*(17), 4577–4588.

GOMEZ-ROMAN, N., FELTON-EDKINS, Z. A., KENNETH, N. S., GOODFELLOW, S. J., ATHNIOS, D., ZHANG, J., RAMSBOTTOM, B. A., INNES, F., KANTIDAKIS, T., KERR, E. R., BRODIE, J., GRANDORI, C., & WHITE, R. J. 2006. Activation by c-Myc of transcription by RNA polymerases I, II and III. *Biochemical Society symposium*, (73), 141–154.

GRANDORI, C., GOMEZ-ROMAN, N., FELTON-EDKINS, Z. A., NGOUENET, C., GALLOWY, D. A., EISENMAN, R. N., & WHITE, R. J. (2005). c-Myc binds to human ribosomal DNA and stimulates transcription of rRNA genes by RNA polymerase I. *Nature cell biology*, *7*(3), 311–318.

GRISENDI, S., BERNARDI, R., ROSSI, M., CHENG, K., KHANDKER, L., MANOVA, K., & PANDOLFI, P. P. 2005. Role of nucleophosmin in embryonic development and tumorigenesis. *Nature*, *437*(7055), 147–153.

GRUMMT I 2013. The nucleolus-guardian of cellular homeostasis and genome integrity. *Chromosoma* 122:487–497

HAMBURGER, A. W. 2008. The role of ErbB3 and its binding partners in breast cancer progression and resistance to hormone and tyrosine kinase directed therapies. *Journal of mammary gland biology and neoplasia,* 13**,** 225-233.

HANNAN, K. M., HANNAN, R. D., SMITH, S. D., JEFFERSON, L. S., LUN, M., & ROTHBLUM, L. I. 2000. Rb and p130 regulate RNA polymerase I transcription: Rb disrupts the interaction between UBF and SL-1. *Oncogene*, *19*(43), 4988–4999.

HANAHAN D, WEINBERG RA. 2000. The hallmarks of cancer. *Cell*.; 100(1):57-70.

HE, H.-C., LING, X.-H., ZHU, J.-G., FU, X., HAN, Z.-D., LIANG, Y.-X., DENG, Y.-H., LIN, Z.-Y., CHEN, G. & CHEN, Y.-F. 2013. Down-regulation of the ErbB3 binding protein 1 in human bladder cancer promotes tumor progression and cell proliferation. *Molecular biology reports*, 40**,** 3799-3805.

HEISS, N. S., GIROD A., SALOWSKY, R., WIEMANN, S., PEPPERKOK, R., & POUSTKA, A. (1999). Dyskerin localizes to the nucleolus and its mislocalization is unlikely to play a rolein the pathogenesis of dyskeratosis congenita. *Human molecular genetics*, *8*(13), 2515–2524.

HELGASON, C. D., DAMEN, J. E., ROSTEN, P., GREWAL, R., SORENSEN, P., CHAPPEL, S. M., BOROWSKI, A., JIRIK, F., KRYSTAL, G., & HUMPIRES, R. K. 1998. Targeted disruption of SHIP leads to hemopoietic perturbations, lung pathology, and a shortened life span. *Genes & development*, *12*(11), 1610–1620.

HENRAS, A. K., SOUDET, J., GERUS, M., LEBARON, S., CAIZERGEUS-FERRER, M., MOUGIN, A., & HENRY, Y. 2008. The post-transcriptional steps of eukaryotic ribosome biogenesis. *Cellular and molecular* life *sciences: CMLS*, *65*(15), 2334–2359.

HOKIN MR, HOKIN LE 1953. Enzyme secretion and the incorporation of P32 into phospholipids of pancreas slices. *J Biol Chem* 203: 967-977**.**

HONDA, A and ISHIHAMA, A. 2004. Structure-function relationships of influenza virus RNA polymerase. In: Options for Control of Influenza Virus. 1263, 21-24

HORVATH, B. M., MAGYAR, Z., ZHANG, Y., HAMBURGER, A. W., BAKO, L., VISSER, R. G., BACHEM, C. W. & BÖGRE, L. 2006. EBP1 regulates organ size through cell growth and proliferation in plants. *The EMBO Journal,* 25**,** 4909-4920.

HUNT A.N. 2006. Dynamic lipidomics of the nucleus. *J. Cell. Biochem.* ; 97:244–251.

HU, B., XIONG, Y., NI, R., WEI, L., JIANG, D., WANG, G., WU, D., XU, T., ZHAO, F. & ZHU, M. 2014. The downregulation of ErbB3 binding protein 1 (EBP1) is associated with poor prognosis and enhanced cell proliferation in hepatocellular carcinoma. *Molecular and cellular biochemistry,* 396**,** 175-185.

Ishikawa, S., Egami, H., Kurizaki, T., Akagi, J., Tamori, Y., Yoshida, N., Tan, X., Hayashi, N., & Ogawa, M. (2003). Identification of genes related to invasion and metastasis in pancreatic cancer by cDNA representational difference analysis. *Journal of experimental & clinical cancer research: CR*, *22*(2), 299–306.

Ilboudo, A., Nault, J. C., Dubois-Pot-Schneider, H., Corlu, A., Zucman-Rossi, J., Samson, M, & Le Seyec, J. (2014). Overexpression of phosphatidylinositol 4-kinase type IIIα is associated undifferentiated status and poor prognosis of human hepatocellular carcinoma. *BMC cancer*, *14*, 7

JACOBSEN, R.G.; MAZLOUMI GAVGANI, F.; EDSON, A.J.; GORIS, M.; ALTANKHUYAG, A.; LEWIS, A.E 2019. Polyphosphoinositides in the Nucleus: Roadmap of Their Effectors and Mechanisms of Interaction. *Adv. Biol. Regul.* 7–21

J. VAN RIGELLEN, A. YETIL, D.W. FELSHER. 2010. MYC as a regulator of ribosome biogenesis and protein synthesis, *Nat. Rev.* Cancer 4 301–309

KAKUK, A., FRIEDLĂNDER E., VEREB, G., Jr, KÁSA, A., BALLA, A., BALLA, T., HEILMEYER, L. M., Jr, GERGLEY, P., & VEREB, G. (2006). Nucleolar localization of phosphatidylinositol 4-kinase PI4K230 in various mammalian cells. *Cytometry. Part A: the journal of the International Society for Analytical Cytology*, *69*(12), 1174–1183.

KAKUK, A., FRIEDLANDER, E., VEREB, G., Jr, LISBOA, D., BAGOSSI, P., TOTH, G., GERGLEY, P., & VEREB, G. (2008). Nuclear and nucleolar localization signals and their targeting function in phosphatidylinositol 4-kinase PI4K230. *Experimental cell research*, *314*(13), 2376–2388.

Kalasova, I., Fáberová, V., Kalendová, A., Yildirim, S., Uličná, L., Venit, T., & Hozák, P. (2016). Tools for visualization of phosphoinositides in the cell nucleus. *Histochemistry and cell biology*, *145*(4), 485–496.

Karlsson, T., Altankhuyag, A., Dobrovolska, O., Turcu, D. C., & Lewis, A. E. (2016). A polybasic motif in ErbB3-binding protein 1 (EBP1) has key functions in nucleolar localization and polyphosphoinositide interaction. *The Biochemical journal*, *473*(14), 2033–2047.

Katan, M., Rodriguez, R., Matsuda, M., Newbatt, Y. M., & Aherne, G. W. (2003). Structural and mechanistic aspects of phospholipase Cgamma regulation. *Advances in enzyme regulation*, *43*, 77–85

Kennah, M., Yau, T. Y., Nodwell, M., Krystal, G., Andersen, R. J., Ong, C. J., & Mui, A. L. 2009. Activation of SHIP via a small molecule agonist kills multiple myeloma cells. *Experimental hematology*, *37*(11), 1274–1283.

KIM, C. K., NGUYEN, T. L., JOO, K. M., NAM, D.-H., PARK, J., LEE, K.-H., CHO, S.-W. & AHN, J.-Y. 2010. Negative regulation of p53 by the long isoform of ErbB3 binding protein Ebp1 in brain tumors. *Cancer research,* 70**,** 9730-9741.

KIM, C. K., LEE, S. B., NGUYEN, T. L., LEE, K.-H., UM, S. H., KIM, J. & AHN, J.-Y. 2012. Long isoform of ErbB3 binding protein, p48, mediates protein kinase B/Akt-dependent HDM2 stabilization and nuclear localization. *Experimental cell research,* 318**,** 136-143.

KOWALINSKI, E., BANGE, G., BRADATSCH, B., HURT, E., WILD, K. & SINNING, I. 2007. The crystal structure of Ebp1 reveals a methionine aminopeptidase fold as binding platform for multiple interactions. *FEBS letters,* 581**,** 4450-4454.

KO, H. R., KIM, C. K. & AHN, J. Y. 2014. Phosphorylation of the N-terminal domain of p48 Ebp1 by CDK2 is required for tumorigenic function of p48. *Molecular carcinogenesis*.

KO, H. R., CHANG, Y. S., PARK, W. S., & AHN, J. Y. 2016. Opposing roles of the two Isoforms of ErbB3 binding protein 1 in human cancer cells. *International journal of cancer*, *139*(6), 1202–1208.

Kumar, A., Redondo-Muñoz, J., Perez-García, V., Cortes, I., Chagoyen, M., & Carrera, A. 2011. Nuclear but not cytosolic phosphoinositide 3-kinase beta has an essential function in cell survival. *Molecular and cellular biology*, *31*(10), 2122–2133.

LAMARTINE, J., SERI, M., CINTI, R., HEITZMANN, F., CREAVEN, M., RADOMSKI, N., JOST, E., LENOIR, G., ROMEO, G. & SYLLA, B. 1997. Molecular cloning and mapping of a human cDNA (PA2G4) that encodes a protein highly homologous to the mouse cell cycle protein p38-2G4.*Cytogenetic and Genome Research,* 78**,** 31-35.

LATONEN, L., MOORE, H., BAI, B., JÄÄMAA, S. & LAIHO, M. 2011. Proteasome inhibitors induce nucleolar aggregation of proteasome target proteins and polyadenylated RNA by altering ubiquitin availability. *Oncogene,* 30**,** 790-805.

LEMMON M. A. 2008. Membrane recognition by phospholipid-binding domains. *Nature reviews. Molecular cell biology*, *9*(2), 99–111.

LESSOR, T. J. & HAMBURGER, A. W. 2001. Regulation of the ErbB3 binding protein Ebp1 by protein kinase C. *Molecular and cellular endocrinology,* 175**,** 185-191.

LESSOR, T. J., YOO, J. Y., XIA, X., WOODFORD, N. & HAMBURGER, A. W. 2000. Ectopic expression of the ErbB-3 binding protein ebp1 inhibits growth and induces differentiation of human breast cancer cell lines. *Journal of cellular physiology,* 183**,** 321-329.

LESLIE, N. R. & DOWNES, C. P. 2002. PTEN: The down side of PI 3-kinase signalling. *Cell Signal,* 14**,** 285-95.

Lewis, A. E., Sommer, L., Arntzen, M. Ø., Strahm, Y., Morrice, N. A., Divecha, N., & D'Santos, C. S. (2011). Identification of nuclear phosphatidylinositol 4,5-bisphosphate-interacting proteins by neomycin extraction. *Molecular & cellular proteomics : MCP*, *10*(2), M110.003376.

LI, M., BROOKS, C. L., WU-BAER, F., CHEN, D., BAER, R. & GU, W. 2003. Mono-versus polyubiquitination: differential control of p53 fate by Mdm2. *Science,* 302**,** 1972-1975

LINDSTRÖM M. S. 2009. Emerging functions of ribosomal proteins in gene-specific transcription and translation. *Biochemical and biophysical research communications, 379*(2), 167–170.

Ling, K., Schill, N. J., Wagoner, M. P., Sun, Y., & Anderson, R. A. (2006). Movin' on up: the role of PtdIns(4,5)P(2) in cell migration. *Trends in cell biology, 16*(6), 276–284

LIU, Z., AHN, J.-Y., LIU, X. & YE, K. 2006. Ebp1 isoforms distinctively regulate cell survival and differentiation. *Proceedings of the National Academy of Sciences,* 103**,** 10917-10922.

LIU, J.-L., SHENG, X., HORTOBAGYI, Z. K., MAO, Z., GALLICK, G. E. & YUNG, W. A. 2005. Nuclear PTEN-mediated growth suppression is independent of Akt down-regulation. *Molecular and cellular biology,* 25**,** 6211-6224.

LOWE, S. W., & SHERR, C. J. 2003. Tumor suppression by Ink4a-Arf: progress and puzzles. *Current opinion in genetics & development*, *13*(1), 77–83.

MAEHEMA T. (2007). PTEN: its deregulation and tumorigenesis. *Biological & pharmaceutical bulletin, 30*(9), 1624–1627.

MAFFUCCI, T. 2012. An introduction to phosphoinositides. *Curr Top Microbiol Immunol,* 362**,** 1-42.

MARCINIAK, R. A., LOMBARD, D. B., JOHNSON, F. B. & GUARENTE, L. Nucleolar localization of the Werner syndrome protein in human cells. 1998. *Proc. Natl Acad*. Sci. USA 95, 6887–6892.

MARTINDILL, D. M., RISEBRO, C. A., SMART, N., FRANCO-VISERAS, M. D. M., ROSARIO, C. O., SWALLOW, C. J., DENNIS, J. W. & RILEY, P. R. 2007. Nucleolar release of Hand1 acts as a molecular switch to determine cell fate. *Nature cell biology,* 9**,** 1131-1141.

MARTIN T.F. 1998. Phosphoinositide lipids as signaling molecules: common themes for signal transduction, cytoskeletal regulation, and membrane trafficking. *Annu. Rev. Cell Dev.* Biol. ; 14:231–264

MASUDA, S., DAS, R., CHENG, H., HURT, E., DORMAN, N. & REED, R. 2005. Recruitment of the human TREX complex to mRNA during splicing. *Genes & development,* 19**,** 1512-1517.

MAYER, C., BIERHOFF, H. & GRUMMT, I. 2005. The nucleolus as a stress sensor: JNK2 inactivates the transcription factor TIF-IA and down-regulates rRNA synthesis. *Genes & development,* 19**,** 933-941

MEI, Y., ZHANG, P., ZUO, H., CLARK, D., XIA, R., LI, J., LIU, Z. & MAO, L. 2014. Ebp1 activates podoplanin expression and contributes to oral tumorigenesis. *Oncogene*, 33**,** 3839-3850.

MICHELL R.H., HEATH V.L., LEMMON M.A., DOVE S.K. 2006. Phosphatidylinositol 3, 5- bisphosphate: metabolism and cellular functions. *Trends Biochem. Sci.*; 31:52–63.

MITCHELL, J. R., WOOD, E. & COLLINS, K. 1999 A telomerase component is defective in the human disease dyskeratosis congenita. Nature 402, 551–555

MONIE, T. P., PERRIN, A. J., BIRTLEY, J. R., SWEENEY, T. R., KARAKASILIOTIS, I., CHAUDHRY, Y., ROBERTS, L. O., MATTHEWS, S., GOODFELLOW, I. G. & CURRY, S. 2007. Structural insights into the transcriptional and translational roles of Ebp1. *The EMBO journal,* 26**,** 3936-3944.

Montanaro, L., Brigotti, M., Clohessy, J., Barbieri, S., Ceccarelli, C., Santini, D., Taffurelli, M., Calienni, M., Teruya-Feldstein, J., Trerè, D., Pandolfi, P. P., & Derenzini, M. 2006. Dyskerin expression influences the level of ribosomal RNA pseudo-uridylation and telomerase RNA component in human breast cancer. *The Journal of pathology*, *210*(1), 10–18.

Moss, T., Langlois, F., Gagnon-Kugler, T., & Stefanovsky, V. 2007. A housekeeper with power of attorney: the rRNA genes in ribosome biogenesis. *Cellular and molecular life sciences: CMLS*, *64*(1), 29–49.

Naoe, T., Suzuki, T., Kiyoi, H., & Urano, T. (2006). Nucleophosmin: a versatile molecule associated with hematological malignancies. *Cancer science*, *97*(10), 963–969.

NGUYEN, L. X., LEE, Y., URBANI, L., UTZ, P., HAMBURGER, A., SUNWOO, J. & MITCHELL, B. 2015. Regulation of ribosomal RNA synthesis in T cells: requirement for GTP and Ebp1. *Blood,* 125**,** 2519.

Nguyen, l., Zhu, L., Lee, Y., Ta, L., & Mitchell, B. S. (2016). Expression and Role of the ErbB3-Binding Protein 1 in Acute Myelogenous Leukemic Cells. *Clinical cancer research: an official journal of the American Association for Cancer Research*, *22*(13), 3320–3327.

Nguyen, D. Q., Hoang, D. H., Nguyen Vo, T. T., Huynh, V., Ghoda, L., Marcucci, G., & Nguyen, L. 2018. The role of ErbB3 binding protein 1 in cancer: Friend or foe? *Journal of cellular physiology*, *233*(12), 9110–9120.

Nguyen, D. Q., Hoang, D. H., Nguyen, T., Ho, H. D., Huynh, V., Shin, J. H., Ly, Q. T., Thi Nguyen, D. D., Ghoda, L., Marcucci, G., & Nguyen, L. (2019). Ebp1 p48 promotes oncogenic activities in human colon cancer cells through regulation of TIF-90-mediated ribosomal RNA synthesis. *Journal of cellular physiology*, *234*(10), 17612–17621.

Ong, C. J., Ming-Lum, A., Nodwell, M., Ghanipour, A., Yang, L., Williams, D. E., Kim, J., Demirjian, L., Qasimi, P., Ruschmann, J., Cao, L. P., Ma, K., Chung, S. W., Duronio, V., Andersen, R. J., Krystal, G., & Mui, A. L. (2007). Small-molecule agonists of SHIP1 inhibit the phosphoinositide 3-kinase pathway in hematopoietic cells. *Blood*, *110*(6), 1942–

OU, K., KESUMA, D., GANESAN, K., YU, K., SOON, S. Y., LEE, S. Y., GOH, X. P., HOOI, M., CHEN, W. & JIKUYA, H. 2006. Quantitative profiling of drug-associated proteomic alterations by combined 2-nitrobenzenesulfenyl chloride (NBS) isotope labeling and 2DE/MS identification. *Journal of proteome research,* 5**,** 2194-2206.

Payrastre, B., Nievers, M., Boonstra, J., Breton, M., Verkleij, A. J., & Van Bergen en Henegouwen, P. M. (1992). A differential location of phosphoinositide kinases, diacylglycerol kinase, and phospholipase C in the nuclear matrix. *The Journal of biological chemistry*, *267*(8), 5078–5084.

PAYRASTRE B, MISSY K, GIURITO S, BODIN S, PLANTAVID M, GRATACAP M 2001. Phosphoinositides: key players in cell signalling, in time and space. Cell Signal; 13:377-387.

PEDERSON, T. & TSAI, R. Y. 2009. In search of non-ribosomal nucleolar protein function and regulation. *The Journal of cell biology,* 184**,** 771-776

Pelletier, J., Thomas, G. & Volarević, S. 2018. Ribosome biogenesis in cancer: new players and therapeutic avenues. *Nat Rev Cancer* **18,** 51–63

PILIPENKO EV, PESTOVA TV, KOLUPAEVA VG, KHITRINA EV, POPERECHNYA AN, AGOL VI, HELLEN CU. 2000. A cell cycle-dependent protein serves as a template-specific translation initiation factor. *Genes Dev* 14:

PINKAS-KRAMARSKI, R., ALROY, I. & YARDEN, Y. 1997. ErbB receptors and EGF-like ligands: cell lineage determination and oncogenesis through combinatorial signaling. *Journal of mammary gland biology and neoplasia,* 2**,** 97-107.

POLITZ, J. C., YAROVOI, S., KILROY, S. M., GOWDA, K., ZWIEB, C. & PEDERSON, T. 2000. Signal recognition particle components in the nucleolus. *Proceedings of the National Academy of Sciences,* 97**,** 55-60.

POLITZ, J. C. R., HOGAN, E. M. & PEDERSON, T. 2009. MicroRNAs with a nucleolar location. *Rna,* 15**,** 1705-1715.

Poortinga, G., Wall, M., Sanij, E., Siwicki, K., Ellul, J., Brown, D., Holloway, T. P., Hannan, R. D., & McArthur, G. A. (2011). c-MYC coordinately regulates ribosomal gene chromatin remodeling and Pol I availability during granulocyte differentiation. *Nucleic acids research*, *39*(8), 3267–3281.

POSTLE A.D., WILTON D.C., HUNT A.N., ATTARD G.S. 2007. Probing phospholipid dynamics by electrospray ionisation mass spectrometry. Prog. Lipid Res. 46:200–224.

R. Lewis VANN, Peter F. B. WOODING, F. Robin IRVINE, Nullin DIVECHA. 1997 Metabolism and possible compartmentalization of inositol lipids in isolated rat-liver nuclei. *Biochem J* 15; 327 (2): 569–576.

RADOMSKI, N. & JOST, E. 1995. Molecular cloning of a murine cDNA encoding a novel protein, p38-2G4, which varies with the cell cycle. *Experimental cell research,* 220**,** 434-445.

REYES-GUTIERREZ, P., RITLAND POLITZ, J. C. & PEDERSON, T. 2014. A mRNA and Cognate MicroRNAs Localize in the Nucleolus. *Nucleus,* 5**,** 636-642.

RODNINA, M. V., & WINTERMEYER, W. 2009. Recent mechanistic insights into eukaryotic ribosomes. *Current opinion in cell biology*, *21*(3), 435–443.

RUGERRO, D., & PANDOLFI, P. P. (2003). Does the ribosome translate cancer?. *Nature reviews. Cancer*, *3*(3), 179–192.

SANTEGOETS, S. J., SCHREURS, M. W., REURS, A. W., LINDENBERG, J. J., KUETER, E. W., VAN DEN EERTWEGH, A. J., HOOIJBERG, E., BRANDWIJK, R. J., HUFTON, S. E. & HOOGENBOOM, H. R. 2007. Identification and characterization of ErbB-3-binding protein-1 as a target for immunotherapy. *The Journal of Immunology,* 179**,** 2005-2012

SBRISSA D, SEMANN L, YANGFEG L, SHISHEVA A, CHINNI SR. 2015. Abstract 5162: phosphatidylinositol 4-kinase type IIIa (PI4KA) expression in prostate cancer. Cancer Res.; 75:5162–5162.

SCHERL, A., COUTÉ, Y., DÉON, C., CALLÉ, A., KINDBEITER, K., SANCHEZ, J.-C., GRECO, A., HOCHSTRASSER, D. & DIAZ, J.-J. 2002. Functional proteomic analysis of human nucleolus. *Molecular biology of the cell,* 13**,** 4100-4109.

SCHRAMP M., HEDMAN A., LI W., TAN X., ANDERSON R. 2012. PIP kinases from the cell membrane to the nucleus. *Subcell. Biochem.* 58:25–59

SHAH, Z. H., JONES, D. R., SOMMER, L., FOULGER, R., BULTSMA, Y., D'SANTOS, C. & DIVECHA, N. 2013. Nuclear phosphoinositides and their impact on nuclear functions. *FEBS J,* 280**,** 6295-310.

SHAW, P., & BROWN, J. 2012. Nucleoli: composition, function, and dynamics. *Plant physiology*, *158*(1), 44–51.

SHAW PJ, HIGHETT MI, BEVEN AF, JORDAN, EG. 1995. The nucleolar architecture of polymerase I transcription and processing. EMBO J **14**: 2896–2906

SHERR C. J. (2001). The INK4a/ARF network in tumour suppression. *Nature reviews. Molecular cell biology*, *2*(10), 731–737.

SMITH, C. D., & WELLS, W. W. (1984). Characterization of a phosphatidylinositol 4-phosphate-specific phosphomonoesterase in rat liver nuclear envelopes. *Archives of biochemistry and biophysics*, *235*(2), 529–537.

SMITH, C. D., & WELLS, W. W. (1983). Phosphorylation of rat liver nuclear envelopes. II. Characterization of in vitro lipid phosphorylation. *The Journal of biological chemistry*, *258*(15), 9368–9373.

.

SMITH, C. D., & WELLS, W. W. (1984). Solubilization and reconstitution of a nuclear envelope-associated ATPase. Synergistic activation by RNA and polyphosphoinositides. *The Journal of biological chemistry*, *259*(19),

SOBOL, M., YILDIRIM, S., PHILIMONENKO, V. V., MARSAEK, P., CASTANO, E., & HOZAK, P. (2013). UBF complexes with phosphatidylinositol 4,5-bisphosphate in nucleolar organizer regions regardless of ongoing RNA polymerase I activity. *Nucleus (Austin, Tex.)*, *4*(6), 478–486.

SQUATRITO, M., MANCINO, M., DONZELLI, M., ARECES, L. B. & DRAETTA, G. F. 2004. EBP1 is a nucleolar growth-regulating protein that is part of pre-ribosomal ribonucleoprotein complexes. *Oncogene,* 23**,** 4454-4465

SQUATRITO, M., MANCINO, M., SALA, L. & DRAETTA, G. F. 2006. Ebp1 is a DsRNA-binding protein associated with ribosomes that modulates eIF2α phosphorylation. *Biochemical and biophysical research communications,* 344**,** 859-868.

SRIVASTAVA, S. P., KUMAR, K. U. & KAUFMAN, R. J. 1998. Phosphorylation of Eukaryotic translation initiation factor 2 mediates apoptosis in response to activation of the double-stranded RNA-dependent protein kinase. *Journal of Biological Chemistry,* 273**,** 2416-2423.

SUN M, FUENTES SM, TIMANI K, SUN D, MURPHY C, LIN Y, AUGUST A, TENG MN, HE B. 2008. Akt plays a critical role in replication of non-segmented negative stranded RNA viruses. *J Virol,* 82: 105-114

TAKENAVA T., & ITOH, T. (2001). Phosphoinositides, key molecules for regulation of actin cytoskeletal organization and membrane traffic from the plasma membrane. *Biochimica et biophysica acta*, *1533*(3), 190–206.

THAPA, N., TAN, X., CHOI, S., LAMBERT, P. F., RAPRAGAER, A. C., & ANDERSON, R. A. (2016). The Hidden Conundrum of Phosphoinositide Signaling in Cancer. *Trends in cancer, 2*(7), 378–390.

THORPE, L. M., YUZUGULLU, H., & Zhao, J. J. (2015). PI3K in cancer: divergent roles of isoforms, modes of activation and therapeutic targeting. *Nature reviews. Cancer*, *15*(1), 7–24.

TOKER A. 2002. Phosphoinositides and signal transduction. *Cell Mol Life Sci*; 59:761-779.

TSUI, M. M. & YORK, J. D. 2010. Roles of inositol phosphates and inositol pyrophosphates in development, cell signaling and nuclear processes. *Advances in enzyme regulation,* 50**,** 324-337.

VANHAESBROEK B, STEPHENS L, HAWKINS P. 2012. PI3K signaling: the path to discovery and understanding. *Nat Rev Mol Cell Biol*.; 13(3):195-203.

Viiri, K. M., Jänis, J., Siggers, T., Heinonen, T. Y., Valjakka, J., Bulyk, M. L., Mäki, M., & Lohi, O. (2009). DNA-binding and -bending activities of SAP30L and SAP30 are mediated by a zinc-dependent module and monophosphoinositides. *Molecular and cellular Biology*, *29*(2), 342–356.

VOLGELSTEIN, B., LANE, D., & LEVINE, A. J. (2000). Surfing the p53 network. *Nature*, *408*(6810), 307–310.

VOIT, R., SCHAFER, K., & GRUMMT, I. (1997). Mechanism of repression of RNA polymerase I transcription by the retinoblastoma protein. *Molecular and cellular biology*, *17*(8), 4230–4237.

VOUSDEN KH, LANE DP. 2007. p53 in health and disease. *Nat Rev Mol Cell Biol*. ;8(4):275-283.

Wang, C., Query, C. C. & Meier, U. T. Immunopurified small nucleolar ribonucleoprotein particles pseudouridylate rRNA independently of their association with phosphorylated Nopp140. *Mol. Cell. Biol*. 22, 8457–8466 (2002)

Waugh M. G. (2012). Phosphatidylinositol 4-kinases, phosphatidylinositol 4-phosphate and cancer. *Cancer letters*, *325*(2), 125–131.

Wendel, H. G., De Stanchina, E., Fridman, J. S., Malina, A., Ray, S., Kogan, S., Cordon-Cardo, C., Pelletier, J., & Lowe, S. W. (2004). Survival signalling by Akt and eIF4E in oncogenesis and cancer therapy. *Nature*, *428*(6980), 332–337.

WĘSIERSKA-GĄDEK, J. & HORKYA, M. 2003. How the Nucleolar Sequestration of p53 Protein or Its Inter-players Contributes to Its (Re) Activation. *Annals of the New York Academy of Sciences,* 1010**,** 266-272.

WJ KEUNE, DR JONES, N DIVECHA. 2013. PtDIns5P and Pin1 in oxidative stress Signaling. *Advances in biological regulation*.

WICKI, A. & CHRISTOFORI, G. 2007. The potential role of podoplanin in tumor invasion. *British journal of cancer,* 96**,** 1-5.

WILD, K., ALEKSIĆ, M., LAPOUGE, K. *et al.* 202. MetAP-like Ebp1 occupies the Human ribosomal tunnel exit and recruits flexible rRNA expansion segments. *Nat Commun* 11, 776.

White, R. J., Trouche, D., Martin, K., Jackson, S. P., & Kouzarides, T. (1996). Repression of RNA polymerase III transcription by the retinoblastoma protein. *Nature*, *382*(6586), 88–

White R. J. 2005. RNA polymerases I and III, growth control and cancer. *Nature reviews. Molecular cell biology*, *6*(1), 69–78.

Woolford, J. L., Jr, & Baserga, S. J. (2013). Ribosome biogenesis in the yeast Saccharomyces cerevisiae. *Genetics*, *195*(3), 643–681.

XIA, X., CHENG, A., LESSOR, T., ZHANG, Y. & HAMBURGER, A. W. 2001a. Ebp1, an ErbB-3 binding protein, interacts with Rb and affects Rb transcriptional regulation. *Journal of cellular physiology,* 187**,** 209-217.

XIA, X., LESSOR, T. J., ZHANG, Y., WOODFORD, N. & HAMBURGER, A. W. 2001b. Analysis of the expression pattern of Ebp1, an ErbB-3-binding protein. *Biochemical and biophysical research communications,* 289**,** 240-244.

XIAN, J., OWUSU OBENG, E., RATTI, S., RUSCIANO, I., MARVI, M. V., FAZIO, A., De Stefano, A., MONGIORGI, S., CAPELLINI, A., RAMAZZOTTI, G., MANZOLI, L., COCCO, L., & FOLLO, M. Y. 2020. Nuclear Inositides and Inositide-Dependent Signaling Pathways in Myelodysplastic Syndromes. *Cells*, *9*(3), 697.

Yin, Y., & Shen, W. H. (2008). PTEN: a new guardian of the genome. *Oncogene*, *27*(41), 5443–5453.

YU, Y.-T., SHU, M.-D., NARAYANAN, A., TERNS, R. M., TERNS, M. P. & STEITZ, J. A. 2001. Internal modification of U2 small nuclear (snRNA) occurs in nucleoli of Xenopus oocytes. *The Journal of cell biology,* 152**,** 1279-1288.

YAMADA, H., MORI, H., MOMOI, H., NAKAGAWA, Y., UEGUCHI, C. & MIZUNO, T. 1994. A fission yeast gene encoding a protein that preferentially associates with curved DNA. *Yeast,* 10**,** 883-894.

Yildirim, S., Castano, E., Sobol, M., Philimonenko, V. V., Dzijak, R., Venit, T., & Hozák, P. (2013). Involvement of phosphatidylinositol 4,5-bisphosphate in RNA polymerase I transcription. *Journal of cell science*, *126*(Pt 12), 2730–2739.

YOO, J., WANG, X., RISHI, A., LESSOR, T., XIA, X., GUSTAFSON, T. HAMBURGER, A. 2000a. Interaction of the PA2G4 (EBP1) protein with ErbB-3 and regulation of this binding by heregulin. *British journal of cancer,* 82**,** 683.

YOO, J. Y., WANG, X. W., RISHI, A. K., LESSOR, T., XIA, X. M., GUSTAFSON, T. A. HAMBURGER, A. W. 2000b. Interaction of the PA2G4 (EBP1) protein with ErbB-3 and regulation of this binding by heregulin. *British journal of cancer,* 82**,** 683-90.

YU, Y., CHEN, W., ZHANG, Y., HAMBURGER, A. W., PAN, H. & ZHANG, Z. 2007. Suppression of salivary adenoid cystic carcinoma growth and metastasis by ErbB3 binding protein Ebp1 gene transfer. *International journal of cancer,* 120**,** 1909-1913.

YUAN, P., TEMAM, S., EL-NAGGAR, A., ZHOU, X., LIU, D. D., LEE, J. J. & MAO, L. 2006. Overexpression of podoplanin in oral cancer and its association with poor clinical outcome. *Cancer,* 107**,** 563-569.

Zhao, K., Wang, W., Rando, O. J., Xue, Y., Swiderek, K., Kuo, A., & Crabtree, G. R. (1998). Rapid and phosphoinositol-dependent binding of the SWI/SNF-like BAF complex to chromatin after T lymphocyte receptor signaling. *Cell*, *95*(5), 625–636.

ZHANG, Y., FONDELL, J. D., WANG, Q., XIA, X., CHENG, A., LU, M. L. & HAMBURGER, A. W. 2002.Repression of androgen receptor mediated transcription by the ErbB-3 binding protein, Ebp1.*Oncogene,* 21**,** 5609-5618.

ZHANG, Y., WANG, X.-W., JELOVAC, D., NAKANISHI, T., YU, M.-H., AKINMADE, D., GOLOUBEVA, O., ROSS, D. D., BRODIE, A. & HAMBURGER, A. W. 2005b. The ErbB3-binding protein Ebp1 suppresses androgen receptor-mediated gene transcription and tumorigenesis of prostate cancer cells. *Proceedings of the National Academy of Sciences of the United States of America,* 102**,** 9890-9895.

ZHANG, Y., WOODFORD, N., XIA, X. & HAMBURGER, A. W. 2003. Repression of E2F1-mediated transcription by the ErbB3 binding protein Ebp1 involves histone deacetylases. *Nucleic acids research,* 31**,** 2168-2177.

ZHANG, Y. & HAMBURGER, A. W. 2004. Heregulin regulates the ability of the ErbB3-binding protein Ebp1 to bind E2F promoter elements and repress E2F-mediated transcription. *Journal of Biological Chemistry,* 279**,** 26126-26133

ZHANG, Y. & HAMBURGER, A. 2005. Specificity and heregulin regulation of Ebp1 (ErbB3 binding protein 1) mediated repression of androgen receptor signaling. *British journal of cancer,* 92**,** 140-146.

ZHANG, Y., AKINMADE, D. & HAMBURGER, A. W. 2005a. The ErbB3 binding protein Ebp1 interacts with Sin3A to repress E2F1 and AR-mediated transcription. *Nucleic acids research,* 33**,** 6024-6033.

ZHANG, F., LIU, Y., WANG, Z., SUN, X., YUAN, J., WANG, T., TIAN, R., JI, W., YU, M. & ZHAO, Y. 2015. A novel Anxa2-interacting protein Ebp1 inhibits cancer proliferation and invasion by suppressing Anxa2 protein level. *Molecular and cellular endocrinology*

ZHANG, Y., LINN, D., LIU, Z., MELAMED, J., TAVORA, F., YOUNG, C. Y., BURGER, A. M. & HAMBURGER, A. W. 2008. EBP1, an ErbB3-binding protein, is decreased in prostate cancer and implicated in hormone resistance. *Molecular cancer therapeutics,* 7**,** 3176-3186.

Zhang, S., Zeng, X., Ding, T., Guo, L., Li, Y., Ou, S., & Yuan, H. (2018). Microarray profile of circular RNAs identifies hsa_circ_0014130 as a new circular RNA biomarker in non-small cell lung cancer. *Scientific reports*, *8*(1), 2878.

Zhang, Q., Zhang, C., Ma, J. X., Ren, H., Sun, Y., & Xu, J. Z. (2019). Circular RNA PIP5K1A promotes colon cancer development through inhibiting miR-1273a. *World journal of gastroenterology*, *25*(35), 5300–5309.

Zhai, W., & Comai, L. (2000). Repression of RNA polymerase I transcription by the tumor suppressor p53. *Molecular and cellular biology*, *20*(16), 5930–5938.

Zhou, H., Mazan-Mamczarz, K., Martindale, J. L., Barker, A., Liu, Z., Gorospe, M., Leedman, P. J., Gartenhaus, R. B., Hamburger, A. W., & Zhang, Y. (2010). Post-transcriptional regulation of androgen receptor mRNA by an ErbB3 binding protein 1 in prostate cancer. *Nucleic acids research*, *38*(11), 3619–3631.

ZU, J. BLENIS J., & YUAN J. 2008. Activation of PI3K/Akt and MAPK pathways regulates Myc-mediated transcription by phosphorylating and promoting the degradation of Mad1, *Proc. Natl. Acad. Sci*. U. S. A. 105 584–6589.

1: Proc Natl Acad Sci USA 105, 15779 (2008); 2. Chem Bio Chem 4, 1147 (2003); 3. J Am Chem Soc 124, 3192 (2003); 4. Angew Chem Int Ed Engl 41, 2596 (2002); 5. Angew Chem Int Ed Engl 40, 2004 (2001).

Appendix

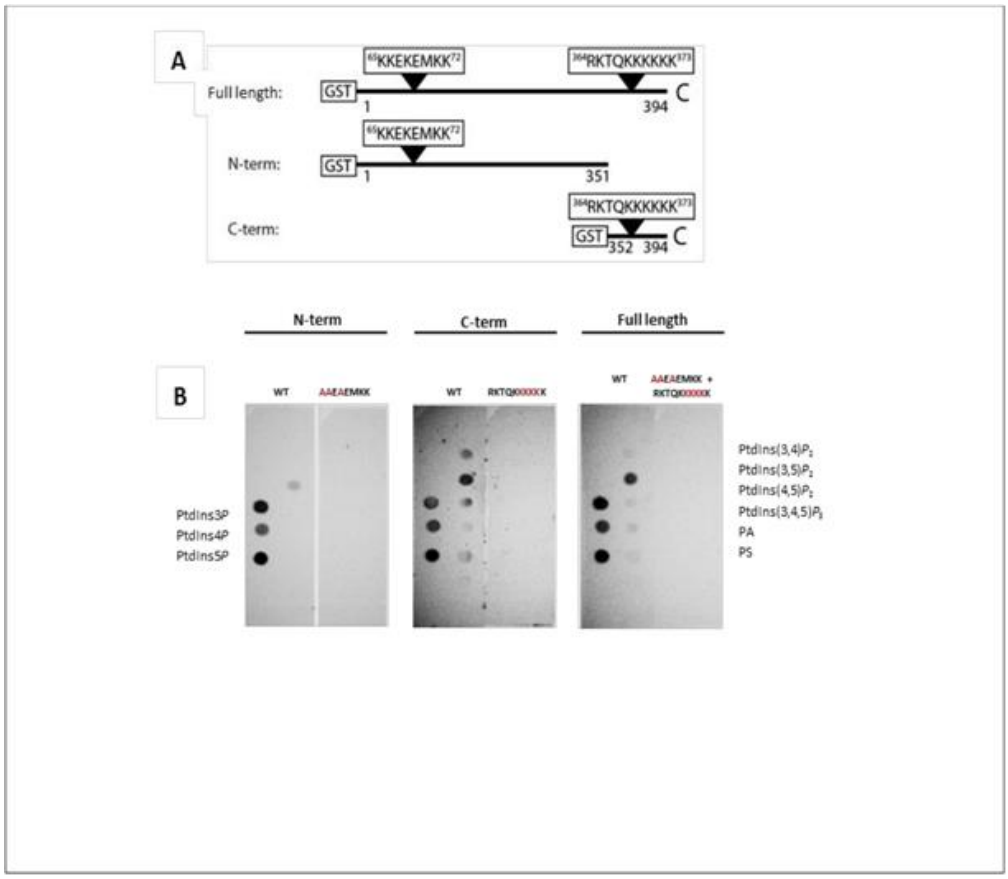

Supplementary figure S-1. In vitro binding of N- and C-terminal EBP1 constructs. A) Representation of the primary structure of the recombinant GST-EBP1 and the deletion constructs. The approximate locations of the lysine-rich regions are indicated by arrows. B) PIP strips incubated with recombinant wild type FL-EBP1 and the N-and C-terminal constructs. All three strips were processed simultaneously using the same amount of protein and same antibody dilution. Figure adapted from (Karlsson, 2011)

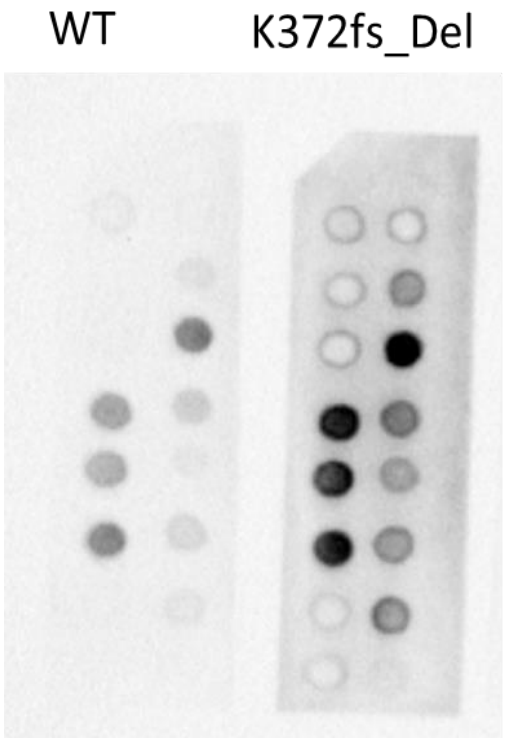

Supplementary figure S2: Increased PPIn interaction with K372Rdel-fs tumor mutant. K372Rdel-fs tumor mutant showing an enhanced binding with PPIn compared to wild type construct. Figure taken from former master's student thesis.

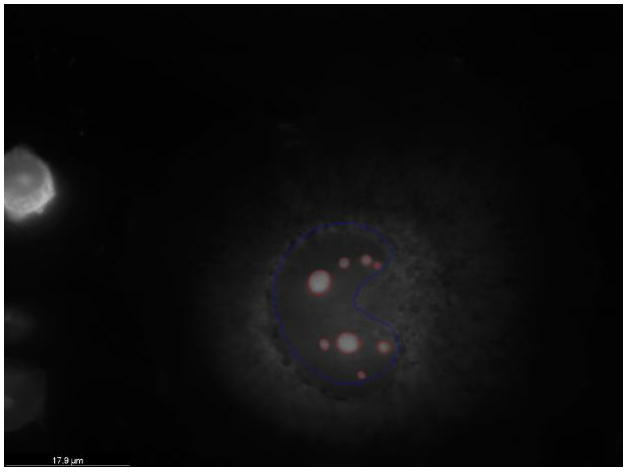

Supplementary figure S3. Detection of nucleoli by Cell Profiler. Pipeline module selects nucleoli in the GFP positive cells based on a specific threshold factor which is adjusted accordingly. Red circles represent the detected nucleoli from a sample run of K372Rdel-fs tumor mutant.